UNIVERSITAS STUDIORUM INSUBRIAE
Ph.D. in Cellular and Molecular Biology
XXV CYCLE


**Ph.D thesis of: RAIMONDI IVAN**

# PROLINE DEHYDROGENASE REGULATION BY THE P53 FAMILY AND THE REGULATORY CIRCUIT WITH HIF-1.

**Scuola di Dottorato in Scienze Biologiche e Mediche.**

**Tutor: Dott. PAOLA CAMPOMENOSI**

**Anno accademico 2011/2012**

**SUMMARY**

Proline differs from the other amino acids because its α-nitrogen is contained within a pyrrolidine ring. Therefore, it cannot be metabolized by the general transaminases and decarboxylases acting on other amino acids. Proline dehydrogenase (PRODH) is a stress-inducible, key enzyme in proline metabolism, catalyzing its conversion into Δ1-pyrroline-5-carboxylate, a crucial compound interconnecting proline metabolism with glutamate and α-ketoglutarate (α-KG) synthesis and with the Tricarboxylic Acids (TCA) and Urea cycles. Consequently, PRODH can influence various cellular pathways, including glutamatergic transmission, glutathione levels as well as the activity of a number of enzymes using α-KG as a substrate.

Proline can also be regarded as an emergency substrate, as abundant stores are released during degradation of intracellular or extracellular matrix proteins (especially collagens). PRODH is localized in the inner membrane of mitochondria and after reduction of the FAD cofactor bound to form the holoenzyme, it can directly transfer electrons to cytochrome C to generate ATP or it can oxidize O2 to generate reactive oxygen species (ROS). Thus when cells are under stress, PRODH has been proposed to act either as a survival factor, favouring maintenance of "survival energy levels", or as a cell death effector, inducing ROS-dependent apoptosis.

Alterations in PRODH protein levels and catalytic activity have been implicated in diseases such as hyperprolinemia, DiGeorge syndrome, schizophrenia and cancer. For cancer in particular, several lines of evidence suggest a central role of PRODH as a mitochondrial tumor suppressor: 1) expression of PRODH is reduced in diverse colorectal and renal cancer cells as compared to normal counterparts; 2) restoration of PRODH expression in human hypo-expressing colon cancer cell lines suppresses their ability to form tumours when injected into SCID mice; 3) PRODH expression is regulated transcriptionally and post-transcriptionally by several cellular sensors of cell health and homeostasis, whose functions are deregulated during carcinogenesis, including p53, PPARγ and mTOR (mammalian target of rapamycin). However, the exact mechanisms by which these proteins control PRODH function have been only partially elucidated.

Understanding transcriptional and post-transcriptional regulation of a gene and its product is clue to understanding its function. In the first two years of

my PhD work we identified and characterized the p53 Response Elements (REs) in the *PRODH* gene, responsible for p53 binding and transactivation of this target. We confirmed p53-dependent induction of endogenous *PRODH* in response to genotoxic damage in cell lines of different histological origin and we established that overexpression of p73β or p63β is sufficient to induce *PRODH* expression in p53-null cells. The p53 family-dependent transcriptional activation of PRODH was linked to specific intronic response elements (REs), among those predicted by bioinformatics tools and experimentally validated by a yeast-based transactivation assay upon modulated expression of p53, p63 and p73 and by p53 occupancy measurements in HCT116 human cells by ChIP. Based on the following pieces of evidence i) it has been proposed that during nutrient stress extracellular matrix (ECM) proteins may be degraded to provide substrates for energy production (ecophagy), ii) an abundant protein in ECM is collagen, that is very rich in proline and hydroxyproline, iii) the key enzyme in hydroxyproline metabolism is hydroxyproline dehydrogenase, homologous to PRODH, whose gene (*PRODH2*) was also shown, although less convincingly, to be a p53 target, we decided to characterize the p53 REs present in this gene as well. We demonstrated that the *PRODH2* gene was not responsive to p63 nor p73 and was at best a weak p53 target, based on minimal levels of PRODH2 transcript induction by genotoxic stress observed only in one of four p53 wild-type cell lines tested. Consistently, all predicted p53 REs in PRODH2 were poor matches to the p53 RE consensus and showed limited responsiveness, only to p53, in the functional assay. Taken together, our results highlight that PRODH but not PRODH2 expression is likely under control of the entire p53 family members, supporting a deeper link between p53 proteins and metabolic pathways, as PRODH functions in modulating the balance of proline and glutamate levels and of their derivative alpha-keto-glutarate in the metabolism under normal and pathological (tumor) conditions.

Another important transcription factor that we considered for a possible role in regulation of PRODH, is the Hypoxia Inducible Factor 1 (HIF-1), whose function influences cellular metabolism and is altered during the tumourigenic process. HIF proteins are composed of two subunits, α and β, both constitutively expressed in cells. However, the α subunits are rapidly degraded by the proteasome at normal oxygen concentrations found in tissues. Key to HIF-1α degradation is its oxygen-dependent hydroxylation at specific residues

(prolines 402 and 564) by Prolyl Hydroxylases (PHD), that target the protein for ubiquitylation and proteasomal degradation in presence of molecular oxygen, α-KG and vitamin C. During hypoxia, HIF-1α subunits become stabilized, which enables them to form heterodimers with HIF-1β, that activate numerous cell survival pathways.

HIF-1 has been shown to control the expression of more than a hundred genes, either by direct transcriptional activation of protein coding genes and microRNAs (miRs), or by interacting or interfering with other transcription factors. HIF-1 activation results in profound alterations in tumour cell behaviour, which include triggering the angiogenic switch, shifting glucose metabolism towards glycolysis, promoting epithelial-to-mesenchymal transition and acquisition of an invasive phenotype, as well as increasing chemo- and radio-resistance. For this reason, tumour cells often maintain HIF-1 overexpression after they return to a normoxic environment.

We tested the hypothesis that an increase in PRODH activity, by increasing α-KG, would provide substrate for the hydroxylation reaction catalyzed by PHDs, thus leading to a decrease in HIF-1 α levels. indeed, ectopic expression of PRODH led to down-regulation of HIF-1α and VEGF protein levels in the U87 glioblastoma cell line. This finding confirmed what was already reported to occur for colon cancer cell lines.

In addition to a role of PRODH in regulating HIF-1 stability in normoxia, we hypothesized that a regulatory circuit between PRODH and HIF-1 could exist. PRODH was found to be downregulated 2-fold in a transcriptomics analysis of genes regulated following induction of focal brain ischemia in rat. On the other hand, however, very recently PRODH was shown to be induced by hypoxia and this induction was AMPK-dependent and HIF-independent. Therefore, the question was still open for investigation. Our expectations are unbiased, because PRODH possesses the ability to promote either cell survival, in conditions in which energy levels are low, by producing ATP or inducing ROS dependent autophagy, or ROS induced apoptotic cell death. Of course a different outcome depending on the cell lines tested as well as on other types of stress acting on the cells concomitantly with the hypoxic stress may be expected.

In a first attempt to verify if PRODH transcript levels were modified by hypoxia, we exposed cancer cell lines of different histological origin (HCT116, colon;

MCF7, breast; U87MG, glia; SHSY-5Y, neural crest) to 1% hypoxia, anoxia or to treatment with $CoCl_2$, a PHDs inhibitor, and compared the levels of expression with those obtained in the same untreated cell lines, by using real time RT-qPCR. All cell lines showed a marked decrease in PRODH transcript, in particular after treatment with $CoCl_2$, and a reduction also in protein levels, although of minor entity compared to transcript decrease. Preliminary results obtained during my PhD work confirm that PRODH-HIF-1 regulatory circuit does indeed exist, and lays the foundations for further investigations, to clarify the relationship between these two proteins to increase knowledge about PRODH regulation and its possible downregulation during the tumourigenic process.

# 1. INTRODUCTION

## 1.1 Cancer and its metabolism.

Although it has been known for long that cancer cells have a unique metabolism compared to normal cells (Warburg, 1956), interest in this topic has revived recently, when several oncogenes and tumour suppressors were shown to affect several aspects of cell metabolism (Figure 1) (Vogelstein and Kinzler, 2004).

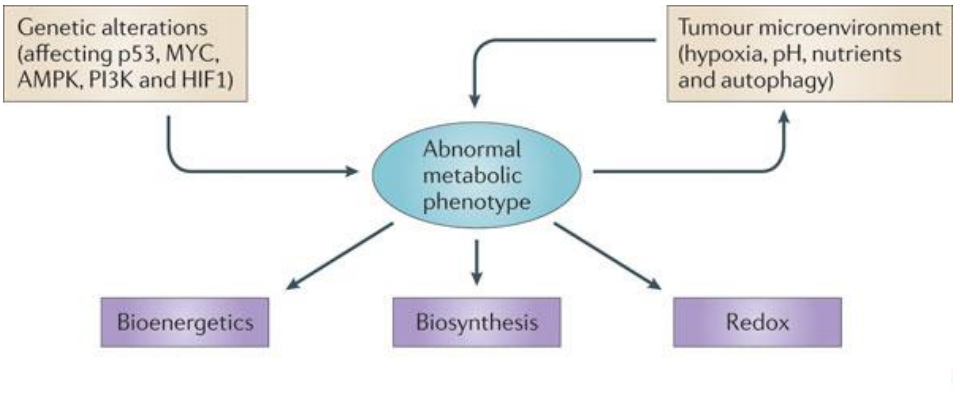


***Figure 1. Determinants of the tumour metabolic phenotype.***
*The metabolic phenotype of tumour cells is controlled by intrinsic genetic mutations and external responses to the tumour microenvironment. Oncogenic signalling pathways controlling growth and survival are often activated by the loss of tumour suppressors (such as p53) or by constitutive activation of oncoproteins (such as PI3K). The resulting altered signalling modifies cellular metabolism to match the requirements of cell division. Abnormal microenvironmental conditions such as hypoxia, low pH and/or nutrient deprivation elicit responses from tumour cells, including autophagy, which further affect metabolic activity. These adaptations optimize tumour cell metabolism for proliferation by providing appropriate levels of energy in the form of ATP, biosynthetic capacity and the maintenance of balanced redox status. AMPK: AMP-activated protein kinase; HIF1: hypoxia-inducible factor 1.*

*From Cairns 2011*

Among these are the PI3K signaling pathway, that perturbs coordination between growth and proliferation signals and central metabolism (Plas and Thompson, 2005), Myc, that promotes mitochondrial gene expression, mitochondrial biogenesis and glutamine metabolism (Li et al., 2005), AMPK, the central energy sensor (Schafer et al., 2009), HIF-1α, that is essential to control oxygen levels and stimulates new vessel formation to improve nutrient uptake, and finally p53, one of the tumour suppressors most recently shown to modulate metabolic reprogramming, by reducing utilization of the glycolytic pathway (Bensaad et al., 2006) and by promoting oxidative phosphorylation (Matoba et al., 2006).

Based on constantly growing evidence, it is now generally accepted that metabolism and bioenergetics play a fundamental role in the development of complex diseases such as cancer. This unique metabolic divergence may be the target for discovery and development of more specific cancer therapies (Vander Heiden et al., 2009).

The altered metabolism is considered fundamental to the transformation of normal cells into cancer cells and is believed to be a characteristic of most, if not all, cancers, including solid tumours, and hematologic malignancies (Suganuma et al., 2010; Altman and Dang, 2012). Metabolic transformation is thought to be initiated by the strongly decreased oxygen availability in a growing tumour as soon as it reaches the size of 1 $mm^3$. This leads to alterations in energy production mechanisms, including a large shift in mitochondrial function from energy production to the creation of biosynthetic intermediates, or building blocks, supporting cell growth and proliferation (Wallace, 2012). Not surprisingly, metabolic requirements and the types of nutrients taken up by cancer cells are altered dramatically compared to normal cells (Dang, 1999; Jones and Thompson, 2009).

Tumour cells face various types of stress as they arise and progress. Early-stage tumours, that have not yet recruited new blood vessels to supply them with nutrients, will have a shortage of both glucose and oxygen, will face metabolic stress, and some cells will acquire anchorage independence(Schafer et al., 2009). Additionally, some mutations, that trigger tumour formation, accelerate certain cellular metabolic programs and thereby cause stress. AMP-activated protein kinase (AMPK) is a central sensor of cellular metabolism. It is activated during metabolic stress situations that lower the intracellular levels of ATP, a crucial energy-supplying molecule (Schafer et al., 2009). AMPK activation influences cellular signalling pathways that are involved in cancer, such as the mTOR and p53 pathways, and inhibits the proliferation of cells in culture (Mihaylova and Shaw, 2011; Hardie et al., 2012).

Aim of this PhD project was to study the regulation and function of Proline dehydrogenase (PRODH), an enzyme key to proline metabolism, able to interfere with cancer metabolism adaptation in at least two different ways.

First of all, as we will see in detail later, two products deriving from the activity of the flavoenzyme PRODH are glutamate and alpha-Ketoglutarate ($\alpha$-KG), the latter of which plays an anaplerotic role in the tricarboxylic acids (TCA) cycle

(Phang et al., 2010). Therefore, PRODH deregulation could perturb TCA steady state and drive metabolic change during tumour growth, when other nutrients or substrates are depleted. It has been demonstrated that PRODH overexpression corresponds to a decrease of essential TCA intermediates such as fumarate and malate, limiting energy production of cells (Liu et al., 2009a). Moreover, $\alpha$-KG is an essential substrate for some enzymes, such as Prolyl Hydroxylases (Tuderman et al., 1977). PRODH catalytic activity also results in production of reducing power, that are transferred on the FAD molecule of this flavoenzyme and can either be donated to the oxidative phosphorylation chain, downstream of Complex I, to produce ATP, or used to produce ROS (Surazynski et al., 2005; White et al., 2007).

Proline dehydrogenase has been shown to play a role in apoptosis, as upregulation of PRODH (for example by p53) leads to increased proline oxidation and superoxide production in mitochondria. Superoxide, in turn, stimulate both the intrinsic and extrinsic apoptotic cell death pathways (Phang et al., 2008). More recently a role of PRODH in regulation of ROS mediated autophagy has been described. Therefore, PRODH can either mediate apoptosis or survival.

Hypoxia is frequently concurrent with nutrient depletion and metabolic changes and it can influence yet another hallmark of cancer, neoangiogenesis. PRODH was recently shown to interfere also with this process, again by its ability to modulate $\alpha$-KG (Liu et al., 2009). Both hallmarks, metabolic changes and neoangiogenesis, are initiated by hypoxia and its main effector, the transcription factor Hypoxia Inducible Factor-1 (HIF-1), but is subsequently sustained by deregulation of the Hypoxia Inducible Factor(s) also in absence of hypoxia.

The two processes just considered are very important for tumour growth, and indeed metabolic changes and neoangiogenesis are considered hallmarks of cancer, e.g. alterations in cellular physiology that are essential to the transformation of normal cells into cancerous cells, as they were historically defined by Douglas Hanahan and Robert Weinberg a decade ago and revised more recently (Hanahan and Weinberg, 2000, 2011).

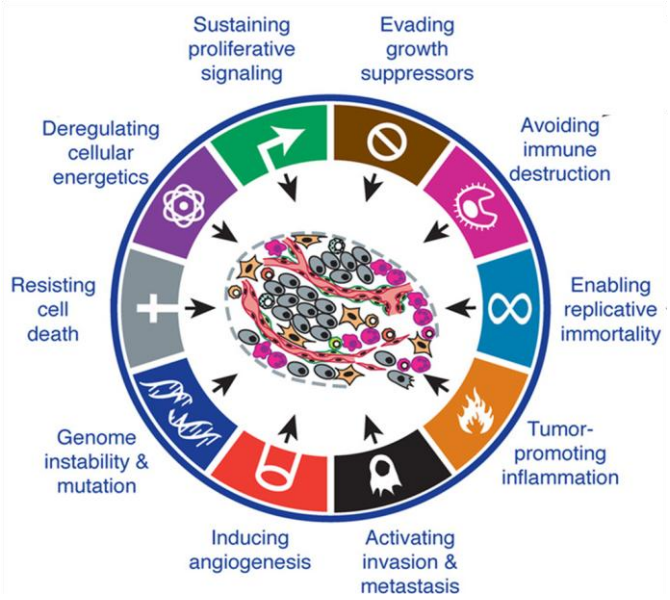


***Figure 2. Hallmarks of cancer.***
*Representation of 10 biological capabilities acquired during the multistep development of human tumors.*
*Modified from Hanahan and Weinberg, 2011*

Several lines of evidence indicate that development of cancer is a multistep process, each step of which is finely regulated and connected with others; genetic or epigenetic alterations in this complicated network can drive the progressive transformation of normal human cell into highly malignant derivatives (Hanahan and Weinberg, 2011).

Knowledge about the regulation of these processes and the links between them are in continue expansion. In view of PRODH involvement in different metabolic pathways, it is essential to reach a deep knowledge of the enzyme regulation and the molecular processes PRODH is involved in, to understand the mechanisms underlying its oncosuppressive role.

**1.2 Prodh.**

The *PRODH* gene maps on human chromosome 22 in the 22q11 region. It encodes for Proline dehydrogenase, a mitochondrial enzyme that catalyzes dehydrogenation of proline to 1-pyrroline-5-carboxylate. PRODH mutations are responsible for the benign mendelian condition termed “type I Hyperprolinemia” (OMIM #239510) and for the complex behavioural disease schizophrenia, so that the gene has been also indicated as *SCZD4*, which stands for “schizophrenia susceptibility locus 4” (Jacquet et al., 2002; Kempf et al., 2008).

PRODH is localized to the inner mitochondrial membrane and possesses a key role in the metabolism of proline, a non essential amino acid characterized by a secondary amino group.

The side-chain of proline, in fact, closes on the nitrogen of the amino group, forming a ring that confers stability and rigidity to protein structures. Several proteins are very rich in proline: for example collagen, an essential component of the extracellular matrix, is characterized by a rigid and regular structure, due to its composition, in which 25% of the residues are represented by proline and hydroxyproline. Indeed, cellular proline uptake derives primarily from dietary proteins but can also be obtained by degradation of extracellular matrix proteins, comprised predominantly of collagen.

Due to its particular structure, proline metabolism requires dedicated enzymes, other than those involved in the metabolism of common amino acids, such as transaminases and decarboxylases.

Proline metabolism occurs through a process called "Proline Cycle", in which compounds shuttle between the mitochondrion and the cytoplasm, as shown in Figure 3. PRODH catalyzes the oxidation of Proline to Δ1-pyrroline-5-carboxylate (P5C), which is in tautomeric equilibrium with its linear form, γ-glutamic semialdehyde (GSA). The P5C can exit the mitochondrion and be again converted into Proline by the cytosolic enzyme P5C-reductase, which uses NADPH as its cofactor.

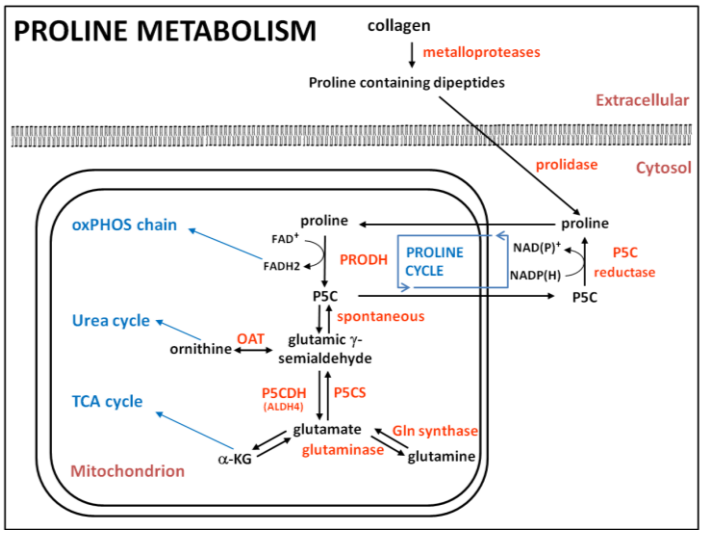


***Figure 3. Schematic of the pathways involved in proline metabolism (see text).*** *PRODH: Proline dehydrogenase; P5C: Δ1pyrroline-5-carboxylate; PC5S: P5C Synthase; PC5DH: P5C dehydrogenase; OAT: ornithine aminotransferase; α-KG: alpha ketoglutarate.*

P5C can also be metabolized to glutamate by P5C dehydrogenase and then converted into α-KG which will enter the Tricarboxylic acid cycle (TCA) or will be used by various cellular enzymes. Glutamate can also be converted back into P5C by the action of P5C synthase (Figure 3). During oxidation of proline, PRODH transfers reducing power to $FAD^+$, which is reduced to $FADH_2$. The reduced cofactor can in turn, donate the pair of electrons to the electron transport chain to generate ATP. Alternatively, the electrons deriving from the oxidation of proline can be used to generate Reactive oxygen species (ROS), reducing the molecular oxygen present in the cell to superoxide anion ($O_2$-), which is subsequently converted to hydrogen peroxide ($H_2O_2$) by superoxide dismutase 2 (SOD2).

Therefore, increased activity of PRODH, by physiological or artificial induction of protein expression and/or activity, may lead to an increased production of ROS, which in turn can lead to the activation of the intrinsic pathway of apoptosis; such process involves the release of Cytochrome C by the mitochondrial membrane, the activation of the caspase cascade and culminates with the condensation of chromatin and formation of apoptotic bodies, thereby leading to cell death (Dobrucki and Darzynkiewicz, 2001). The proline dehydrogenase can also lead to cell death by activating the extrinsic pathway apoptosis: the overexpression of this protein, in fact, leads to an increase of protein levels of NFAT (Nuclear Factor of Activated T-cells), a

transcription factor that allows the activation of the transcription of TRAIL (Related Apoptosis Inducing Ligand), which, upon binding to its receptor, activates the caspase cascade (Liu et al., 2006). Several lines of evidence suggest that this function, apoptosis induction, plays a major role in the tumour suppressive role of PRODH, as it will be described later. Nevertheless, recently PRODH was also described to play a role in induction of autophagy, as its overexpression is sufficient to induced cell protective autophagy in a colon cancer cell line (Zabirnyk et al., 2010). Autophagy is a process known as 'self-eating', which serves a housekeeping role and degrades damaged or unwanted organelles. Autophagy also serves to derive energy during stress conditions. Beyond a threshold, this process may eventually lead to cell death (Galluzzi et al., 2008). Therefore, PRODH seems to act as a balance between survival and apoptosis, likely depending on the type and extent of stress that is inducing it.

### 1.3 Prodh in cancer.

Several pieces of evidence published in the literature support the tumor suppressor function played by PRODH during tumour formation. Immunohistochemical staining with specific antibodies performed on tumor tissue sections and their related normal counterparts, revealed that the expression of PRODH is significantly reduced in tumors compared with adjacent normal tissues (Figure 4). Moreover, restoring the expression of PRODH in a colon carcinoma cell line, can markedly reduce cell proliferation and tumor growth both *in vitro* and *in vivo* (Liu et al., 2009).

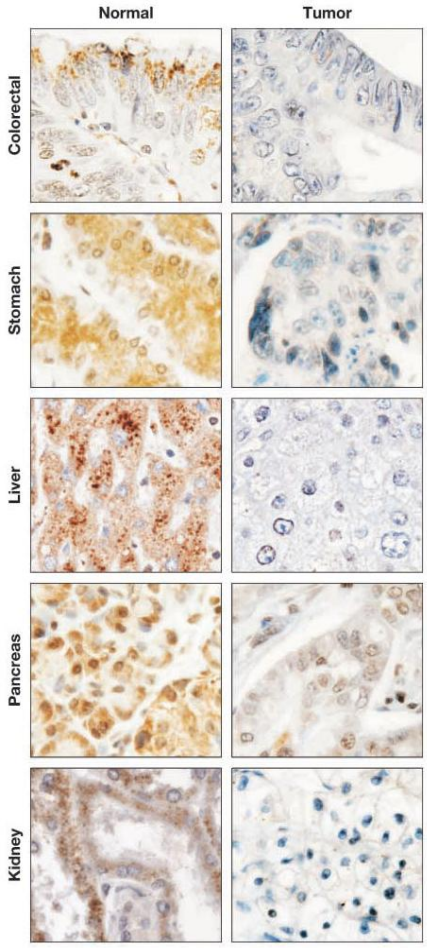


***Figure 4. The reduced expression of PRODH in human tumour tissues.***
*Paired samples of human cancers and normal tissues from the same patient, were used to detect PRODH expression levels by immunohistochemistry. Shown are some representative images from normal colon, stomach, liver, pancreas, and kidney tissues and paired tumours .*

*From Liu et al, 2010*

Moreover, the gene encoding PRODH is located in a chromosomal region undergoing frequent genetic rearrangements such as deletions and translocations; some reports associated loss of this region with an increased predisposition to cancer, although these results are far from being conclusive (McDonald-McGinn et al., 2006; Liu et al., 2009a). In the same region, 1.4 Mb away from the gene, an unprocessed pseudogene (ψ PRODH) has been mapped, that carries a deletion encompassing exons 3 to 7 and several mutations that could be transferred on PRODH with high frequency due to a phenomenon known as gene conversion (Bender et al., 2005). Nevertheless, a systematic search for PRODH mutations in cancer has never been performed. The presence of the pseudogene in antisense orientation could also favor chromosomal rearrangements and in particular deletions .

*PRODH* has been extensively studied as a tumor suppressor gene in colorectal and renal cancers (Liu et al., 2009a), but there are indications that its expression and function may be altered more widely during the tumorigenic process.

PRODH has been described to play its oncosuppressive role through overproduction of ROS, leading to the activation of the apoptotic process. As it will be outlined later, we propose that there are other mechanisms by which PRODH can prevent tumor growth: in particular, in this thesis, we investigated the regulation of HIF-1α by PRODH and its possible consequences, including a role in the control of neoangiogenesis.

PRODH expression and activity were recently found associated with an increase in α-KG level, leading to downregulation of HIF-1α and VEGF protein levels in colorectal cancer cell lines (Liu et al., 2009a). This is not an unexpected finding, as prolyl-hydroxylases require α-KG in addition to molecular oxygen and vitamin C for their activity. Therefore, by increasing α-KG, PRODH can stimulate HIF-1α proline hydroxylation and degradation by the proteasome. The regulation of prolyl hydroxylases by modulation of α-KG substrate levels is very important in light of recent findings reporting that the reactivation of HIF prolyl hydroxylases, obtained using a derivatized α-KG able to permeate cells, induced metabolic catastrophe and cell death in tumor cells (Tennant et al., 2009). This characteristic could be exploited in order to induce tumor cell death and would also explain, at least in part, the mechanism of tumor suppression by PRODH.

Therefore, the importance of PRODH as a mitochondrial tumor suppressor is supported by several lines of evidence: its low expression in various types of human tumors, -in particular colorectal cancer and renal cancer-, and the fact that inducing re-expression of PRODH in human tumorigenic cell lines, suppresses their ability to form tumors when injected into SCID mice. In addition, PRODH expression and activity are controlled by proteins with a central role in tumourigenesis and metabolism, including mTOR, p53, and PPARγ (Polyak et al., 1997; Pandhare et al., 2006, 2009; Liu and Phang, 2012).

**1.4 Prodh regulation.**

An important step needed to understand the contribution of PRODH in metabolic processes, particularly during the tumourigenic process, involves investigating how this enzyme is regulated.

At the transcriptional level, the expression of the *PRODH* gene is regulated by various transcription factors. Among these, one of the first positive regulators identified was PPARγ (peroxisome proliferator activated receptor-gamma) for which a response element in the promoter of the gene has been described (Pandhare et al., 2006, 2009). PPARγ is a stress responsive nuclear receptor, activated by inflammatory drugs belonging to the class of thiazolidinediones, used in the treatment of diabetes mellitus type II (Pandhare et al., 2006). Recent studies have shown that tumor cells treated with these drugs show a reduced growth rate, which may be explained, at least in part, by their activity on PRODH (Pandhare et al., 2009).

Another important transcription factor involved in regulation of *PRODH* expression is p53, whose role in the control of tumourigenesis has been known for a long time, such that it has been defined "guardian of the genome" [Lane, 1992]. In fact, in response to various types of stress such as genotoxic damage or hypoxia, p53 is stabilized and acts by inducing cell cycle arrest or apoptosis, mainly through its activity as a transcription factor.

PRODH was identified as one of the genes, called PIGs (p53 Induced Genes), strongly induced by p53 after treatment with Adriamycin (Polyak et al., 1997). In particular, PRODH was named PIG6 after its identification in a SAGE analysis (Serial Analysis of Gene Expression), a technique used to determine changes in

the transcriptome after induction of p53. Of the 7202 genes analyzed, 14 were found to be induced more than 7 times, including *PRODH* (Polyak et al., 1997). PRODH has been considered one of the proapoptotic targets induced by p53. However in recent years p53 has acquired new roles, including the control of angiogenesis and metabolism, which are well suited to be mediated by PRODH (Teodoro et al., 2006; Vousden and Ryan, 2009). In spite of the fact that PRODH has long been known as a p53 target, identification and validation of the p53 RE(s) responsible for p53 responsivity in this gene has never been carried out, except for one study (Maxwell and Kochevar, 2008). For this reason PRODH has not been included in recent reviews listing known p53 targets (Riley et al., 2008; Beckerman and Prives, 2010a)

Regulation of PRODH also occurs at the post-transcriptional level. An increase in proline dehydrogenase activity, in fact, has been observed after inhibition of mTOR (mammalian Target Rapamycin) by treatment with rapamycin in various cell lines (Pandhare et al., 2009). When the cell undergoes nutrient stress, for example in the absence of glucose (such as tumours can encounter in the initial stages of tumour development, before neoangiogenesis is activated), mTOR is inhibited, thus allowing the passage from the biosynthetic state to a survival one. mTOR is a ubiquitous protein kinase that can form two types of multimeric complex, mTORC1 and mTORC2 (Lian et al., 2008). mTORC1 acts as a metabolic sensor, receiving signals from the intra- and extra-cellular environment, e.g. glucose abundance and nutrients availability, to which it responds by stimulating various cellular processes, the best characterized of which is protein synthesis. The outcome of all processes activated by mTORC1 is a stimulation of cell growth and proliferation (Laplante and Sabatini, 2012). Under normal conditions and plenty of nutrients, therefore, mTOR promotes cell growth, while during stress, the complex of mTOR is inhibited and so is cell growth. Not surprisingly, in conditions of stimulation of protein synthesis, the activity of proline dehydrogenase is inhibited, while physiological or pharmacological inhibition of mTOR leads to an increase in PRODH levels, allowing the utilization of the proline as an energy resource, either because of the consequent increase in $\alpha$-KG that can enter the TCA or be used for other reactions, or by donating the electrons obtained by proline oxidation to the electron transport chain, to maintain active oxidative phosphorylation (Phang et al., 2010). Noteworthy, p73, a member of the p53 family, was recently

shown to be induced by mTORC1 inhibition by rapamycin (Rosenbluth and Pietenpol, 2009). This prompted us to investigate transactivation of the *PRODH* gene by the whole p53 family, as a first step to elucidating the mechanism by which mTOR could increase PRODH expression.

Also AMPK activation has been shown to induce PRODH expression, and increase the production of ATP by this although the mechanisms underlying this activation have not been elucidated [Pandhare et al, 2009]. Nevertheless, AMPK is known to negatively regulate mTOR during nutrient stress and the action of these regulators could therefore partially overlap (Kimura et al., 2003).

Finally, another mechanism to finely regulate PRODH levels at the post-transcriptional level has been demonstrated very recently in cell lines derived from human renal cell carcinoma, where PRODH transcript was shown to be targeted by various microRNAs, in particular of miR-23b* (Liu et al., 2010) MicroRNAs are endogenous small RNAs, 18 to 25 nucleotides long, capable of binding the 3'UTR (UnTranslated Region) of mRNAs, thus inhibiting protein synthesis according to two main mechanisms: degradation or sequestering of mRNAs and repression of their translation (Pillai et al., 2007; Braun et al., 2011; van Kouwenhove et al., 2011).

All regulatory factors involved in the control of PRODH play a very important role in the control of the onset of cancer; indeed, they are often directly or indirectly deregulated, giving way to the neoplastic process. However, the mechanisms by which some of them, such as mTOR, exert their control on the activity of PRODH have been only partially elucidated. In any case, the fact that the main proteins involved in the control of tumor development have PRODH among their targets, suggests that the latter may have an important role in maintaining cellular homeostasis and also that its expression may influence tumour formation.

**1.5 Prodh2.**

Hydroxyproline is an aminoacid present in some proteins, that is not found in such form as a free aminoacid, but derives from post-translational modification of proline. Like proline, hydroxyproline requires a specific enzyme for its metabolism, hydroxyproline dehydrogenase *(*OH-PRODH or PRODH2*)*. The *PRODH2* gene, encoding this enzyme, maps to the 19q13.1 chromosomal region and little is known about its expression or function, except that it is associated with a rare inborn error of metabolism known as hydroxyprolinemia (OMIM #237000).
In the mitochondria, proline and hydroxyproline are oxidized to yield $\Delta^1$-pyrroline-5-carboxylate (P5C) and $\Delta^1$-pyrroline-3-hydroxy-5-carboxylate (OH-P5C), by PRODH and OH-PRODH, respectively. These two intermediates can be converted to glutamate and γ-hydroxy glutamate by a common enzyme, $\Delta^1$-pyrroline-5-carboxylate dehydrogenase. A research led by Adams and Goldstone showed that $\Delta^1$-pyrroline-5-carboxylate reductase can reduce either P5C or OH-P5C to proline or hydroxyproline, respectively (Phang et al., 2008). As for PRODH, also PRODH2 gene has been proposed to be a transcriptional target of p53 and to induce ROS dependent apoptosis (Cooper et al., 2008). Coordinated regulation may be envisaged, due to the existence of common sources for substrates of both enzymes. For this reason, we decided to investigate regulation of both genes by the p53 family.

In the following sections some of the proteins known or hypothesized to regulate PRODH expression are described, as the mechanisms of their regulation of PRODH expression will be the subject of this PhD thesis.

**1.6 The p53 family.**

The large part of the work described in this thesis is based on the identification and validation of the putative p53 response elements (REs) present in the *PRODH* and *PRODH2* genes, in order to deepen the knowledge about p53 control of their transcription and to investigate their possible transactivation by the other members of the p53 family.

The protein encoded by the tumor suppressor gene *p53* responds to various types of stress by activating and modulating different biological processes such as apoptosis, cell-cycle arrest, DNA repair, cellular differentiation and senescence (Vousden and Prives, 2009); p53 status is altered in over 50% of spontaneous tumors in humans (Greenblatt et al., 1994; Harris and Levine, 2005). In addition to mutations in sporadic tumours, germ-line mutations in p53 are found in the cancer prone Li-Fraumeni syndrome which predisposes carriers to a wide spectrum of early-onset cancers (Hainaut and Hollstein, 2000). Normally, p53 is expressed in a latent form and is maintained at low levels through ubiquitin mediated degradation. However, in response to DNA damage or other forms of cellular stress, p53 is activated to function as a transcription factor, resulting in a cascade of events that eventually prevents tumor development (Harris and Levine, 2005).

The p53 pathway responds to a wide variety of stress signals. These include: telomere shortening, hypoxia, mitotic spindle damage, heat or cold shock, unfolded proteins, improper ribosomal biogenesis, nutrient deprivation in transformed cell, etc. (Figure 5, step 1). These stress signals are detected by various sensors (Figure 5, step 2), the activities of which channel information to p53 through a plethora of protein modifications, to the p53 protein itself or to its negative regulator, MDM2. The latter is a direct p53 transcriptional target and functions as a ubiquitin ligase, capable of blocking p53 transcriptional activity directly and also by ubiquitination and targeting the p53 protein for proteasomal degradation. Thus the two proteins create a feedback loop, to keep p53 activity low in unstressed or cells or after the cellular response to damage has been carried out (Figure 5, step 3) (Levine, 1997). Stabilization of the p53 protein allows the activation of a plethora of target genes, by interaction with the specific p53 consensus sequence in the DNA (Figure 5, step 6).

p53 can also recruit cofactors such as histone acetyltransferases (HATs) and TATA-binding protein-associated factors (TAFs) to regulate gene expression (figure 5, step 7 and 8), after binding to DNA, p53 mediates transactivation of its target gene (fig 5, step 9), which are involved in various pathways such as DNA repair, cell-cycle arrest, apoptosis, and many others more recently discovered, like metabolism and angiogenesis. (figure 5, step 10). Evidence suggests that the type and extent of stress and by the cell type under stress, is

channeled onto the p53 protein by means of different post-translational modifications, thus leading to induction of a specific subset of target genes (Beckerman and Prives, 2010b).

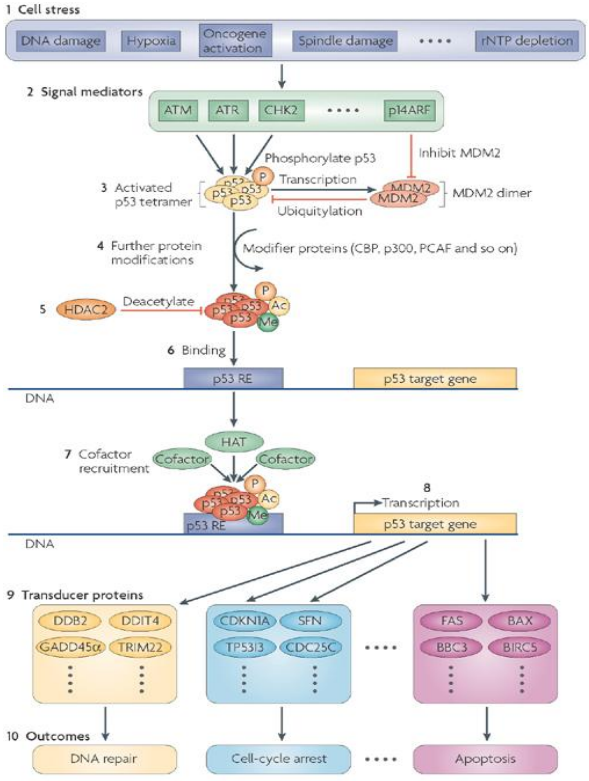


***Figure 5. Mechanisms of p53 activation and regulation of downstream targets.***
*Sequence of events leading to p53 stabilization and activation and the relative outcomes.*
*From Riley et al, 2008*

The p53 consensus site (or Response Element, RE) is composed by two half-sites RRRCWWGYYY -where W can be A or T, and R and Y stand for purine and pyrimidine bases, respectively- separated by a spacer of variable length (range 0–21 base pairs, although the most efficient REs show no spacer at all), (figure 6) (Riley et al., 2008).

Some p53 REs can have more than two contiguous half-sites, and are therefore referred to as cluster sites. Various experiments have shown that the level of binding affinity and subsequent transactivation increases linearly with the number of adjacent half-sites (Kern et al., 1991; Bourdon et al., 1997).

Finally, some genes contain multiple p53-binding sites in different locations within the gene and promoter region, and each p53 RE can contribute to the p53 response.

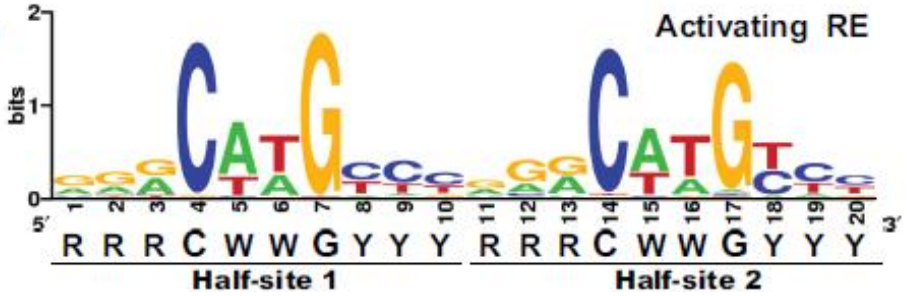


***Figure 6. p53 consensus sequence.***
*p53 RE motifs from 123 validated activating p53REs (A) and 39 validated repressing p53REs (B) drawn with WebLogo software.*

*From Wang 2009*

P53 is the founding member of a gene family, consisting of the tumor suppressor p53, and its more recently identified (although more ancient relatives) homologues p63 and p73. The high level of sequence similarity between p63, p73 and p53 proteins, particularly in the DNA binding domain, allows p63 and p73 to transactivate the same p53-responsive genes, causing cell cycle arrest and apoptosis. However, the function of the three family member is not functionally redundant and the primary role of each p53 family member – as determined by the analysis of knockout mice - illustrates that each protein has its own unique functions.

For example, p63-deficient mice are born alive but their limbs are absent or truncated owing to a malfunctioning of the apical ectodermal ridge (Mills et al., 1999; Yang et al., 1999). They fail to develop a stratified epidermis and most epithelial tissues (for example, hair follicles, teeth, prostate, lacrimal and salivary glands, and mammary glands), indicating its important role in stratified epithelia development.

The p73 knock-out mice have profound developmental defects including hippocampal dysgenesis, hydrocephalus, chronic infections and inflammation (Abraham and Meyer, 2003). They also exhibit abnormal reproductive and social behavior due to defects in pheromone detection, attributed to a dysfunctional nasal organ that normally expresses high levels of p73 (Johnson

et al., 2005). Until recently p73 was not considered a tumour suppressor gene, as p73 knock-out mice showed no increased susceptibility to spontaneous tumorigenesis (Yang et al., 2000; Stiewe and Pützer, 2002). By knocking out specific p73 isoforms, however, Tomasini et al showed that the TAp73 beta isoform does indeed possess tumour suppressive activity (Rosenbluth and Pietenpol, 2008; Tomasini et al., 2008).

Among the three typical outcomes deriving from activation of the p53 family members, namely apoptosis, senescence or cell-cycle arrest, the first two are terminal for the cell, whereas cell-cycle arrest allows for repair processes to take place and remove DNA damage, so that the cell survives. With time, however, research has expanded the roles of these transcription factors to new fields, i.e. metabolism, and they were found to be crucial for the general maintenance of cell health, both in physiological and pathological conditions. In fact, p53, but also p63 and p73, are at the center of a complex network within the cell, which maintains cellular homeostasis.

The proteins encoded by this gene family have considerable similarity in structure and domain organization; there is an N-terminal transactivation domain, a central DNA binding domain showing the highest level of conservation, and a C-terminal oligomerization domain (figure 7).


***Figure 7. Architectures of human TP53, TP73, and TP63 genes.***
*TP53, TP73, and TP63 genes encode the transactivation (TAD), DNA binding (DBD), and oligomerization (OD) domains. TP73 and TP63 contain additional SAM (Sterile Alpha Motif) domain in some of their isoforms. Percentage homology of residues between p53, p63, and p73 is shown.*

*From Wei 2012*

Despite structural similarity and the high level of conservation of the DNA binding domains of the p53 family members (Figure 7), significant differences in DNA binding ability and specificity have been reported. This implies that each member of the p53 family may have differential affinity for different DNA binding sites. For this reason, it is important to expand the analysis of the PRODH regulation to all members of this gene family.
The identification and characterization of the REs present in target genes of the p53 family will facilitate the unraveling of the complicated signaling networks of these transcription factors.

### 1.7 Hypoxia-inducible-factor (HIF-1).

Another important objective of this work was aimed at characterizing function and regulation of PRODH, was to investigate the relationship between proline dehydrogenase and the Hypoxia-inducible-factor (HIF-1).
The transcription factor hypoxia-inducible factor-1 (HIF-1) is a key regulator of genes responsible for adaptation and survival of cells and the whole organism to hypoxia (1% $O_2$, compared to 21% $O_2$ in normoxia) (Wang et al., 1995; Semenza, 1998). Since its identification, 2 decades ago, knowledge of HIF biology in normal and tumour cells has grown exponentially, because of the realization that hypoxia has a strong impact on cell biology and mammalian physiology and pathology (ischemia, stroke, cancer).
This transcription factor functions as a heterodimer composed of two subunits: HIF-1β, constitutively expressed, and HIF-1α, whose levels are tightly regulated at the post-translational level. Inhibition of HIF-1α during embryogenesis, leads to abnormalities in the development of blood vessels and heart, and abortion. Even the inactivation of HIF-2α causes the death of the embryo, although showing a phenotype less pronounced with regard to cardiovascular problems, indicating that the major isoform involved in the process of angiogenesis is HIF-1α (Kaur et al., 2005).
HIF-1 was discovered after the identification of its consensus sequence, the hypoxia response element (HRE; 5'-RCGTG-3') in the 3' enhancer of the erythropoietin (EPO) gene, encoding a hormone that stimulates erythrocyte proliferation and whose transcription is induced during hypoxia (Goldberg et al., 1988; Semenza et al., 1991). Subsequent studies identified the protein that

bound the HRE under hypoxic conditions as HIF-1, a heterodimeric complex consisting of a hypoxically inducible subunit HIF-1α and a constitutively expressed subunit HIF-1β (Wang et al., 1995). HIF-1β is also known as the aryl hydrocarbon nuclear translocator (ARNT), because it was originally identified as a binding partner of the aryl hydrocarbon receptor (Reyes et al., 1992).

When the oxygen tension in the cell decreases, HIF-1α is stabilized and translocated to the nucleus, where it dimerizes with the HIF-1β subunit, whose expression is constitutive and independent from intracellular oxygen concentrations. The active heterodimer form interacts with its coactivators and recognizes HREs (Hypoxia Responsive Elements) sequences present in the promoters of target genes to induce transcription (Brahimi-Horn and Pouysségur, 2006).

As I said, HIF-1α levels are subject to oxygen-dependent regulation, controlled by prolyl-hydroxylase (PHD), which are able to hydroxylate the ODD domain, in presence of α-KG, vitamin C and oxygen. The hydroxylation of two proline residues (P402 and P564) in normoxia, induces ubiquitination by the VHL E3 ubiquitin ligase and the rapid degradation of HIF-1α by the proteasome(Pugh et al., 1997). During hypoxia, absence of oxygen prevents PHD activity and HIF-1α accumulates leading to heterodimer formation and activation as a transcription factor.

The hypothesis that we wanted to test in this thesis is that PRODH may influence the degradation of HIF-1α in normoxia (figure 8, right). In fact, one of the products that is formed downstream of the metabolism of proline, of which PRODH is the key enzyme, is α-KG, substrate of the PHDs. The hypothesis is therefore that an increase of the levels of PRODH can lead to an accumulation of this molecule, stimulating an increased activity of PHDs and consequently causing a decrease in the levels of HIF-1α due to an increase in the degradation pathway. We chose as model glioblastoma cell lines, that show frequently HIF-1 deregulation. Glioblastoma is a highly vascularized, deadly tumour with very poor prognosis. Mutations in Isocitrate dehydrogenase (IDH) and succinate dehydrogenase (SDH), influencing the levels of α-KG or succinate (respectively substrate and product of PHD activity) have been shown to be selected for in this type of tumour and to influence neoangiogenesis (Parsons et al., 2008; Jones and Thompson, 2009). Of note, increasing the levels of α-KG in these cells by the use of a non degradable α-KG

derivative has been shown to induce tumour cell death (Tennant et al., 2009). If our hypothesis was confirmed, then PRODH would act as an oncosuppressor by inducing tumour apoptosis or by inhibiting the metabolic and neoangiogenic switches observed in tumors.

Therefore, understanding the mechanisms of PRODH regulation and how it is downregulated in tumours could open new possibilities to restore its expression, thus contributing to tumourigenic control.

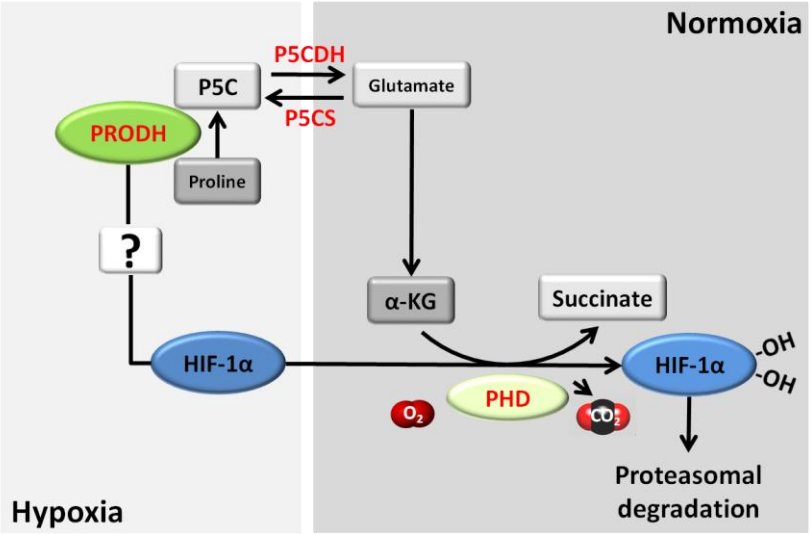


***Figure 8. Scheme depicting the hypothesized regulatory circuit between PRODH and HIF-1α:***
*At physiological $O_2$ concentrations, PRODH cooperates with PHD in keeping HIF-1 levels low, by providing the essential PHD substrate α-KG. At low $O_2$ concentrations or in situations of overexpressed HIF-1, such as those observed in some tumours, HIF-1 may in turn regulate PRODH.*

On the other hand, we hypothesized that in hypoxic conditions or in situations of HIF-1 overexpression (i.e. in tumours, not necessarily in presence of hypoxia) , HIF-1α could modulate PRODH levels (figure 8, left), in order to escape apoptosis or, alternatively, facilitate survival. Our hypothesis is supported on one side by a study showing that PRODH is among the transcripts downregulated by inducing brain ischemia in the rat (Schmidt-Kastner et al., 2002). On the other side, very recently PRODH was shown to be upregulated during nutrient and/or hypoxic stress in an AMPK-dependent but HIF-independent manner (Liu et al., 2012).

## 2. AIMS OF THE Ph.D. THESIS

This PhD work aims to expand knowledge about regulation of proline metabolism by two cancer-associated factors, p53 and HIF-1α, to understand the contribution of PRODH in metabolic processes, particularly during the tumourigenic process.

Our first goal was to fill in a gap in the literature, by identifying and validating the p53-REs in the *PRODH* and *PRODH2* genes. Both genes had previously been shown (more or less convincingly, as it will be discussed in this thesis) to be induced by p53; but the REs possibly responsible for this induction had not been identified nor validated. Moreover, we expanded the work to investigate the regulation of *PRODH* and *PRODH2* genes by the other members of the p53 family, p63 and p73.

During the final year of my PhD work, I worked at the hypothesis that there is a reciprocal control between HIF-1 and PRODH; in this circuit, PRODH stimulates PHD hydroxylating activity on prolines 402 and 564 of the HIF-1α subunit, tagging the protein for VHL dependent ubiquitylation and proteasome degradation. HIF-1, in turn, when physiologically (hypoxia) or pathologically (neoplasia) stabilized, would be responsible for down-regulating PRODH at the transcriptional or post-transcriptional level.

## 3. MATERIALS AND METHODS

### 3.1 Reagents.

Nutlin-3A was purchased from Alexis Biochemicals (Enzo Life Sciences, Exeter, UK). All oligonucleotides were from *Eurofins MWG Operon* (Ebersberg, Germany*).* Bacteriological reagents (Bactoagar, Yeast extract, Peptone) were from DIFCO (BD Biosciences, Milan, Italy). Doxorubicin, 5-fluorouracil (5FU) and cobalt chloride ($CoCl_2$) and all other reagents were from Sigma Aldrich (Milan, Italy) unless otherwise specified.

### 3.2 Cell lines and treatments.

The human breast adenocarcinoma-derived MCF7 cell line was obtained from the InterLab Cell Line Collection bank, ICLC (Genoa, Italy); the colon adenocarcinoma HCT116 (p53+/+) cell line and its p53−/− derivative were a gift from B. Vogelstein (The Johns Hopkins Kimmel Cancer Center, Baltimore, Maryland, USA) (Bunz et al., 1998). LoVo colon adenocarcinoma cells were a gift from M. Broggini (Istituto Farmacologico Mario Negri, Milan Italy) (Drewinko et al., 1976), the hepatocellular carcinoma derived HepG2 cells were a generous gift from A. Provenzani (Laboratory of Genomic Screening, CIBIO, University of Trento), neuroblastoma cell line SHSY-5Y was a generous gift from A. Quattrone (Laboratory of Translational Genomics, CIBIO, University of Trento) while the U87MG glioblastoma cell line was obtained from ATCC. Cells were maintained in McCoy's, DMEM or RPMI media supplemented with 10% FBS, 1% glutamine and antibiotics (100 units/ml penicillin plus 100 µg/ml streptomycin), as advised by the suppliers.
To study PRODH expression in response to p53 induction or stabilization, cells were seeded at 80% confluence and treated with genotoxic agents or Nutlin-3A at the indicated concentrations for 16 hours.
For transient transfection experiments, 7 x $10^5$ cells were seeded in 6-well plates 24 hours before transfection to reach ~70% confluency on transfection day. Cells were transfected using 2 µg plasmid DNA/well and the TransIT-LT1 transfection reagent (Mirus, Milan, Italy) according to the manufacturer's instructions. Human p53 was expressed from the pC53-SN3 plasmid (Kern et al., 1991), while p63beta, p73beta and PRODH cDNAs were expressed from pCDNA3.1 (Ciribilli et al., 2010).

All mammalian constructs were extracted from XL1blue *E. coli* cells using the endotoxin free PureYield plasmid midi-prep kit, according to the manufacturer's protocol (Promega, Milan, Italy). In all experiments, cells were harvested 24 hours after transfection, trypsinized and collected for RNA extraction.
For generation of stable clones, U87 cells were plated in 6-well plates the day before experiment to reach ~80% confluence at transfection, using pCDNA3_PRODH construct or empty vector as control, which was performed with FuGENE HD (Promega), according to the manufacturer's instructions. The day after transfection, cells were trypsinized and replated onto 100mm cell culture plates with G418-supplemented medium (400μg/ml). After two weeks, transfected clones were isolated using cloning rings, grown separately into 24 wells plates and processed as soon as possible to check for PRODH expression analysis.
For hypoxia treatment cells were incubated at 37°C in a humidified atmosphere with $pO_2$ of 21% for 24 hours and subsequently incubated in a hypoxic chamber (Modular Incubator Chamber and Flow Meter, Billups-Rothenberg,) for 24 hours. The mixture of gas present inside the chamber is composed of $N_2$ (94%), $CO_2$ (5%) and $O_2$ (1%), with a flow of 20 LPM (liters per minute).
Chemical hypoxia was obtained by treatment with cobalt chloride ($CoCl_2$). Cells were seeded and grown at standard conditions for 24 hours, then treated with $CoCl_2$ (100 μM) for 24 hours (Yuan et al., 2003).
To generate anoxic condition cell lines were packed for 24 hours into a plastic incubation bag containing an Anaerocult A mini sachet (Merck) according to the manufacturer's instructions.

**3.3 Analysis of PRODH and PRODH2 transcript levels.**

To quantify PRODH and PRODH2 mRNAs following treatments or transfections, cells were harvested and washed once with PBS. Total RNA was extracted using the RNeasy Kit (Qiagen, Milan, Italy) according to the manufacturer's instructions. For real-time quantitative PCR (qPCR), cDNA was generated from 2 μg of RNA by using the RevertAid First Strand cDNA Synthesis Kit (Fermentas, Milan, Italy) or the iScript Reverse Transcription Supermix for RT-qPCR (Biorad). qPCR was performed on a RotorGene 3000 thermal cycler (Corbett Life Science, Ancona, Italy) or on a StepOne thermal cycler (AB, Milan, Italy) using the KAPA Probe Fast

Universal 2X qPCR Master Mix (Resnova, Rome, Italy) with Taqman assays (AB, Milan, Italy) or the Sso Advanced Sybr Green Supermix (Biorad). Relative mRNA quantification was obtained using the ΔΔCt method, where the glyceraldehyde 3-phosphate dehydrogenase (*GAPDH*), hypoxanthine phosphorybosyl transferase (HPRT) or the β2-microglobulin (B2-M) genes served as internal control. *P21* was used as positive control for the efficacy of the induction of p53 family members by the specific treatment, while VEGF was used as positive control for HIf-1α stabilization after hypoxic treatments. All primers used are reported in Table 1.

**3.4 Construction of yeast reporter strains and media.**

Nine different *Saccharomyces cerevisiae* reporter strains were constructed, containing the firefly luciferase gene under the control of the p53 RE found by bioinformatics tools (see below) in the *PRODH* and *PRODH2* genes. To insert the putative p53 RE upstream of the luciferase reporter genes the "*delitto perfetto approach"* for *in vivo* mutagenesis was used (Storici et al., 2001), starting from the available master reporter strain yLFM-ICORE. The master strain contains the luciferase cDNA integrated in the yeast genome downstream a minimal promoter derived from the CYC1 gene. The counter selectable ICORE cassette is located 5' to the minimal promoter and confers high targeting efficiency of the locus by oligonucleotides that contain the desired RE sequences (Table 2) (Storici et al., 2001). The recombinant yeast strains were checked by colony PCR and direct sequencing for proper positioning of the inserted REs (BMR Genomics, Padua, Italy). Yeast cells were grown in YPDA medium (1% yeast extract, 2% peptone, 2% dextrose with the addition of 200 mg/L adenine). For plating, YPDA medium was supplemented with 2% bactoagar, while selective minimal plates lacking tryptophan or leucine but containing adenine (200 mg/L) and dextrose as carbon source were used to isolate transformant clones with expression vectors for p53 family proteins. 5-Fluoroorotic acid (FOA) and geneticin (G418) were added to the plates when necessary (Storici et al., 2001).

**3.5 Constructs for the expression of p53 family members in *S. cerevisiae.***

To express members of the p53 family in yeast, the pTSG- (TRP1) or pLSG-based (LEU2) constructs, harbouring respectively p73β and p63β cDNAs (TA isoforms)

under the control of the *GAL1,10* inducible promoter, were used (Inga et al., 1997; Jordan et al., 2008). This promoter allows to modulate the expression of the proteins under study by varying the galactose concentration in the culture medium. The wild type p53 cDNA was similarly expressed using the pLS89 expression vector (TRP1) (Inga et al., 1997). Empty vectors pRS-314 or pRS-315 were used as controls; these vectors contain respectively the TRP1 (as pTSG) or LEU2 (as pLSG-) yeast selectable markers.

**3.6 Luciferase assays in yeast.**

To measure the transactivating capacity of p53 family members on the putative p53 REs identified in *PRODH* and *PRODH2* genes, the expression vectors described above were transformed into the yLFM-RE strains using the lithium acetate method. After transformation the yeast strains were grown on minimal medium lacking tryptophan or leucine but containing adenine (200 mg/L) and dextrose as carbon source, to keep the expression of p53 family members inhibited. After 2-3 days at 30°C, transformants were streaked onto the same type of plates and grown for an additional day. For each reporter strain, the basal luciferase activity was measured from the empty vectors pRS314- or pRS315-transformed colonies. Transformant colonies were grown in 100 µL of selective medium containing raffinose as the sole carbon source in a transparent 96-well plate for 16-24 hours at 30°C. Different concentrations of galactose (0.008% and 1%) were added to induce low or high levels of expression of the p53 family members. OD600 was directly measured in the multi-well plate to normalize for cell density using a multilabel plate reader (Infinite M200-Pro, Tecan, Milan, Italy). Ten µL of cells suspension were transferred to a white 384 plate (BrandTech Scientific Inc., Essex, CT, USA) and mixed with an equal volume of PLB buffer 2X (Passive Lysis Buffer, Promega). After 15 minutes of shaking at room temperature, 10 µL of *Firefly* luciferase substrate (Bright Glo Luciferase Reporter Assay, Promega) were added. Luciferase activity was measured and results were expressed as fold of induction compared to empty vectors.

### 3.7 Chromatin immunoprecipitation experiments in HCT116 cell line.

Chromatin immunoprecipitation (ChIP) assays were performed as previously described (Menendez et al., 2006, 2009) using the EZ Magna ChIP kit (Upstate Biotechnology, Millipore, Lake Placid, NY, USA). Briefly, HCT116 p53+/+ and p53-/- cells were plated onto 150-mm dishes, let to grow for one day and treated with 1.5 μM doxorubicin for 16 h or left untreated. Cells were then cross-linked with 1% formaldehyde for 10 min at 37 °C and treated subsequently with 125 mM glycine for 5 min. Samples were processed following the manufacturer's instructions. Cell lysates were then sonicated using conditions that enabled us to evaluate the distinct contribution of the different REs. Sonication was done using a Misonix 4000 instrument equipped with a multiplate horn (Misonix, Qsonica LLC., Newtown, CT, USA). Samples were sonicated using twelve cycles of 20 seconds pulses at 80% of amplitude with a 40 seconds pause in-between and the accuracy of shared chromatin fragments was checked on a 2% agarose gel. The p53-specific monoclonal antibody DO- 1 (Santa Cruz Biotechnology, Milan, Italy) and magnetic Protein G beads were used in the ChIP assay. As a negative control we used mouse IgG (Santa Cruz Biotechnology). Once reverted the crosslinks, PCR amplifications were performed on immunoprecipitated and purified chromatin using primers to amplify specific regions in the PRODH promoter, introns and in the *CCNB1* gene, that does not contain any p53 REs (No Binding Site, NBS) (Table S1). Furthermore, qPCR was used to quantify the fold change in site occupancy. The qPCR reaction was performed with 2 μL of each sample and using the Power SYBR® Green PCR Master Mix (Applied Biosystems, Foster City, CA, USA) following manufacturer's procedures. To determine the fold change in site occupancy the SuperArray ChIP-qPCR Data Analysis tool was used (SA Biosciences, Frederick, MD, USA). The enrichment values were obtained after normalization against the input, then computing the ratio between the doxorubicin vs mock treatment.

### 3.8 Western blot analysis.

Cells for intracellular extracts were mechanically scraped from 100mm plates in PBS+5mM $Na_2$ EDTA, counted and resuspended in RIPA buffer supplemented with protease inhibitors (PMSF, benzamidine, aprotinin, and leupeptin), when cells

reached ~70% confluency. Quantification of total protein was performed with Bradford reagent before SDS–PAGE, using bovine serum albumin as a standard.
Eighty to 100 micrograms of intracellular lysate were loaded for PRODH detection. Proteins were transferred onto Immobilon-P transfer membrane (Millipore, USA) and protein of interest were identified using anti-PRODH mouse polyclonal antibody (Abnova, code ABIN519294), anti-HIF1α mouse monoclonal antibody (BD Bioscience, code 610958, clone 54/HIF-1α ) and anti-β-Actin rabbit polyclonal antibody (Santacruz, code sc-1616 ) as loading control.
Immunoblot analyses were performed using standard procedures and the immunorecognition was detected using the ECL Plus Western Blotting Detection System (GE Healthcare, USA). When appropriate, acquired images were quantified using the program ImageJ (NIH, free PC version).

**3.9 Intracellular staining for VEGF production.**

Three U87 stable clones transfected with either pcDNA3-PRODH and pcDNA3 vector as control were seeded in 6-well plates and grown for 24 hours, then cells were treated with Monensin for 2 hours where indicated (Golgi Stop, BD). After trypsinization, $3x10^5$ cells per FACS tube (BD) were treated with 250 μL of Cytofix/Cytoperm fixation and permeabilization solution (BD) and incubated for 15 minutes at 4°C, followed by 2 washes in PermWash solution (BD). 5 μL of PhycoErithryn-labelled anti-human VEGF antibody (R&D) was added in each tube, and incubated for 20 minutes at 4°C. After two washes in PermWash buffer, cells were resuspended in 500 μl of PBS per tube, and FACS analyses were performed with a FACSCanto II instrument (BD). Viable cells were gated based on physical parameters (SSC-FSC), followed by quantification of VEGF specific fluorescence.

**3.10 Statistics.**

All statistical analyses were made using Prism (GraphPad Software). Data are reported as mean +s.d. and statistical analyses were performed by using the Student's t-test. Results were considered statistically significant when a $P<0.05$ was obtained.

**3.11 Bioinformatics analysis.**

Sequences of the human PRODH and PRODH2 reference mRNAs (NM_016335.4 and NM_021232.1, respectively) were retrieved from NCBI (http://www.ncbi.nlm.nih.gov/nucleotide), and the genomic organization was obtained with the UCSC Blat algorithm at http://genome.ucsc.edu/ followed by extension of the promoter region retrieved, using the function "gene sorter" at UCSC.
To search for the p53 REs in the *PRODH* and *PRODH2* genes, the following sites were consulted:
-TESS (http://www.cbil.upenn.edu/tess.);
-p53MH algorithm (http://linkage.rockefeller.edu/ott/p53MH.htm.) (Hoh et al., 2002);
-p53 FamTaG ( http://p53famtag.ba.itb.cnr.it/index.php.) (Sbisà et al., 2007);
-TFBIND (http://tfbind.hgc.jp/) (Tsunoda and Takagi, 1999)

### 3.12 Table 1. Oligonucleotides used in this work.

| **NAME** | **SEQUENCE (**5' - 3' orientation) | **USE** |
|---|---|---|
| **ade2_Fw** | AAGTTGCCTAGTTTCATGAA | Yeast colony PCR & |
| **luc1_Rv** | CATAGCTTCTGCCAACCGAA | Sequencing after "delitto perfetto" |
| | | |
| **PIG6_prom-3.1_F** | TGCCCCATTATCACCCTAGCTTCT | qPCR after ChIP |
| **PIG6_prom-3.1_R** | TGCCCAACATGGAGGCTTTTCT | |
| **PIG6_prom-0.9_F** | ATACTCACCAGGCTCCACTATGGG | |
| **PIG6_prom-0.9_R** | CGGCCACAAGTTGTATGGTTCGTT | |
| **PIG6_int2+1.7_F** | CCACATCTAAGGGGCATCCCAAAA | |
| **PIG6_int2+1.7_R** | CACAAGGTGGGCATGGCTTCT | |
| **PIG6_int2+2.8_F** | TGGTTGCTTTGCTGTGGAGTCA | |
| **PIG6_int2+2.8_R** | AGACAGGGTTTCACGATGTTGCTC | |
| **PIG6_int2+4.7_F** | CTGTGGACTGTCATCTAGCTCA | |
| **PIG6_int2+4.7_R** | TGTTCCCTCTTATCCCAAGTCC | |
| **PIG6_int3+6.8_F** | AAGGGGAGGGAAAGGCAGTCA | |
| **PIG6_int3+6.8_R** | CAAAACAGCCAATCGCAAGGCA | |
| **CCNB1_FW (NBS)** | TATGCCACATCGAAGCATGCTAA | |
| **CCNB1_RV (NBS)** | ACAGATGGCACATGGTGCCAATT | |
| | | |
| **PRODH FW sybr** | CAGCCACATGGAGACATTCTTG | qPCR |
| **PRODH RV sybr** | AGCCGTCATCGCTGACTCTAC | |
| **P21 FW sybr** | CTGGAGACTCTCAGGGTCGAAA | |
| **P21 RV sybr** | GATTAGGGCTTCCTCTTGGAGAA | |
| **VEGFsybrFw** | CTTGCCTTGCTGCTCTACCT | |
| **VEGFsybrRv** | GCAGTAGCTGCGCTGATAGA | |
| **Beta-2MG FW sybr** | AGGCTATCCAGCGTACTCCA | |
| **Beta-2MG RV sybr** | ATGGATGAAACCCAGACACA | |
| **GAPDH FW sybr** | GAAGGTGAAGGTCGGAGTC | |
| **GAPDH RV sybr** | GAAGATGGTGATGGGATTTC | |
| **HPRT FW sybr** | AGACTTTGCTTTCCTTGGTCAGG | |
| **HPRT Rv sybr** | GTCTGGCTTATATCCAACACTTCG | |
| | | |
| **PRODH** | Hs00271933_m1 | AB Taqman assays |
| **PRODH2** | Hs00560403_m1 | |
| **Beta-2MG** | Hs00984230_m1 | |

### 3.13 Table 2. Oligonucleotides used for the creation of PRODH and PRODH2 yeast reporter strains by the "Delitto Perfetto" approach.

| Name | Sequence of the Response Element |
|---|---|
| **PRODH -3.1** | CGACTTGTCCTCAATGACCACGCTC (25)* |
| **PRODH -0.9** | CACCAGGCTCCACTATGGGCTTGTCTTCGTGTGACTTCTGT (41) |
| **PRODH +1.7** | GGGCAAGGACGGGCATGCTA (20) |
| **PRODH +2.8** | TTACAAGCCCTAGGCTCATGCCTAGGCATGGTGGCTCATGCCTGTAATTCT AGCAC (56) |
| **PRODH +4.7** | GTCCTTGTTGCCAGGGCATGCCT (23) |
| **PRODH +6.8** | AGGCTTGCCTCAGCATGTCG (20) |
| **PRODH2 -1.3** | TCCCAGCATGTTGGGAGGACAAGTAG (26) |
| **PRODH2 -0.5** | ACTCTAGCCTGGGCAACAAGAGT (23) |
| **PRODH2 -0.27** | GTACATGTTTCCTGCTGTCCATGTTT (26) |

** The number in brackets indicates the length of the Response Element in nucleotides. In the complete oligonucleotide used for "delitto perfetto" the sequence of each Response Element is surrounded at both sides by the sequences needed for homologous recombination in yeast; these sequences are:*

***5' CORE** GCGGAATTGACTTTTTCTTGAATAATACAT (30)*

***3' CORE** GCAGATCCGCCAGGCGTGTATATAGCGTGG (30)*

*the total length of each oligonucleotide is the sum of 5'core+PRODH RE+3' core.*

# 4.RESULTS

## 4.1 PRODH regulation by p53 family members.

During the first two years of my PhD project I worked at verifying and improving knowledge about the regulation of the *PRODH* gene by p53 and at expanding the analyses to the other members of this important family of transcription factors, namely p63 and p73. It has long been known that *PRODH* is a p53 inducible gene (Polyak et al., 1997) but a systematic search and validation of the p53 REs in this gene has never been carried out. The work presented in this section of the Results has been used for a manuscript that is under revision for publication in PLoS ONE and that is attached at the end of this PhD thesis.

## 4.2 PRODH levels increase upon genotoxic stress or p53 stabilization.

To confirm previous data reporting that PRODH is inducible by genotoxic stress via p53, we treated several cancer cell lines of different histological origin (HCT116 $p53^{+/+}$, HCT116 $p53^{-/-}$, and LoVo: colon; MCF7: breast; HepG2: liver) with doxorubicin or 5-fluorouracil, two genotoxic agents known to induce p53. Variations in PRODH or control transcripts were measured by Reverse transcription followed by quantitative real time PCR (RT-qPCR). All cell lines tested showed an increase in PRODH transcript levels after the treatments, compared to untreated controls, particularly evident in the HepG2 and LoVo cell lines. The induction observed was, in most cases, comparable (or even higher in HepG2 and LoVo) to that obtained for p21, one of the best characterized and efficiently transactivated target of p53, confirming that the *PRODH* gene is a strong p53 target. The only exception was the colon cancer cell line HCT116 $p53^{-/-}$, derived from HCT116 $p53^{+/+}$ by *p53* gene knock-out. In this case, we did not observe any PRODH induction upon genotoxic damage, confirming that the induction observed in the other cell lines was indeed p53 dependent (Figure 9).

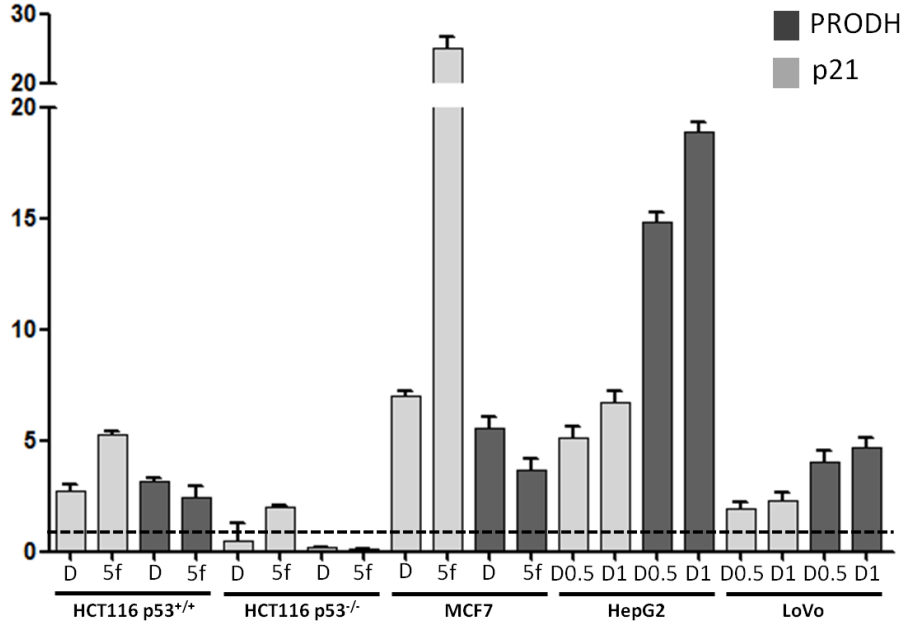


***Figure 9 Genotoxic stress induces a p53-dependent increase of PRODH transcript levels.*** *HCT116 p53+/+, HCT116 p53-/-, MCF7, HepG2 and LoVo cell lines were treated with the genotoxic compounds Doxorubicin (D, 0.5, 1 or where not indicated,1.5 µM) or with 5-Fluorouracil (5f, 375 µM) for 16 hours before proceeding to total RNA extraction, cDNA preparation and real time q-PCR. The established p53 target gene p21 is shown for comparison (lighter bars). Bars indicate the average folds of induction obtained in treated versus untreated cell samples, plotted together with the standard deviation of three biological replicates. The values obtained in untreated cell lines were set to 1 and shown in the figure as a horizontal broken line.*

We also tested transactivation of the *PRODH* gene after treatment with Nutlin-3A. This drug can stabilize p53 by disrupting its interaction with the negative regulator MDM2, therefore in absence of genotoxic stress. To do this, we again measured PRODH transcript levels after treatment of the p53 competent cell line, HCT116 $p53^{+/+}$ with two doses of the drug. A dose dependent increase in PRODH transcript was observed; more specifically, a 3,8 and 6,1 fold induction (over the value obtained in untreated cells, arbitrarily set to 1) in PRODH mRNA was observed at 5 or 10 mM Nutlin, respectively. As a positive control, p21 transcript levels were also measured in the same conditions (Figure 10).

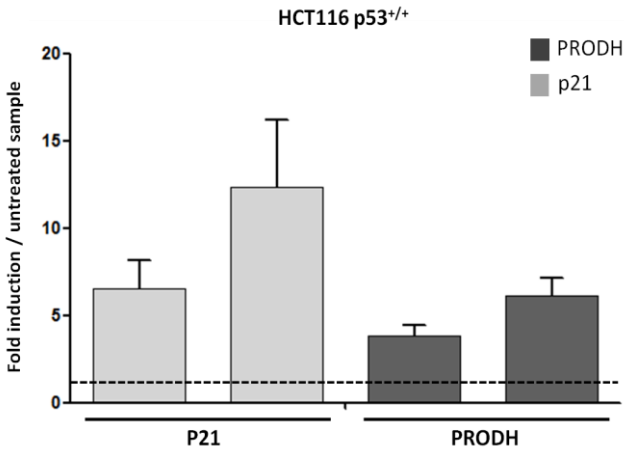


***Figure 10. p53 stabilization result in a p53-dependent increase of PRODH transcript levels.*** *HCT116 p53+/+ cell line was treated with the the p53 stabilizer Nutlin-3A (Nutlin, 5 or 10 μM) for 16 hours before proceeding to total RNA extraction, cDNA preparation and real time q-PCR. The established p53 target gene p21 is shown for comparison (lighter bars). Bars indicate the average folds of induction obtained in treated versus untreated cell samples, plotted together with the standard deviation of three biological replicates. The values obtained in untreated cell lines were set to 1 and shown in the figure as a horizontal broken line.*

### 4.3 p63 and p73 can transactivate PRODH in mammalian cells.

We decided to test the ability of the other transcription factors of the p53 family, p63 and p73, to transactivate PRODH. We chose the beta isoforms of both transactivators, because they are known to possess the highest transactivating activity among all isoforms (Ueda et al., 2001; Ghioni et al., 2002). The p53 null colon cancer cell line HCT116 $p53^{-/-}$ was transiently transfected with constructs expressing the three transcription factors belonging to the family or with the corresponding empty vector as a negative control. Subsequently, we measured the levels of PRODH mRNA by RT q-PCR. The results showed that also p63 and p73 are able to induce the proline dehydrogenase transcription, although less efficiently than p53. Indeed, a three- and almost four-fold induction was observed with p63 and p73, respectively, compared to the 7 fold induction obtained with p53 (figure 11). We therefore demostrated that PRODH is a target for all members of this family of transcription factors.

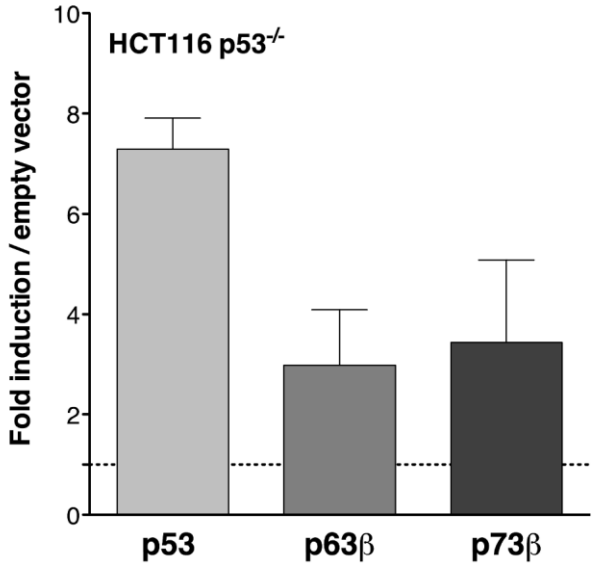


***Figure 11. Ectopic expression of p53 family members p53, p63β, p73β induces PRODH expression in mammalian cells.*** *Expression constructs for p53, p63β, p73β were transfected in HCT116p53$^{-/-}$ cells and the PRODH transcript induction was assayed by RT-qPCR and compared to the empty vector, used as reference and indicated by the broken line. All the experiments shown derive from three biological replicates.*

### 4.4 The *PRODH* gene contains numerous putative p53 REs

After confirming PRODH responsivity to p53 and demonstrating that it is transactivated also by the other family members, we analyzed the nucleotide sequence of the gene to search and map p53 response elements (REs) responsible for direct transactivation, as this piece of information is still lacking in the literature. As I said before, there is only one report on a p53 RE present in the promoter, about 1100 bp upstream of the transcriptional start site (TSS) (Maxwell and Kochevar, 2008).

As first steps toward the *in silico* identification of p53 consensus sequences, we retrieved the whole genomic sequence from Genbank, encompassing 3 kb of sequence upstream of the predicted transcriptional start site; then we built the exon-intron organization by using the UCSC-Blat algorithm and the PRODH mRNA reference sequence NM_016335.4, to generate a "gene map".
The search for p53 REs in the whole genomic sequence was performed using a combination of four bioinformatic tools for identifying p53 specific binding sites (p53MH, p53FamTag) or transcription factors consensus sequences in general (Tess, TFBIND). This was accompanied by a manual search as well.
By combining all bioinformatic predictions results, we isolated nine putative p53 REs that have been named according to their distance from the

Transcription Start Site (TSS) based on reference sequence NM_016335.4 (Table 3).

Three of them were excluded from further analysis because they did not respond to one or more of the criteria taken into consideration for functional REs, based on data collected by several groups and summarized in recent reviews (Jordan et al., 2008; Riley et al., 2008; Beckerman and Prives, 2010), such as distance from the transcription start site (TSS) (> 10 kb) (+14.3 and +15.8 REs), the presence of a long spacer (> 7 bp) between the two half sites of the consensus (+6.4 RE) or mismatches in the CWWG core sequence (none of the PRODH REs were affected).

Table 3. p53 Response elements in the PRODH gene

| | Name | Location (bp from TSS) | Mismatches HS 1 | Mismatches HS 2 | Spacer (bp) | Sequence |
|---|---|---|---|---|---|---|
| 1 | **-3.1** | Promoter -3,158 | 1 | 2 | 5 | **cGACTTGTCC***TCAAT***GAcCAcG CTC** |
| 2 | **-0.9** | Promoter -917 | - | 1 in ¼ site, 3 in a HS | 7, 5 | CACC**AGgCT***CCACTAT***GGGCTT GTCT***TCGTG***tGACTTcTgT*** |
| 3 | **+1.7** | Intron 2 +1,694 | 2 | 1 | - | **GGGCAAGgaCGGGCATGCTa** |
| 4 | **+2.8** | Intron 2 +2,816 | 2, 2, 2, 2, 3 in each of the five half sites | | 3, 0, 0, 3 bp respecti vely | **ttACAAGCCC***TAGG***ctCATGCCT AGGCATGgTgGctCATGCCT***GT A***AttCTAGCaC°** |
| 5 | **+4.7** | Intron 2 +4,727 | 3 | - | 3 | **GtcCTTGTTg***CCA***GGGCATGCCT** |
| 6 | +6.4 | Intron 3 +6,453 | 1 | 2 | 8 | **GGtCTTGCTC***TGTTGCCC***AGGC TAGagT** |
| 7 | **+6.8** | Intron 3 +6,817 | - | 2 | - | **AGGCTTGCCTcAGCATGTCg** |
| 8 | +14.3 | Intron 8 +14,269 | 2 | 1 | 2 | **AGcCATGgTT***CC***AGcCAAGCCC** |
| 9 | +15.8 | Intron 9 +15,832 | - in ¼ site | 1 | 5 | **TGTTT***GTTAG***AAGCATGTCa** |

** same RE described in (Maxwell and Kochevar, 2008).*
*° Cluster formed by 5 half-sites: the 3 central half-sites contain a CATG core and are separated by 0 bp spacer, while the two external half sites are separated by the central 3 by 3 bp spacers. All of the 5 half-sites contain at least 2 mismatches each, although they never involve the core of the consensus.*
*Bold name: REs selected for experimental validation.*
*Bold/underlined: bases belonging to the indicated RE; italic: spacers; minuscule: mismatches within RE*

By positioning the selected REs on the "gene map" (figure 12A) it was possible to observe that only 2 of the REs are located in the promoter region of the *PRODH* gene, at positions -3.1 and -0.9 kb from the TSS. The latter has already been described (Maxwell and Kochevar, 2008) and was investigated, although it did not completely fulfil the chosen parameters. The discrepancy in the numbering between Maxwell paper and our work is attributable to the newer

reference sequence we used. The other REs were located in intron 2 (+1.7, +2.8 and +4.7 kb) and 3 (+6.8 kb), respectively. The latter RE, +6.8, falls within a genomic region previously identified in a ChIP (chromatin immunoprecipitation)-sequencing experiment but not further characterized (Wei et al., 2006). In that paper, the RE was reported in intron 1, although it is in intron 3 according to a more recent genomic assembly and the PRODH mRNA version NM_016335.4 used in the present work.

The two REs in the promoter contained only one half-site with either one (-3.1) or no (-0.9) mismatches (Figure 2A). An additional half-site with two mismatches, one of which involving a base in the CWWG core sequence, was present in the -3.1 RE, separated from the first half-site by a 5 bp spacer; in the -0.9 RE, a quarter site with one mismatch and a half-site with three mismatches (that can alternatively be considered a quarter site with one mismatch) were presented, separated by the first half-site by 7 and 5 nucleotide spacers, respectively. Among the intronic REs, two of them (+1.7 and +6.8) had no spacers, while the +4.7 had a 3 bp spacer; the +4.7 and +6.8 REs had a consensus half-site and a second half-site with two mismatches outside the CWWG core motif, while the +1.7 had mismatches (one or two) in each half-site (Figure 2A). The +2.8 RE was identified as a full site composed of two half-sites (GctCATGCCT-AGGCATGgTg) by the TFbind software. Upon careful analysis of the nearby sequence, this RE turned out to be surrounded by other half-sites, thus constituting a cluster with a total of 5 half-sites, of which the 3 central contained a CATG core and were devoid of any spacers, while the two external half-sites were separated from the central 3 REs by 3 bp spacers (Figure 2A). All of the 5 half-sites in the +2.8 RE contained at least 2 mismatches each, none involving the CWWG core motif of the consensus. Interestingly, the +6.8 was the only RE identified by the p53SCAN algorithm in the genomic region encompassing the *PRODH* gene (Menendez et al., 2009).

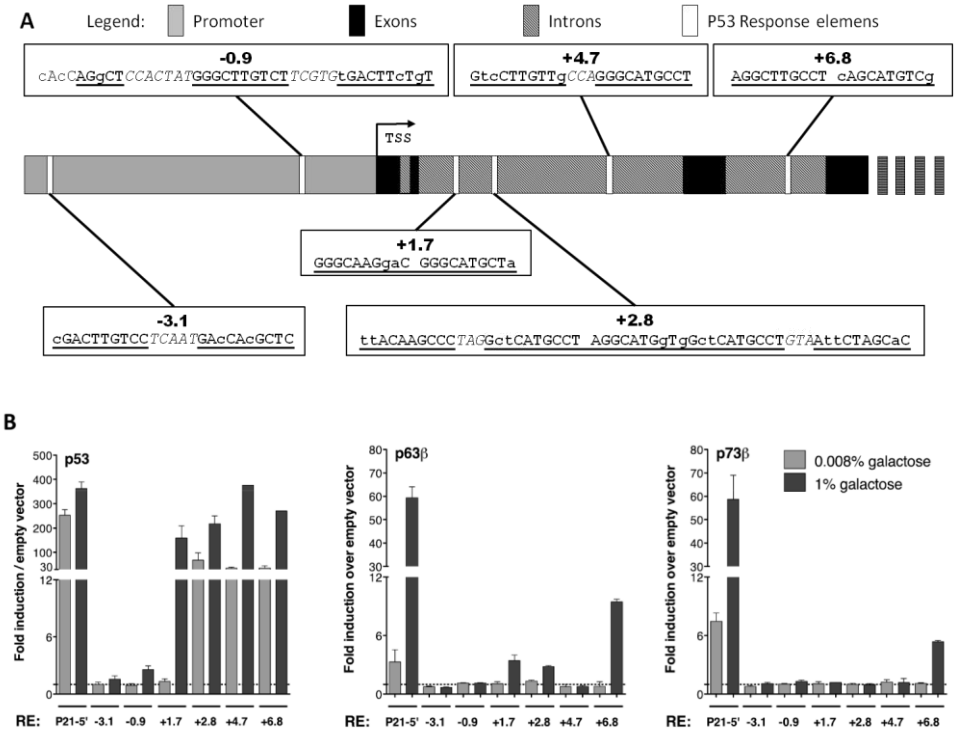


***Figure 12. The PRODH gene contains several putative p53 REs, some of which are differentially transactivated by p53 family members in yeast. A.*** *Scheme depicting genomic location and sequence of the six p53 REs in the PRODH gene that were selected for further analyses. The first 4 exons are indicated as black boxes and numbered. The sequence of the REs at the various indicated locations is shown (lowercase = mismatches from consensus; italics = spacer between half-sites)* ***B.*** *The REs in the PRODH gene were assayed with different p53 family members p53, p63β and p73β at different levels of galactose induction (0.008%, lighter bars and 1%, darker bars) in the yeast transactivation assay. As a positive control, the yeast strain carrying one of the p53 REs present in P21 gene (P21-5') was included. Bars represent the fold of induction on each RE by the specified p53 family expression construct over the values obtained with the relative empty vector (negative control) (set to 1 and indicated by a broken line across each graph) used as negative control.*

## 4.5 The p53 family members differentially transactivate from the PRODH REs in yeast .

Validation of the 6 selected consensus sequences was performed by using a transactivation assay in yeast. The first step was to create reporter strains in the yeast Saccharomyces cerevisiae, by integrating the PRODH REs in the yeast genome, upstream of a reporter gene. To do this we chose to exploit a well-known procedure called "Delitto perfetto approach", that takes advantage of the yeast ability to efficiently perform homologous recombination (Storici et

al., 2001; Storici and Resnick, 2003). Briefly, using a previously engineered yeast strain (*yLFM-ICORE*), we inserted oligonucleotides carrying the sequence of the single REs of interest at a specific site upstream of the luciferase reporter gene. With this method the RE+reporter are integrated into a yeast chromosome, maintaining its chromatin organization and thus reproducing what occurs physiologically during eukaryotic gene expression. Transformation of the strains obtained with constructs expressing the p53 protein family members under control of a galactose inducible promoter allowed us to determine the responsivity of each RE at different levels of transcription factors expression.

As shown in Figure 12B, The four intronic REs (+1.7, +2.8, +4.7 and +6.8) were induced by p53 in a dose dependent manner and showed strong response at the higher level of induction (1% galactose). At moderate induction (0.008% galactose), the +2.8, +4.7 and +6.8 already showed at least a 35-fold increase above background in luciferase activity. In all cases, a yeast strain carrying the P21-5' RE was used as a positive control. Overall, the levels of p53-dependent induction of the intronic REs by p53 were comparable to those obtained with the positive control strain, bearing the p21-5' RE, which has been previously shown to be strongly induced by the p53 family members in yeast (Inga et al., 2002). The REs in the promoter (-3.1 and -0.9) instead, showed no (-3.1) or extremely weak (-0.9: 2.5-fold) induction over the basal level even at 1% galactose, suggesting lack of responsiveness to p53 (Figure 12B).
Also the other p53 family members could weakly transactivate luciferase reporter expression from some REs, at 1% galactose. More specifically, the +1.7, +2.8 were very weakly transactivated upon p63β but not p73β expression, while the + 6.8 RE was transactivated following p63β or p73β expression (5 to 10-fold) (Figure 12B). At low galactose induction of p63β and p73β, no detectable increase in luciferase activity was observed in any of the PRODH REs.

### 4.6 P53 binding capacity *in vivo* in mammalian cells.

To study p53 binding to the PRODH gene *in vivo*, HCT116 $p53^{+/+}$ cell line and its p53 knock-out derivative (HCT116 $p53^{-/-}$) were treated with DOXO or left untreated (mock) and cell extracts were subject to Chromatin ImmunoPrecipitation (ChIP) and amplification of the DNA fragments containing each RE.

The data confirmed that the +6.8 RE is the most efficiently bound by p53 in HCT116 $p53^{+/+}$ under the conditions tested, showing almost a 4-fold enrichment in binding by p53 after genotoxic treatment over the untreated sample, followed by +2.8 (3-fold enrichment), +1.7 (2-fold enrichment) and finally -3.1 RE. The -0.9 and +4.7 REs showed very low enrichment (Figure 13). For comparison, enrichment of p53 binding in DOXO treated over untreated cells is shown for a genomic region not containing a p53 RE (*CCNB1*) (indicated as Non Binding Site, NBS, in figure 13), used as negative control and for a region of the p21 promoter surrounding the well established P21-5' RE, used as positive control.

The +6.8 RE showed the highest p53 binding *in vivo* (Figure 13). Interestingly, this RE is the one most efficiently transactivated by all p53 family members in yeast assays (Figure 12B).

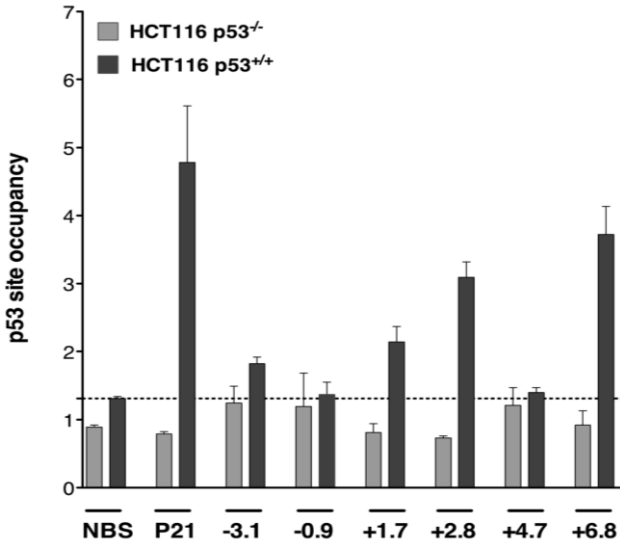


***Figure 13. Relative p53 occupancy levels at PRODH sites containing p53 REs.*** *ChIP experiments were performed in the HCT116 p53+/+ cell line and its isogenic derivative HCT116 p53-/- (negative control), treated with DOXO or left untreated. Binding of p53 to the different REs was analysed by qPCR. The broken line indicates the level of p53 bound to the No Binding Site (NBS) after DOXO treatment of HCT116 p53+/+ cells, used as a negative control. The enrichment for the P21 promoter 22 region, containing the P21-5' RE, of DOXO treated over untreated cells is reported as a positive control.*
*The data are representative of two independent experiments.*

### 4.7 PRODH2 regulation by p53.

It was previously demonstrated that, like PRODH, PRODH2 is induced by genotoxic stress and by p53 (Cooper et al., 2008). We therefore decided to confirm these pieces of evidence in mammalian cells, on one side, while searching for p53 REs in the *PRODH2* gene.

To this aim, we treated the same cell lines known to harbour wild type p53 with Doxorubicin or 5-Fluorouracil that I described for induction of PRODH. Consistent with the literature, these genotoxic treatments resulted in a slight increase of PRODH2 transcript in LoVo cells, but we were unable to calculate the fold induction as basal levels fell below the detection limits of our qPCR (Figure 14A). In HCT116 $p53^{+/+}$ and MCF7 cell lines, basal levels were undetectable and no induction was observed (Figure 14A). Finally, when the HepG2 hepatocarcinoma cell line, which turned out to have detectable basal levels, was treated with DOXO, no induction of the PRODH2 gene was observed (Figure 14B). Concomitantly, a slight repression was detected, in spite of efficient induction of the p21 transcript, used as a positive control. These findings led us to assume that *PRODH2* is a gene with a limited responsiveness to p53.

**A**

| CELL LINE | BASAL EXPRESSION | INDUCIBILITY BY DOXORUBICIN |
|---|---|---|
| HCT116 | no | no |
| MCF7 | no | no |
| LoVo | no | yes |
| HepG2 | yes | no |

**B**

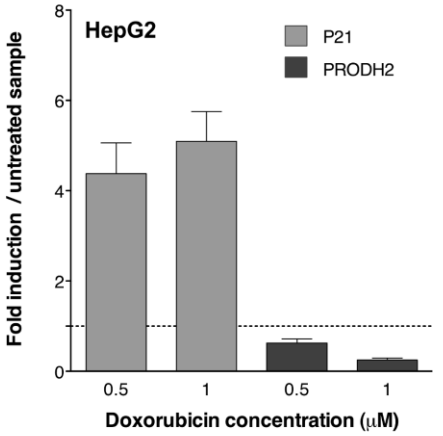


***Figure 14. p53 weakly induces PRODH2 expression in some cell lines. A.*** *The ability of DOXO to induce expression of the PRODH2 gene was analysed in four cell lines harbouring endogenous wildtype p53, namely HCT116 (p53+/+), MCF7, LoVo and HepG2.* ***B.*** *Levels of PRODH2 (darker bars) and p21 (lighter bars, positive control) transcripts in HepG2 cells treated with DOXO were determined by RT-qPCR. The value obtained in the untreated cell line was normalized to 1 (broken line). All the experiments were performed in triplicate.*

To verify if the low responsiveness is attributable to the presence of poor quality p53 REs in the *PRODH2* gene, we followed the same procedure and used the same algorithms applied for searching p53 REs in the *PRODH* gene. Five putative p53 consensus sequences were identified in the *PRODH2* gene, three of which were in the promoter, while two were located in intron 9 at more than 10 kb from the TSS (first nucleotide present in the NM_021232.1 reference PRODH2 mRNA) (Table 4). The latter two REs consisted of just one half-site (Table 3); for this reason, and for the distance from the TSS, they were excluded from further analysis. Of the three REs identified in the promoter (Table 3 and Figure15A), two had a 3 bp spacer and at least four mismatches in the two half-sites, not involving the core sequence (-1.3 and -0.5), and the third (-0.27) had a 6 bp spacer and one or two mismatches in the two half-sites (Table 4 and figure 15A).

Table 4. p53 Response elements in the *PRODH2* gene

| | Name | Location (bp from TSS) | Mismatches HS 1 | Mismatches HS 2 | Spacer (bp) | Sequence |
|---|---|---|---|---|---|---|
| 1 | **-1.3** | Promoter -1,281 | 2 | 2 | 3 | **cAGCATGTTg***GGA***GGACAAGTag** |
| 2 | **-0.5** | Promoter -0,534 | 2 | 3 | 3 | **ActCTAGCCT***GGG***cAACAAGagT** |
| 3 | **-0.27** | Promoter, -0,267 | 1 | 2 | 6 | **GtACATGTTT***CCTGCT***GtcCATGTTT** |
| 4 | +10.5 | Intron 9 +10,519 | 2 | NA | NA | **cAGCAAGaCC** |
| 5 | +10.7 | Intron 9 +10,685 | - | NA | NA | **AAGCAAGTCC** |

*Bold: REs selected for experimental validation.*
*Bold/underlined: bases that are part of the indicated RE; italic: spacers; minuscule: mismatches within RE*

Yeast strains carrying the -1.3, -0.5 and -0.27 REs upstream of the chromosomally located luciferase reporter, and otherwise isogenic with the previously described PRODH RE strains, were constructed. Again, an isogenic strain carrying the P21-5' RE was used as positive control. Activity of the

reporter was only slightly increased by high-level p53 expression in the three PRODH2 strains, with -0.27 being the most efficiently transactivated (9-fold induction) (Figure 15B). A 4-fold increase in luciferase activity over the empty vectors, used as negative control, was obtained with the -1.3 RE but only a 2-fold with the -0.5 RE. Expression of p63β and p73β did not result in any detectable induction of luciferase activity (Figure 15B). Taken together, and compared with the induction levels obtained with PRODH, PRODH2 should be considered as a weak p53 target with low expression levels and limited responsiveness in human cells.

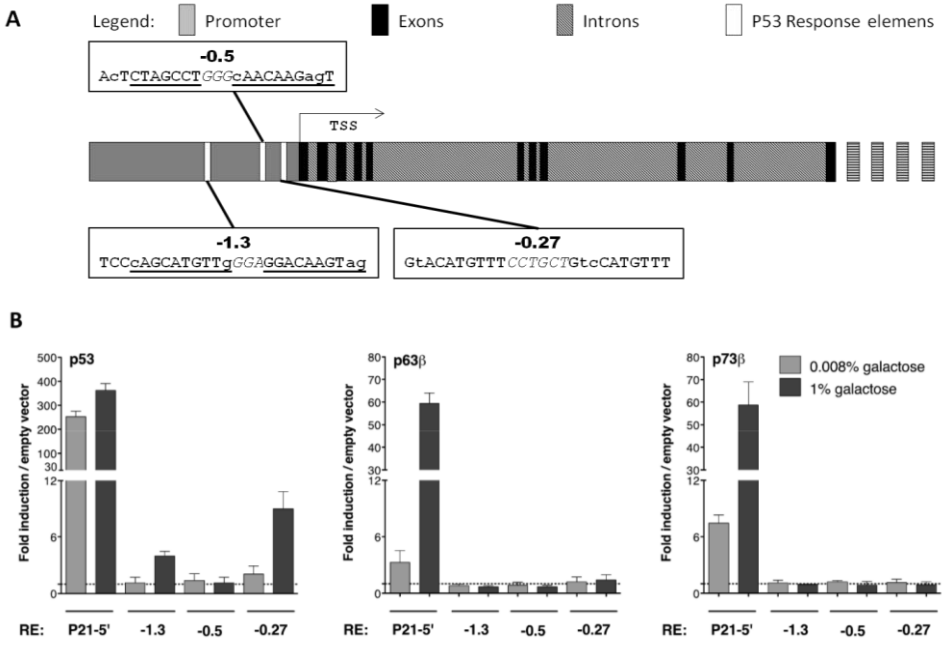


***Figure 15. The PRODH2 gene contains three putative p53 REs, two of which are poorly transactivated only by p53 in yeast. A.*** *Scheme depicting chromosomal location and sequence of the p53 REs in the PRODH2 gene, selected for analysis in the yeast transactivation assay.* ***B.*** *The REs in the PRODH2 gene were assayed with different p53 family members p53, p63ϐ and p73ϐ at different levels of galactose induction (0.008%, lighter bars and 1%, darker bars) in the yeast transactivation assay. As a positive control, the yeast strain carrying the P21-5' RE was included. Bars represent the fold of induction of each RE by the specified p53 family expression construct over the values obtained with the relative empty vector (negative control) (set to 1 and indicated by a broken line across each graph). All the experiments shown derive from at least three biological replicates.*

In conclusion, in the first two years of my PhD, I demonstrated that all members of the p53 family can induce the transcription of PRODH and we obtained a detailed map of the p53 response elements in the *PRODH* gene. This will allow us to continue our studies on the regulation of this enzyme, for

example, looking for polymorphisms possibly affecting binding of the p53 family members to the response elements. In addition, with the yeast strains we constructed, we can carry out a screening of several missense mutants of p53 to assess their effects on the metabolism of proline and in cellular metabolism in general. More generally, we have enriched the information emerging in recent study on the interconnection between the p53 family and the control of metabolism, a topic that we plan to investigate in more detail in our laboratory, studying the network of transcriptional and post-transcriptional regulations between the p53 family and the important sensor of cellular homeostasis, mTOR, that integrates the various internal and external signals to promote growth and cell proliferation on one side, and p53, mTOR and the hypoxia inducible factor HIF-1, on the other.

**4.8 The HIF 1α-PRODH regulatory circuit.**

The second aim of this PhD project was to investigate the existence of a reciprocal regulatory circuit between the hypoxia inducible factor HIF-1 and PRODH. On one hand, this would increase the knowledge of the mechanisms by which PRODH could suppress tumorigenesis, other then the well known induction of apoptosis. On the other hand it would improve the knowledge on PRODH regulation by adding to the list of its regulators another important transcription factor often deregulated in tumours. As we described in the introduction section and in the aims of the work, this mutual control would occur in different conditions, e.g. PRODH would contribute to PHD activity by providing α-KG, ultimately leading to increased HIF-1α degradation during normoxia, and this may have a positive impact in those tumours over-expressing HIF-1α in absence of hypoxic stress. HIF-1α could in turn control PRODH expression when either induced by hypoxia or over-expressed, a phenomenon often occurring in tumours.

### 4.9 PRODH overexpression results in a decrease of HIF-1α levels in the U87 cell line.

As it was shown in Figure 3, the enzymatic reaction of PRODH can trigger a cascade of events that results in an increased level of α-KG, substrate that prolyl-hydroxylase (PHD) utilizes, together with molecular $O_2$, to hydroxylate its target protein HIF1-α, a modification that is followed by ubiquitination by pVHL and degradation by the proteasome complex (Tennant et al., 2009).
To confirm that an increase in PRODH protein levels can affect HIF-1α stability, we stably transfected a construct expressing PRODH in the U87 glioblastoma cell line. We considered this a suitable cell line for this type of analysis, since it has low endogenous levels of PRODH and high levels of HIF-1α, allowing us to evaluate the effects of overexpression of the first on the decrease of the second.
Five out of 6 stable clones overexpressing PRODH showed a corresponding decrease in the levels of HIF-α, compared to clones stably transfected with empty vector (used as controls), thus indicating that our hypothesis is correct (Figure 16). The remaining clone, among those ectopically expressing PRODH, showed no significant changes in the levels of HIF-1α (lane 3, fig 16), but this may be attributable to specific characteristics of that clone.

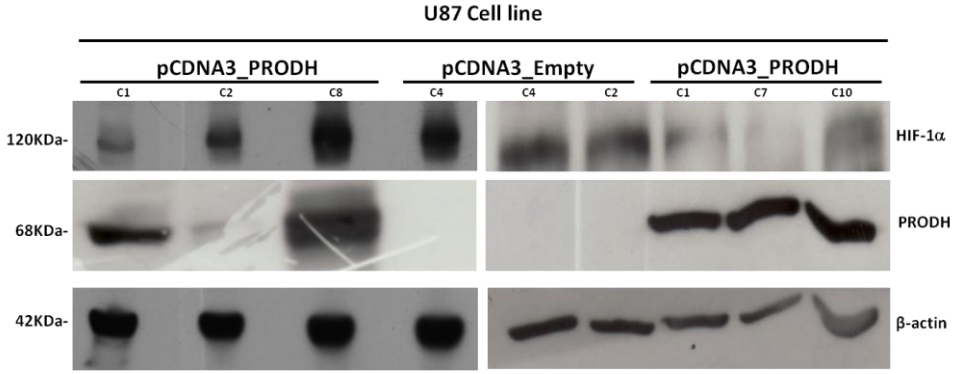


***Figure 16. PRODH expressing, stably transfected clones show decreased levels of HIF-1α compared to control clones.*** *Western blot analysis of PRODH and HIF-1α protein levels in U87 clones stably tranfected with either a construct overexpressing PRODH (pcDNA3_PRODH, lanes 1, 2, 3, 7, 8 and 9) or empty vector as control (pcDNA3, lanes 4, 5 and 6). Detection was performed using antibodies specific for PRODH, HIF-1α and to β-actin for loading normalization (see Materials and methods).*

To overcome the variability among clones, we decided to perform the same experiment using protein extracts from pools of stable clones, either transfected with PRODH expression constructs or empty vector as control. Moreover, we performed the same analyses on transiently transfected U87 cells, using the same constructs as above. These approaches should allow us to observe a general trend, obtained in most of the cells by PRODH overexpression. With both approaches we were able to observe a decrease in HIF-1α protein levels of about 50% when PRODH was overexpressed, compared to control clones (Figure 17, A and B).

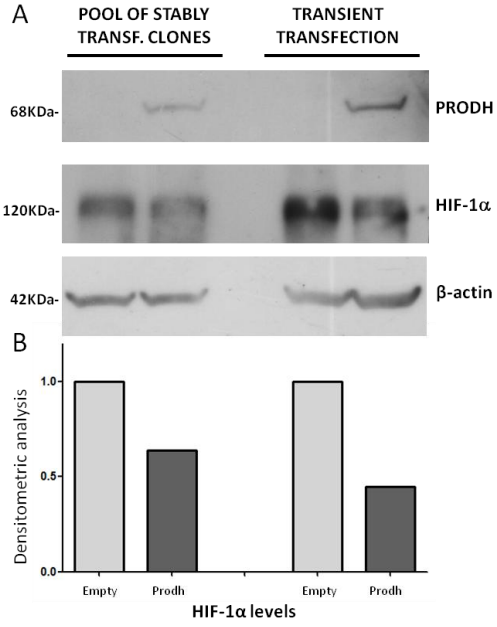


***Figure 17. HIF-1α protein levels are reduced by PRODH overexpression.***

***A****. Western blot analysis of PRODH and HIF-1α protein levels, on extracts from cellular pools obtained after stable transfection (left side) or following transient transfections (right side) of PRODH encoding plasmid or empty vector. 80 ug of protein extract, prepared seeding and harvesting cells as described in materials and methods, were used for SDS PAGE and immunoblotting.*
*Analysis was performed using a specific antibodies for PRODH, HIF-1α and β-actin to normalize loading.*
***B.*** *Densitometric analysis of protein levels with the free on line software Image-J. Bars represent the fold of reduction of HIF-1α by overexpression of PRODH compared to the values obtained with the relative empty vector, arbitrarily set to 1.*

In conclusion we confirmed the hypothesis that PRODH overexpression leads to decreased levels of HIF-1α in normoxic conditions.

**4.10 HIF-1α reduction by PRODH leads to a reduction of VEGF, the protein product of one of HIF-1 transcriptional targets.**

Next, we decided to investigate if the inverse correlation we observed between HIF-1α and PRODH could have functional consequences on the transcriptional response activated by HIF-1.
To do this, some of the U87 clones stably transfected with PRODH expression construct, where a reduction in HIF-1α had been previously observed, or empty vector transfected clones as controls, were used for a quantitative analysis of VEGF. The intracellular VEGF levels were analyzed by cytofluorimetric detection of the VEGF cytokine, using a specific antibody for intracellular staining. The analysis was performed both in presence or absence of Monensin, an inhibitor of vesicular intracellular protein transport. Monensin treatment leads to an accumulation of most cytokine proteins, being synthesized in the secretory pathway, in the Golgi complex and thereby enhances VEGF staining signals to facilitate detection and to better quantify possible differences.
VEGF levels decreased in PRODH expressing clones, compared to clones tranfected with empty vector, used as controls. The difference was even more evident when cells were pretreated with the Golgi inhibitor, resulting in a significative reduction in VEGF levels in PRODH expressing clones compared to controls (Figure 18). The average and standard deviation are indicated.

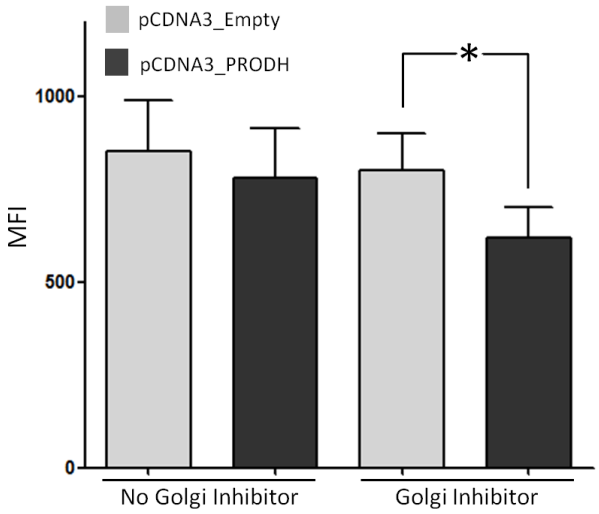


***Figure 18. VEGF levels decrease following PRODH overexpression.*** *Cytofluorimetric quantification of VEGF protein levels in U87 cell clones transfected with PRODH expressing construct or empty vector alone. Upon reaching 80% confluency, cells were trypsinized, fixed and permeabilized prior to intracellular VEGF staining using a specific antibody. Then, FACS analysis was performed to measure VEGF levels. Bars indicate the average value obtained in stable clones treated or not with Golgi inhibitor. Error bars indicate the s.d. of the mean obtained from three independents clones. *P<0.05.*

In conclusion, we provide evidence for a new mechanism of tumour suppression by PRODH that occurs by modulating the activity of the transcription factor HIF-1, often deregulated in tumours, such as glioblastoma even in absence of a hypoxic stress.

### 4.11 Increased expression and activity of HIF-1α affects PRODH expression.

We then decided to investigate if hypoxic stress and other treatments leading to HIF-1α stabilization could affect the expression of PRODH. To test this hypothesis we selected several tumour cell lines of different histological origin and exposed them to hypoxia or cobalt chloride, a molecule able to mimic low oxygen condition, by chemically inhibiting PHDs (and consequently increasing HIF-1α levels). The same cells, left in normoxic conditions, were used as control. First, we analyzed PRODH transcript levels by RT-qPCR. In all cell lines a strong reduction of PRODH mRNA in response to cobalt chloride was observed (Figure 19). The effect of hypoxia was more variable, but generally

less marked than cobalt chloride, possibly due to its pleiotropic effect, i.e. activation of different pathways in the cells, possibly having opposite effects on PRODH expression, thus resulting in a reduced net effect.

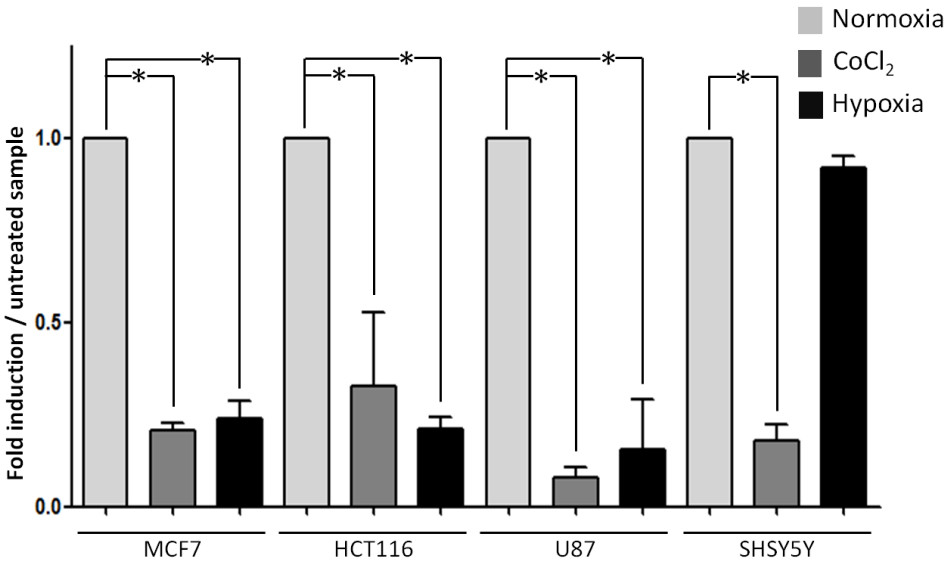


***Figure 19. HIF1-α stabilization leads to a decrease in PRODH transcript levels.*** *MCF7, HCT116, U87 and SHSY5Y cell lines were treated with the PHD inhibitor $CoCl_2$ (100 μM), or hypoxia (1%) for 24 hours before proceeding to total RNA extraction, cDNA preparation and real time q-PCR. Bars indicate the average fold of reduction obtained in treated versus untreated samples, plotted together with the standard deviation of three biological replicates. The values obtained in untreated cell lines were set to 1. *P<0.01*

As a control for effectiveness of the treatments performed, RT qPCR analyses are undergoing to check VEGF expression levels, that should be increased by the treatments described above, as it is a well known transcriptional target of HIF-1. As a preliminary result, the levels of expression after treatment of the HCT116 colon cancer cell line are shown in Figure 20.

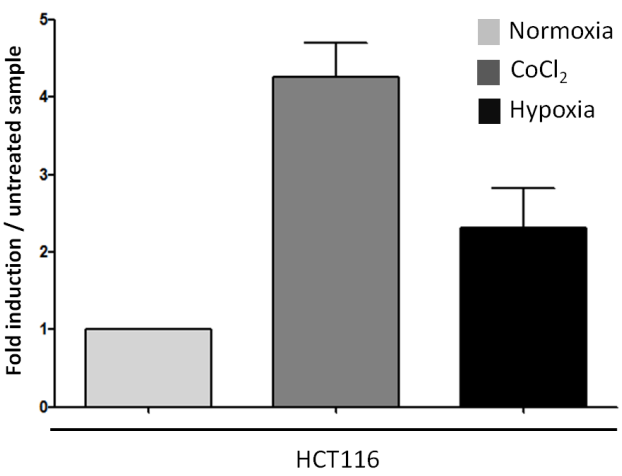


***Figure 20. HIF1-α stabilization leads to an increase in VEGF transcript levels.*** *HCT116 cell line was treated with the PHD inhibitor $CoCl_2$ (100 μM), for 24 hours before proceeding to total RNA extraction, cDNA preparation and real time q-PCR. Bars indicate the average fold of induction obtained in treated versus untreated samples, plotted together with the standard deviation of three biological replicates. The values obtained in untreated cell lines were set to 1.*

Next, we asked if the reduction we observed at the mRNA level resulted also in a reduction at the protein levels. To answer this question we chose two cell lines where PRODH protein is detectable by western blot analysis, IGROV1 and MCF7. After treatment of the cells with one or more of the conditions used to determine transcript levels, protein extracts were prepared and used for western blot analysis. A reduction in PRODH levels was observed in all hypoxic conditions, although the decrease was less evident than that observed for PRODH transcript. This observation is the result of only one preliminary experiment and has to be confirmed. Moreover, the light protein decrease compared to transcript decrease could be due to the experimental procedure the time of incubation in the various, in our conditions, RNA degradation is faster than protein degradation (figure 21). Time course experiments after exposure to $CoCl_2$ are undergoing, to determine variations in transcript and protein levels at each time point.

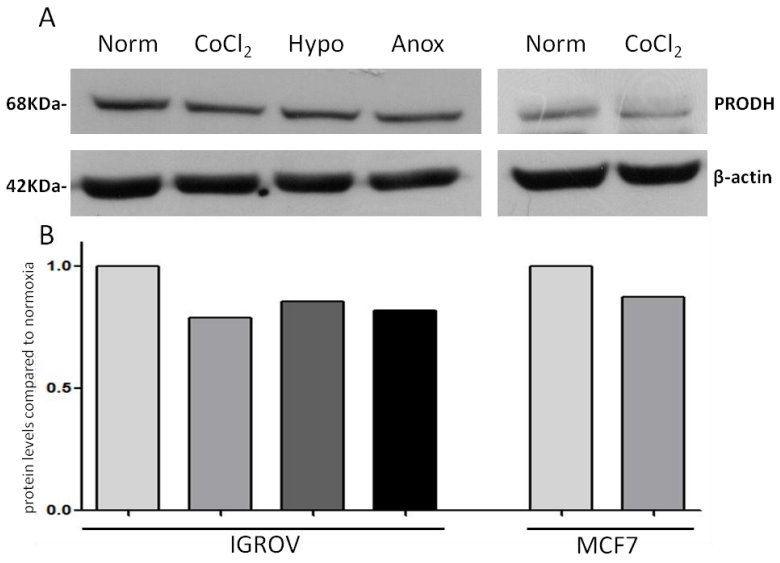


***Figure 21. HIF1-α stabilization leads to a decrease in PRODH protein levels.*** *MCF7 and IGROV cell lines were treated with the PHD inhibitor $CoCl_2$ (100 µM), hypoxia (1%) or Anoxia (0%) for 24 hours before proceeding to total protein extraction, 100 ug of protein extract, prepared seeding and harvesting cells as described in materials and methods, were used for SDS PAGE and immunoblotting.*
*Analysis was performed using a specific antibodies for PRODH and β-actin to normalize loading.*
***B.*** *Densitometric analysis of protein levels with the free on line software Image-J. Bars represent the fold of reduction of PRODH protein by Hypoxic tratments compared to the values obtained with the normoxia sample, arbitrarily set to 1.*

We hypothesize that the reduction observed in PRODH transcript and protein could be due mainly to one or both of the following mechanisms:

1) HIF-1 modulation PRODH through one or more of its direct microRNA targets. In particular, a hypoxic microRNA signature has been described (Kulshreshtha et al., 2007) and some of the microRNAs induced by hypoxia have the potential to target PRODH 3'UTR (miR-23b/*, miR-26b/*, miR-27a/*, miR-30b/*, miR-125b-1/*).
2) Another mechanism by which hypoxia/HIF-1 could modulate PRODH expression is by inducing epigenetic modifications, i.e. DNA methylation and/or histone modifications, either directly or indirectly, through one of its targets.

Experiments to validate these hypotheses are actually undergoing in our laboratory, and the results obtained will contribute to clarify the relationship between HIF-1 and PRODH and will increase knowledge about PRODH regulation and its possible downregulation during the tumourigenic process.

## 5. DISCUSSION AND CONCLUSIONS.

Proline dehydrogenase (PRODH) is a flavoenzyme that catalyzes the first, fundamental step in the metabolism of proline. In humans, the gene encoding this enzyme maps in the chromosomal region 22q11.2. This region is frequently involved in rearrangements causal of the DiGeorge Syndrome (or 22q Deletion Syndrome), characterized, among others, from psychiatric symptoms. Mutations reducing PRODH catalytic activity are responsible for type I hyperprolinemia and for susceptibility to schizophrenia, so that PRODH is considered as one of the susceptibility loci for this mental disorder (SCZD4) (Karayiorgou and Gogos, 2004; Bender et al., 2005; Kempf et al., 2008). Moreover, in the last few years several pieces of evidence have been accumulating about a tumour suppressor role for this protein (Maxwell and Rivera, 2003; Liu et al., 2009a, 2010). Indeed, PRODH hypoexpression was reported in many types of tumours compared to normal tissues and restoration of its expression led to a strong decrease in tumour growth, due to induction of apoptosis, mediated by the accumulation of ROS produced by the oxidation of proline (Maxwell and Rivera, 2003; Liu et al., 2009b, 2010). Nevertheless, it is likely that there are other mechanisms underlying its tumour suppressor function, mediated for example by PRODH contribution to α-KG production, a compound that can profoundly alter several aspects of metabolism. The starting point, driving the work described in this thesis, was that by understanding its regulation, we would have been able to better understand PRODH functions and involvement in tumour suppression.

Although the work mainly focuses on regulation of PRODH, we also analyzed the regulation of its homologous PRODH2, that catalyzes OH-proline metabolism, by p53, to test the hypothesis of a co-regulation of PRODH2 with PRODH. Moreover, we present preliminary data on the existence of a regulatory circuit between PRODH and the hypoxia inducible transcription factor HIF-1α.

## 5.1 P53 family members modulate the expression of PRODH, but not PRODH2, via intronic p53 response elements.

In the first part of my PhD work, the identification and characterization of the p53 REs in the *PRODH* and *PRODH2* genes is described. These genes have been previously described as p53 targets (Polyak et al., 1997; Cooper et al., 2008; Maxwell and Kochevar, 2008), although the REs were not characterized, and their encoded proteins are involved in similar but not identical metabolic processes in the cell, i.e. a) their catalytic activity is directed on very similar substrates with limited cross-reactivity with each other (Downing et al., 1977), b) their substrates have common origin (dietary protein or collagen degradation) and c) they have been shown to be capable of inducing apoptosis via ROS production (Donald et al., 2001; Cooper et al., 2008).

In spite of the fact that the role of PRODH as p53 apoptosis effector has been known for a long time (Polyak et al., 1997), there is very limited information on the regulatory elements that mediate p53 responsiveness of this gene. This could explain why PRODH was not included in the list of 129 genes responding to at least three out of four of the criteria -namely the presence of a p53 RE, demonstration of its upregulation by wild-type p53, functional confirmation of responsiveness of the identified RE in functional assays and physical binding of RE by p53- to be classified as a p53 regulated gene (Riley et al., 2008; Menendez et al., 2009). We extended the characterization of PRODH responsiveness to p53 beyond genotoxic induction, by showing that it was also strongly induced by p53 stabilization following Nutlin-3A treatment (Figure 1). We also showed, by use of a yeast transactivation assay, that p53 exhibits transactivation potential towards all intronic REs in the *PRODH* gene (Figure 2B). The identified intronic REs presented at least two complete half-sites and no mismatches in the core sequences, in contrast to the REs present in the promoter (Table 3). Ultimately, the extent of p53-dependent transactivation of the *PRODH* gene may be due to the sum of the contribution of each RE that can be bound and transactivated. Moreover, depending on p53 levels of induction one might expect titration of p53 to the REs based on its affinity and therefore different levels of PRODH induction, which may influence its activity (Phang et al., 2008a, 2010; Zabirnyk et al., 2010).

Concerning PRODH2, our results could not conclusively demonstrate its responsiveness to p53, in fact the experimental results suggest that it is at best a very weak p53 target gene. This conclusion is based on the functional analysis of the identified p53 REs in yeast and on the quantification of the endogenous gene expression in different cell lines upon genotoxic stress-dependent induction of p53 (Figures 5 and 6). The latter analysis was limited by the extremely low level of PRODH2 expression in several cell lines examined (i.e. HCT116, MCF7, LoVo), with the exception of HepG2. However, we did not observe any induction of PRODH2 by activation of p53 in this cell line, confirming the results obtained by Shinmen et al (Shinmen et al., 2009). The detection of PRODH2 in basal conditions only in the hepatocellular carcinoma cell line confirms that this gene is indeed liver - and kidney- specific, although recently the group led by Phang demonstrated its expression in RKO and its induction by p53 in RKO and LoVo cell lines (Cooper et al., 2008). In our experimental conditions LoVo cells did not show any detectable basal levels of PRODH2 but showed a potential activation upon genotoxic stress, that was however at the limit of detection by qPCR.

Therefore, although a coordinated expression of PRODH and PRODH2 would be justified by the existence of proteins, like collagen, rich both in proline and OH-proline, respectively the substrates of the two enzymes, this does not seem the case (Phang et al., 2008b). Indeed, PRODH has a broad expression and could contribute to cell metabolism, by the production of glutamate and α-KG from P5C, compounds in turn involved in many metabolic reactions and pathways in the cell. On the lack of a coordinated p53-dependent expression of PRODH and PRODH2 some considerations can be taken into account. First, and notably, the step downstream of the PRODH reaction in the pathway, leading from proline to glutamate, is catalyzed by P5C dehydrogenase, whose gene (*ALDH4*) was reported as a p53 target (Yoon et al., 2004). Second, other p53 transcriptional targets, such as TIGAR (Bensaad et al., 2006; Green and Chipuk, 2006), can modulate $\alpha$-KG levels. This suggests an important, and only partially elucidated, contribution of the latter compound in p53 mediated responses and stresses the contribution of PRODH in the metabolic pathways controlled by p53 (Vousden and Ryan, 2009).

Finally, in this work we also addressed the responsiveness of the *PRODH* gene to other members of the p53 family. Indeed, we found that p63$\beta$ and p73$\beta$

could also induce PRODH even though at lower levels compared to p53 (Figure 2A). To our knowledge, no data are available on p73 ability to transcriptionally regulate PRODH expression, while PRODH was found as one of the genes expressed more than 4-fold upon expression of a tetracyclin-inducible TAp63γ isoform (Osada et al., 2005). The lower levels of induction with respect to p53 were not unexpected, as several other p53 targets show a decreased responsiveness to p63 and p73. Furthermore, this result could be explained, among others, by the fact that p63 and p73 show somewhat different DNA binding affinity and transactivation potential towards canonical p53 REs, possibly in part dependent on tetramer assembly and conformation stability, as recently revealed by the comparison of crystal structures of p63 and p73 bound to DNA (Kitayner et al., 2006; Chen et al., 2011, 2012; Ethayathulla et al., 2012). It is interesting to note that the three REs that were transactivated by p63 (namely +1.7, +2.8 and +6.8) and the one transactivated by p73 (+6.8) have no spacer, consistent with previous studies indicating both for p63 and p73 a marked preference for adjacent half-site REs (Jegga et al., 2008; Menendez et al., 2010; Ethayathulla et al., 2012). The +6.8kb RE turned out to be the most efficiently recognized not only by p53 but also by p63 and p73. The reason for this may be that this RE has no spacer and that the mismatches present in one half-site affects the first and last base of the consensus, which is not involved in establishing direct protein:DNA interactions and does not preclude high affinity binding of p53 (Espinosa and Emerson, 2001; Weinberg et al., 2005; Veprintsev and Fersht, 2008; Menendez et al., 2009). However, as in mammalian cells p63 and p73 transactivated equally the *PRODH* gene, induction appears not to be strictly correlated to the relative transactivation potentials measured in the yeast-based assay. Notably, also p73, besides p53, has been recently implicated in regulation of metabolism and autophagy and was shown to be regulated by mTOR (Rosenbluth et al., 2008, 2011; Rosenbluth and Pietenpol, 2009). As proline dehydrogenase is induced by rapamycin (Pandhare et al., 2009) it is tempting to speculate that this may be achieved at least in part through p73.

In conclusion, this work demonstrates that PRODH is a target of the p53 family and provides new clues for a deeper involvement of p53 proteins in metabolic pathways. In fact, in light of the recently described link between glutamine and proline, p53 acquires a more profound role in metabolism of these non

essential aminoacids as well as their derivative alpha-ketoglutarate and in antagonizing c-Myc, that was recently found to downregulate PRODH as an important contribution to Myc metabolic reprogramming and induction of cell proliferation (Hu et al., 2010; Suzuki et al., 2010; Dang, 2011; Liu et al., 2012b).

### 5.2 The regulatory circuit between PRODH and Hypoxia/HIF-1.

Despite the obvious and widely recognized fact that cells need $O_2$ for aerobic metabolism, and that blood vessels supply $O_2$ and nutrients to tissues, the contribution of metabolic switch to cancer development and the link between metabolism and angiogenesis have been largely ignored for a long time, but they are now being (re)discovered at a rapid pace (Semenza, 1998; Esteban and Maxwell, 2005).

To give an example, the peroxisome proliferator-activated receptors (PPARs), are transcription factors that regulate cellular differentiation, development, metabolism (carbohydrate, lipid, protein) and tumourigenesis. Three isoforms have been described (PPARα, PPARβ, and PPARγ), each with distinct roles (Evans et al., 2004; Barish et al., 2006; Lefebvre et al., 2006); two can inhibit angiogenesis and one promotes vessel growth. PPARβ, a regulator of lipid oxidation (Evans et al., 2004), stimulates microvessel maturation (Müller-Brüsselbach et al., 2007), in contrast, PPARα and PPARγ inhibit angiogenesis.

PPARγ transactivates genes regulating glucose and fat metabolism (Rosen and MacDougald, 2006), and is expressed in tumour endothelial cells; PPARγ-selective ligands inhibit endothelial cells proliferation in vitro and exhibit antiangiogenic properties in vivo (Panigrahy et al., 2002). However, the precise mechanisms of action of PPARγ remain unclear, although perturbation on the expression of VEGF and its receptors have been reported (Panigrahy et al., 2002; Chintalgattu et al., 2007). It was previously shown that PPAR*γ* is a strong activator of PRODH transcription (Pandhare et al., 2006).

On the other hand, a growing body of evidence is accumulating indicating that also p53 can suppress angiogenesis through several different mechanisms, which include 1)the enhanced production of anti-angiogenic molecules in the

extracellular matrix, derived from collagen by the activity of a(II) collagen prolyl-4-hydroxylase, a transcriptional target of p53 (Teodoro et al., 2006); 2) repression of transcription of pro-angiogenic molecules such as VEGF and bFGF (Teodoro et al., 2006); 3) stimulation of HIF1α degradation by direct binding (Ravi et al., 2000); 4) modulation of microRNA such as miR107 targeting HIF-1β (Yamakuchi et al., 2010); and inhibition of the angiogenic switch in tumors in concert with p19ARF (Ulanet and Hanahan, 2010). p53 may negatively regulate angiogenesis also by induction of PRODH, that, by increasing α-KG, could modulate PHD activity on HIF-1α. This hypothesis has been investigated in this thesis and preliminary results have been shown.

In addition, Schmidt-Kastner et al demonstrated that *PRODH* is one of the genes whose expression is decreased in a model of brain ischemia in rat (Schmidt-Kastner et al., 2002), suggesting the existence of a regulatory circuit between PRODH and hypoxia, possibly involving the main regulator of cellular response to hypoxia, HIF-1. All of these observations suggest the importance of PRODH, and proline metabolism, for cellular response to various types of stress, among which hypoxic stress.

Therefore, we first showed that PRODH can indeed modulate HIF-1α and VEGF levels in a glioblastoma model cell line. This model was chosen because glioblastoma is characterized by a strong vascularization and invasivity (Alves et al., 2011), a rapid progression and resistance to treatment, leading to very poor prognosis. Our findings are supported by literature data, showing that PRODH induction in renal cancer cell lines can indeed lead to a decrease in HIF-1α, and consequently VEGF (Liu et al., 2009a).

We also suggest that inhibition of angiogenesis, observed by activation of PPARγ and p53, is mediated, at least in part, by their induction of PRODH. Moreover, as angiogenesis is only one of several features regulated by HIF-1, this finding opens new field of investigation on PRODH contribution to the control of the metabolic switch.

The regulation of HIF-1α by PRODH described here occurs in normoxia, nevertheless could have an important role in control of tumourigenesis where hypoxia is often only a transient state that determines the onset of the metabolic switch, although hypoxia can persist also later on in limited areas of the tumour.

Interestingly, other enzymes involved in the regulation of α-KG levels, such as

fumarate hydratase, succinate dehydrogenase and isocitrate dehydrogenase, have all been found to be deregulated in tumours where they drive progression to the malignant phenotype, mostly owing to aberrant activation of HIF-1-dependent pathways (Cervera et al., 2008; Zhao et al., 2009; O'Flaherty et al., 2010). Regulation of PHDs by modulation of α-KG is very important in the light of recent findings indicating that reactivation of HIF specific PHDs by a cell-permeable derivatized α-KG induced metabolic catastrophe and cell death in tumour cells under hypoxic conditions (Tennant et al., 2009).

The HIF-1α regulation exerted by PRODH, described above, is in our opinion only one side of the medal. We hypothesized that hypoxia could in turn induce PRODH down-regulation. We based this hypothesis on literature data describing that ischemia in rat leads to induction of several transcriptional targets of HIF-1, but also to a marked decrease in the mRNA levels of other genes, including PRODH (Schmidt-Kastner et al., 2002). Exposure of different cell lines to hypoxia or treatment with $CoCl_2$, which induces HIF-1α stabilization by inhibiting PHDs, led to a decrease in PRODH transcript levels. The only exception was the SHSY-5Y neuroblastoma cell line in hypoxic conditions. Neuroblastoma derived cell lines have been shown to rely only on HIF-2α, and not HIF-1α, to respond to hypoxic conditions (Jögi et al., 2004). This may partly explain the difference between the results obtained with SHSY-5Y cell line and those obtained with the other cell lines included in the analysis. In a preliminary experiment, we observed that the decrease in PRODH transcript was accompanied by a decrease in PRODH protein levels, although modest compared to the decrease in mRNA. This result seems to suggest that mRNA regulation is faster than protein regulation, and we will test mRNA and protein levels in a time course experiment, starting from short exposure times. Moreover, the IGROV1 cell line differs from other cell lines by the high levels of PRODH expression and the transcript levels in response to all "hypoxic" stimuli has yet to be performed, so that we do not know how these treatment will be effective in this cell line.

Very recently, while this work was already undergoing, PRODH was shown to be up-regulated during nutrient and/or hypoxic stress in an AMPK-dependent but HIF-independent manner (Liu et al., 2012a). This result is in contrast with what we observed in the present work. Nevertheless, there are some

differences in the experimental plan that could partly account for the different results: the medium used for culturing cells, for example, has been shown to affect profoundly the HIF-1 pathway (Torii et al., 2011). In an experiment with the HCT116 cell line, we tried either DMEM or McCoy's medium to culture the cells, and RT-qPCR results were affected by composition of the medium. Therefore, we always used the media advised by ATCC for each cell line. We used hypoxic chambers at 1% $O_2$ concentrations, which is the standard concentration found in most of the papers studying HIF-1. Moreover, also in our experimental settings, hypoxia had in general a less marked effect than $CoCl_2$ treatment, suggesting that during hypoxia different pathways converge on PRODH with opposing effects, while $CoCl_2$ mimics a more defined stimulus. Experiments are also undergoing on selected cell lines by transfecting a construct that encodes a non-hydroxylable form of HIF-1α (P402G/P564A).
Finally, while performing additional experiments to complete and refine the data and fill in the gaps in our preliminary results, we are also starting to investigate two possible mechanisms by which hypoxia or possibly HIF-1 could negatively regulate PRODH transcript levels: 1) regulation by epigenetic mechanisms, through transcriptional regulation or recruitment of chromatin modifying enzymes (Perez-Perri et al., 2011); 2) regulation by induction of one or more microRNAs (miRNAs). Indeed, several miRNAs, upregulated during low oxygen tension, could be able to target the 3'UTR of PRODH. Bioinformatic analysis aimed at finding miRNAs potentially capable of targeting PRODH and at the same time expressed in the hypoxia signature (Kulshreshtha et al., 2007), revealed that at least 5 microRNA (miR-125b-1*, miR-26b*, miR-27a*, miR-30b* and miR-23b*) upregulated during hypoxia, could downregulate PRODH. One of them, miR-23b*, has been previously confirmed as a negative regulator of PRODH expression (Liu et al., 2010).

In conclusion, we gathered preliminary data about the existence of a regulatory circuit between PRODH and HIF-1. This work demonstrates that HIF-1α protein levels is in part under the control of PRODH in normoxic conditions, while during hypoxia or when HIF-1 is pathologically overexpressed, the latter can decrease PRODH mRNA levels by an as yet undetermined mechanism. In light of the important contribution of PRODH in control of metabolic reprogramming and in keeping a balance between apoptotic and survival

signals, we underline the importance of further studying the control of *PRODH* expression exerted by known oncogenes and tumour suppressor genes.

**REFERENCES**.

Abraham, H., and Meyer, G. (2003). Reelin-expressing neurons in the postnatal and adult human hippocampal formation. Hippocampus 13, 715–727.

Altman, B.J., and Dang, C. V (2012). Normal and cancer cell metabolism: lymphocytes and lymphoma. The FEBS Journal 279, 2598–2609.

Alves, T.R., Lima, F.R.S., Kahn, S.A., Lobo, D., Dubois, L.G.F., Soletti, R., Borges, H., and Neto, V.M. (2011). Glioblastoma cells: a heterogeneous and fatal tumor interacting with the parenchyma. Life Sciences 89, 532–539.

Barish, G.D., Narkar, V.A., and Evans, R.M. (2006). PPAR delta: a dagger in the heart of the metabolic syndrome. The Journal of Clinical Investigation 116, 590–597.

Beckerman, R., and Prives, C. (2010). Transcriptional regulation by p53. Cold Spring Harbor Perspectives in Biology 2, a000935.

Bender, H.-U., Almashanu, S., Steel, G., Hu, C.-A., Lin, W.-W., Willis, A., Pulver, A., and Valle, D. (2005). Functional consequences of PRODH missense mutations. American Journal of Human Genetics 76, 409–420.

Bensaad, K., Tsuruta, A., Selak, M. a, Vidal, M.N.C., Nakano, K., Bartrons, R., Gottlieb, E., and Vousden, K.H. (2006). TIGAR, a p53-inducible regulator of glycolysis and apoptosis. Cell 126, 107–120.

Bourdon, J.C., Deguin-Chambon, V., Lelong, J.C., Dessen, P., May, P., Debuire, B., and May, E. (1997). Further characterisation of the p53 responsive element--identification of new candidate genes for trans-activation by p53. Oncogene 14, 85–94.

Brahimi-Horn, C., and Pouysségur, J. (2006). The role of the hypoxia-inducible factor in tumor metabolism growth and invasion. Bulletin Du Cancer 93, E73–80.

Braun, J.E., Huntzinger, E., Fauser, M., and Izaurralde, E. (2011). GW182 proteins directly recruit cytoplasmic deadenylase complexes to miRNA targets. Molecular Cell 44, 120–133.

Bunz, F., Dutriaux, A., Lengauer, C., Waldman, T., Zhou, S., Brown, J.P., Sedivy, J.M., Kinzler, K.W., and Vogelstein, B. (1998). Requirement for p53 and p21 to sustain G2 arrest after DNA damage. Science (New York, N.Y.) 282, 1497–1501.

Cairns, R. a, Harris, I.S., and Mak, T.W. (2011). Regulation of cancer cell metabolism. Nature Reviews. Cancer 11, 85–95.

Cervera, A.M., Apostolova, N., Crespo, F.L., Mata, M., and McCreath, K.J. (2008). Cells silenced for SDHB expression display characteristic features of the tumor phenotype. Cancer Research 68, 4058–4067.

Chen, C., Gorlatova, N., and Herzberg, O. (2012). Pliable DNA conformation of response elements bound to transcription factor p63. The Journal of Biological Chemistry 287, 7477–7486.

Chen, C., Gorlatova, N., Kelman, Z., and Herzberg, O. (2011). Structures of p63 DNA binding domain in complexes with half-site and with spacer-containing full response elements. Proceedings of the National Academy of Sciences of the United States of America 108, 6456–6461.

Chintalgattu, V., Harris, G.S., Akula, S.M., and Katwa, L.C. (2007). PPAR-gamma agonists induce the expression of VEGF and its receptors in cultured cardiac myofibroblasts. Cardiovascular Research 74, 140–150.

Ciribilli, Y., Andreotti, V., Menendez, D., Langen, J.-S., Schoenfelder, G., Resnick, M.A., and Inga, A. (2010). The coordinated p53 and estrogen receptor cis-regulation at an FLT1 promoter SNP is specific to genotoxic stress and estrogenic compound. PloS One 5, e10236.

Cooper, S.K., Pandhare, J., Donald, S.P., and Phang, J.M. (2008). A novel function for hydroxyproline oxidase in apoptosis through generation of reactive oxygen species. The Journal of Biological Chemistry 283, 10485–10492.

Dang, C. V (1999). c-Myc target genes involved in cell growth, apoptosis, and metabolism. Molecular and Cellular Biology 19, 1–11.

Dang, C. V (2011). Therapeutic targeting of Myc-reprogrammed cancer cell metabolism. Cold Spring Harbor Symposia on Quantitative Biology 76, 369–374.

Dobrucki, J., and Darzynkiewicz, Z. (2001). Chromatin condensation and sensitivity of DNA in situ to denaturation during cell cycle and apoptosis--a confocal microscopy study. Micron (Oxford, England : 1993) 32, 645–652.

Donald, S.P., Sun, X.Y., Hu, C.A., Yu, J., Mei, J.M., Valle, D., and Phang, J.M. (2001). Proline oxidase, encoded by p53-induced gene-6, catalyzes the generation of proline-dependent reactive oxygen species. Cancer Research 61, 1810–1815.

Downing, S.J., Phang, J.M., Kowaloff, E.M., Valle, D., and Smith, R.J. (1977). Proline oxidase in cultured mammalian cells. Journal of Cellular Physiology 91, 369–376.

Drewinko, B., Romsdahl, M.M., Yang, L.Y., Ahearn, M.J., and Trujillo, J.M. (1976). Establishment of a human carcinoembryonic antigen-producing colon adenocarcinoma cell line. Cancer Research 36, 467–475.

Espinosa, J.M., and Emerson, B.M. (2001). Transcriptional regulation by p53 through intrinsic DNA/chromatin binding and site-directed cofactor recruitment. Molecular Cell 8, 57–69.

Esteban, M.A., and Maxwell, P.H. (2005). NEWS AND VIEWS HIF , a missing link between metabolism and cancer. 11, 1047–1048.

Ethayathulla, A.S., Tse, P.-W., Monti, P., Nguyen, S., Inga, A., Fronza, G., and Viadiu, H. (2012). Structure of p73 DNA-binding domain tetramer modulates p73 transactivation. Proceedings of the National Academy of Sciences of the United States of America 109, 6066–6071.

Evans, R.M., Barish, G.D., and Wang, Y.-X. (2004). PPARs and the complex journey to obesity. Nature Medicine 10, 355–361.

Galluzzi, L., Vicencio, J.M., Kepp, O., Tasdemir, E., Maiuri, M.C., and Kroemer, G. (2008). To die or not to die: that is the autophagic question. Current Molecular Medicine 8, 78–91.

Ghioni, P., Bolognese, F., Duijf, P.H.G., Van Bokhoven, H., Mantovani, R., and Guerrini, L. (2002). Complex transcriptional effects of p63 isoforms: identification of novel activation and repression domains. Molecular and Cellular Biology 22, 8659–8668.

Goldberg, M.A., Dunning, S.P., and Bunn, H.F. (1988). Regulation of the erythropoietin gene: evidence that the oxygen sensor is a heme protein. Science (New York, N.Y.) 242, 1412–1415.

Green, D.R., and Chipuk, J.E. (2006). p53 and metabolism: Inside the TIGAR. Cell 126, 30–32.

Greenblatt, M.S., Bennett, W.P., Hollstein, M., and Harris, C.C. (1994). Mutations in the p53 tumor suppressor gene: clues to cancer etiology and molecular pathogenesis. Cancer Research 54, 4855–4878.

Hainaut, P., and Hollstein, M. (2000). p53 and human cancer: the first ten thousand mutations. Advances in Cancer Research 77, 81–137.

Hanahan, D., and Weinberg, R. a (2011). Hallmarks of cancer: the next generation. Cell 144, 646–674.

Hanahan, D., and Weinberg, R.A. (2000). The Hallmarks of Cancer Review University of California at San Francisco. 100, 57–70.

Hardie, D.G., Ross, F.A., and Hawley, S.A. (2012). AMPK: a nutrient and energy sensor that maintains energy homeostasis. Nature Reviews. Molecular Cell Biology 13, 251–262.

Harris, S.L., and Levine, A.J. (2005). The p53 pathway: positive and negative feedback loops. Oncogene 24, 2899–2908.

Vander Heiden, M.G., Cantley, L.C., and Thompson, C.B. (2009). Understanding the Warburg effect: the metabolic requirements of cell proliferation. Science (New York, N.Y.) 324, 1029–1033.

Hoh, J., Jin, S., Parrado, T., Edington, J., Levine, A.J., and Ott, J. (2002). The p53MH algorithm and its application in detecting p53-responsive genes. Proceedings of the National Academy of Sciences of the United States of America 99, 8467–8472.

Hu, W., Zhang, C., Wu, R., Sun, Y., Levine, A., and Feng, Z. (2010). Glutaminase 2, a novel p53 target gene regulating energy metabolism and antioxidant function. Proceedings of the National Academy of Sciences of the United States of America 107, 7455–7460.

Inga, A., Iannone, R., Monti, P., Molina, F., Bolognesi, M., Abbondandolo, A., Iggo, R., and Fronza, G. (1997). Determining mutational fingerprints at the human p53 locus with a yeast functional assay: a new tool for molecular epidemiology. Oncogene 14, 1307–1313.

Inga, A., Storici, F., Darden, T.A., and Resnick, M.A. (2002). Differential transactivation by the p53 transcription factor is highly dependent on p53 level and promoter target sequence. Molecular and Cellular Biology 22, 8612–8625.

Jacquet, H., Raux, G., Thibaut, F., Hecketsweiler, B., Houy, E., Demilly, C., Haouzir, S., Allio, G., Fouldrin, G., Drouin, V., et al. (2002). PRODH mutations and hyperprolinemia in a subset of schizophrenic patients. Human Molecular Genetics 11, 2243–2249.

Jegga, A.G., Inga, A., Menendez, D., Aronow, B.J., and Resnick, M.A. (2008). Functional evolution of the p53 regulatory network through its target response elements. Proceedings of the National Academy of Sciences of the United States of America 105, 944–949.

Johnson, J., Lagowski, J., Sundberg, A., and Kulesz-Martin, M. (2005). P53 family activities in development and cancer: relationship to melanocyte and keratinocyte carcinogenesis. The Journal of Investigative Dermatology 125, 857–864.

Jones, R.G., and Thompson, C.B. (2009). Tumor suppressors and cell metabolism : a recipe for cancer growth. 537–548.

Jordan, J.J., Menendez, D., Inga, A., Noureddine, M., Nourredine, M., Bell, D.A., Bell, D., and Resnick, M.A. (2008). Noncanonical DNA motifs as transactivation targets by wild type and mutant p53. PLoS Genetics 4, e1000104.

Jögi, A., Vallon-Christersson, J., Holmquist, L., Axelson, H., Borg, A., and Påhlman, S. (2004). Human neuroblastoma cells exposed to hypoxia: induction of genes associated with growth, survival, and aggressive behavior. Experimental Cell Research 295, 469–487.

Karayiorgou, M., and Gogos, J.A. (2004). The molecular genetics of the 22q11-associated schizophrenia. Brain Research. Molecular Brain Research 132, 95–104.

Kaur, B., Khwaja, F.W., Severson, E.A., Matheny, S.L., Brat, D.J., and Van Meir, E.G. (2005). Hypoxia and the hypoxia-inducible-factor pathway in glioma growth and angiogenesis. Neuro-oncology 7, 134–153.

Kempf, L., Nicodemus, K.K., Kolachana, B., Vakkalanka, R., Verchinski, B. a, Egan, M.F., Straub, R.E., Mattay, V. a, Callicott, J.H., Weinberger, D.R., et al. (2008). Functional polymorphisms in PRODH are associated with risk and protection for schizophrenia and fronto-striatal structure and function. PLoS Genetics 4, e1000252.

Kern, S.E., Kinzler, K.W., Bruskin, A., Jarosz, D., Friedman, P., Prives, C., and Vogelstein, B. (1991). Identification of p53 as a sequence-specific DNA-binding protein. Science (New York, N.Y.) 252, 1708–1711.

Kimura, N., Tokunaga, C., Dalal, S., Richardson, C., Yoshino, K., Hara, K., Kemp, B.E., Witters, L.A., Mimura, O., and Yonezawa, K. (2003). A possible linkage between AMP-activated protein kinase (AMPK) and mammalian target of rapamycin (mTOR) signalling pathway. Genes to Cells : Devoted to Molecular & Cellular Mechanisms 8, 65–79.

Kitayner, M., Rozenberg, H., Kessler, N., Rabinovich, D., Shaulov, L., Haran, T.E., and Shakked, Z. (2006). Structural basis of DNA recognition by p53 tetramers. Molecular Cell 22, 741–753.

van Kouwenhove, M., Kedde, M., and Agami, R. (2011). MicroRNA regulation by RNA-binding proteins and its implications for cancer. Nature Reviews. Cancer 11, 644–656.

Kulshreshtha, R., Ferracin, M., Wojcik, S.E., Garzon, R., Alder, H., Agosto-Perez, F.J., Davuluri, R., Liu, C.-G., Croce, C.M., Negrini, M., et al. (2007). A microRNA signature of hypoxia. Molecular and Cellular Biology 27, 1859–1867.

Laplante, M., and Sabatini, D.M. (2012). mTOR signaling in growth control and disease. Cell 149, 274–293.

Lefebvre, P., Chinetti, G., Fruchart, J.-C., and Staels, B. (2006). Sorting out the roles of PPAR alpha in energy metabolism and vascular homeostasis. The Journal of Clinical Investigation 116, 571–580.

Levine, A.J. (1997). p53, the cellular gatekeeper for growth and division. Cell 88, 323–331.

Li, F., Wang, Y., Zeller, K.I., Potter, J.J., Wonsey, D.R., O'Donnell, K.A., Kim, J.-W., Yustein, J.T., Lee, L.A., and Dang, C. V (2005). Myc stimulates nuclearly encoded mitochondrial genes and mitochondrial biogenesis. Molecular and Cellular Biology 25, 6225–6234.

Lian, J., Yan, X.-H., Peng, J., and Jiang, S.-W. (2008). The mammalian target of rapamycin pathway and its role in molecular nutrition regulation. Molecular Nutrition & Food Research 52, 393–399.

Liu, W., Glunde, K., Bhujwalla, Z.M., Raman, V., Sharma, A., and Phang, J.M. (2012a). Proline oxidase promotes tumor cell survival in hypoxic tumor microenvironments. Cancer Research 72, 3677–3686.

Liu, W., Le, A., Hancock, C., Lane, A.N., Dang, C. V, Fan, T.W.-M., and Phang, J.M. (2012b). Reprogramming of proline and glutamine metabolism contributes to the proliferative and metabolic responses regulated by oncogenic transcription factor c-MYC. Proceedings of the National Academy of Sciences of the United States of America 109, 8983–8988.

Liu, W., and Phang, J.M. (2012). Proline dehydrogenase (oxidase), a mitochondrial tumor suppressor, and autophagy under the hypoxia microenvironment. Autophagy 8, 1407–1409.

Liu, W., Zabirnyk, O., Wang, H., Shiao, Y.-H., Nickerson, M.L., Khalil, S., Anderson, L.M., Perantoni, a O., and Phang, J.M. (2010). miR-23b targets proline oxidase, a novel tumor suppressor protein in renal cancer. Oncogene 29, 4914–4924.

Liu, Y., Borchert, G.L., Donald, S.P., Diwan, B. a, Anver, M., and Phang, J.M. (2009a). Proline oxidase functions as a mitochondrial tumor suppressor in human cancers. Cancer Research 69, 6414–6422.

Liu, Y., Borchert, G.L., Donald, S.P., Diwan, B. a, Anver, M., and Phang, J.M. (2009b). Proline oxidase functions as a mitochondrial tumor suppressor in human cancers. Cancer Research 69, 6414–6422.

Liu, Y., Borchert, G.L., Surazynski, A., Hu, C.-A., and Phang, J.M. (2006). Proline oxidase activates both intrinsic and extrinsic pathways for apoptosis: the role of ROS/superoxides, NFAT and MEK/ERK signaling. Oncogene 25, 5640–5647.

Matoba, S., Kang, J.-G., Patino, W.D., Wragg, A., Boehm, M., Gavrilova, O., Hurley, P.J., Bunz, F., and Hwang, P.M. (2006). p53 regulates mitochondrial respiration. Science (New York, N.Y.) 312, 1650–1653.

Maxwell, S. a, and Rivera, A. (2003). Proline oxidase induces apoptosis in tumor cells, and its expression is frequently absent or reduced in renal carcinomas. The Journal of Biological Chemistry 278, 9784–9789.

Maxwell, S.A., and Kochevar, G.J. (2008). Identification of a p53-response element in the promoter of the proline oxidase gene. Biochemical and Biophysical Research Communications 369, 308–313.

McDonald-McGinn, D.M., Reilly, A., Wallgren-Pettersson, C., Hoyme, H.E., Yang, S.P., Adam, M.P., Zackai, E.H., and Sullivan, K.E. (2006). Malignancy in chromosome 22q11.2 deletion syndrome (DiGeorge syndrome/velocardiofacial syndrome). American Journal of Medical Genetics. Part A 140, 906–909.

Menendez, D., Inga, A., and Resnick, M.A. (2009). The expanding universe of p53 targets. Nature Reviews. Cancer 9, 724–737.

Menendez, D., Inga, A., and Resnick, M.A. (2010). Potentiating the p53 network. Discovery Medicine 10, 94–100.

Menendez, D., Krysiak, O., Inga, A., Krysiak, B., Resnick, M.A., and Schönfelder, G. (2006). A SNP in the flt-1 promoter integrates the VEGF system into the p53 transcriptional network. Proceedings of the National Academy of Sciences of the United States of America 103, 1406–1411.

Mihaylova, M.M., and Shaw, R.J. (2011). The AMPK signalling pathway coordinates cell growth, autophagy and metabolism. Nature Cell Biology 13, 1016–1023.

Mills, A.A., Zheng, B., Wang, X.J., Vogel, H., Roop, D.R., and Bradley, A. (1999). p63 is a p53 homologue required for limb and epidermal morphogenesis. Nature 398, 708–713.

Müller-Brüsselbach, S., Kömhoff, M., Rieck, M., Meissner, W., Kaddatz, K., Adamkiewicz, J., Keil, B., Klose, K.J., Moll, R., Burdick, A.D., et al. (2007). Deregulation of tumor angiogenesis and blockade of tumor growth in PPARbeta-deficient mice. The EMBO Journal 26, 3686–3698.

Osada, M., Park, H.L., Nagakawa, Y., Yamashita, K., Fomenkov, A., Kim, M.S., Wu, G., Nomoto, S., Trink, B., and Sidransky, D. (2005). Differential recognition of response elements determines target gene specificity for p53 and p63. Molecular and Cellular Biology 25, 6077–6089.

O'Flaherty, L., Adam, J., Heather, L.C., Zhdanov, A. V, Chung, Y.-L., Miranda, M.X., Croft, J., Olpin, S., Clarke, K., Pugh, C.W., et al. (2010). Dysregulation of hypoxia pathways in fumarate hydratase-deficient cells is independent of defective mitochondrial metabolism. Human Molecular Genetics 19, 3844–3851.

Pandhare, J., Cooper, S.K., and Phang, J.M. (2006). Proline oxidase, a proapoptotic gene, is induced by troglitazone: evidence for both peroxisome proliferator-activated receptor gamma-dependent and -independent mechanisms. The Journal of Biological Chemistry 281, 2044–2052.

Pandhare, J., Donald, S.P., Cooper, S.K., and Phang, J.M. (2009). Regulation and function of proline oxidase under nutrient stress. Journal of Cellular Biochemistry 107, 759–768.

Panigrahy, D., Singer, S., Shen, L.Q., Butterfield, C.E., Freedman, D.A., Chen, E.J., Moses, M.A., Kilroy, S., Duensing, S., Fletcher, C., et al. (2002). PPARgamma ligands inhibit primary tumor growth and metastasis by inhibiting angiogenesis. The Journal of Clinical Investigation 110, 923–932.

Parsons, D.W., Jones, S., Zhang, X., Lin, J.C.-H., Leary, R.J., Angenendt, P., Mankoo, P., Carter, H., Siu, I.-M., Gallia, G.L., et al. (2008). An integrated genomic analysis of human glioblastoma multiforme. Science (New York, N.Y.) 321, 1807–1812.

Perez-Perri, J.I., Acevedo, J.M., and Wappner, P. (2011). Epigenetics: new questions on the response to hypoxia. International Journal of Molecular Sciences 12, 4705–4721.

Phang, J.M., Donald, S.P., Pandhare, J., and Liu, Y. (2008a). The metabolism of proline, a stress substrate, modulates carcinogenic pathways. Amino Acids 35, 681–690.

Phang, J.M., Liu, W., and Zabirnyk, O. (2010a). Proline Metabolism and Microenvironmental Stress.

Phang, J.M., Liu, W., and Zabirnyk, O. (2010b). Proline metabolism and microenvironmental stress. Annual Review of Nutrition 30, 441–463.

Phang, J.M., Pandhare, J., and Liu, Y. (2008b). The metabolism of proline as microenvironmental stress substrate. The Journal of Nutrition 138, 2008S–2015S.

Pillai, R.S., Bhattacharyya, S.N., and Filipowicz, W. (2007). Repression of protein synthesis by miRNAs: how many mechanisms? Trends in Cell Biology 17, 118–126.

Plas, D.R., and Thompson, C.B. (2005). Akt-dependent transformation: there is more to growth than just surviving. Oncogene 24, 7435–7442.

Polyak, K., Xia, Y., Zweier, J.L., Kinzler, K.W., and Vogelstein, B. (1997). A model for p53-induced apoptosis. Nature 389, 300–305.

Pugh, C.W., O'Rourke, J.F., Nagao, M., Gleadle, J.M., and Ratcliffe, P.J. (1997). Activation of hypoxia-inducible factor-1; definition of regulatory domains within the alpha subunit. The Journal of Biological Chemistry 272, 11205–11214.

Ravi, R., Mookerjee, B., Bhujwalla, Z.M., Sutter, C.H., Artemov, D., Zeng, Q., Dillehay, L.E., Madan, A., Semenza, G.L., and Bedi, A. (2000). Regulation of tumor angiogenesis by p53-induced degradation of hypoxia-inducible factor 1alpha. Genes & Development 14, 34–44.

Reyes, H., Reisz-Porszasz, S., and Hankinson, O. (1992). Identification of the Ah receptor nuclear translocator protein (Arnt) as a component of the DNA binding form of the Ah receptor. Science (New York, N.Y.) 256, 1193–1195.

Riley, T., Sontag, E., Chen, P., and Levine, A. (2008). Transcriptional control of human p53-regulated genes. Nature Reviews. Molecular Cell Biology 9, 402–412.

Rosen, E.D., and MacDougald, O.A. (2006). Adipocyte differentiation from the inside out. Nature Reviews. Molecular Cell Biology 7, 885–896.

Rosenbluth, J.M., Mays, D.J., Jiang, A., Shyr, Y., and Pietenpol, J.A. (2011). Differential regulation of the p73 cistrome by mammalian target of rapamycin reveals transcriptional programs of mesenchymal differentiation and tumorigenesis. Proceedings of the National Academy of Sciences of the United States of America 108, 2076–2081.

Rosenbluth, J.M., Mays, D.J., Pino, M.F., Tang, L.J., and Pietenpol, J.A. (2008). A gene signature-based approach identifies mTOR as a regulator of p73. Molecular and Cellular Biology 28, 5951–5964.

Rosenbluth, J.M., and Pietenpol, J.A. (2008). The jury is in: p73 is a tumor suppressor after all. Genes & Development 22, 2591–2595.

Rosenbluth, J.M., and Pietenpol, J.A. (2009). mTOR regulates autophagy-associated genes downstream of p73. Autophagy 5, 114–116.

Sbisà, E., Catalano, D., Grillo, G., Licciulli, F., Turi, A., Liuni, S., Pesole, G., De Grassi, A., Caratozzolo, M.F., D'Erchia, A.M., et al. (2007). p53FamTaG: a database resource of human p53, p63 and p73 direct target genes combining in silico prediction and microarray data. BMC Bioinformatics *8 Suppl 1*, S20.

Schafer, Z.T., Grassian, A.R., Song, L., Jiang, Z., Gerhart-Hines, Z., Irie, H.Y., Gao, S., Puigserver, P., and Brugge, J.S. (2009). Antioxidant and oncogene rescue of metabolic defects caused by loss of matrix attachment. Nature 461, 109–113.

Schmidt-Kastner, R., Zhang, B., Belayev, L., Khoutorova, L., Amin, R., Busto, R., and Ginsberg, M.D. (2002). DNA microarray analysis of cortical gene expression during early recirculation after focal brain ischemia in rat. Brain Research. Molecular Brain Research 108, 81–93.

Semenza, G.L. (1998). Hypoxia-inducible factor 1: master regulator of O2 homeostasis. Current Opinion in Genetics & Development 8, 588–594.

Semenza, G.L., Nejfelt, M.K., Chi, S.M., and Antonarakis, S.E. (1991). Hypoxia-inducible nuclear factors bind to an enhancer element located 3' to the human erythropoietin gene. Proceedings of the National Academy of Sciences of the United States of America 88, 5680–5684.

Shinmen, N., Koshida, T., Kumazawa, T., Sato, K., Shimada, H., Matsutani, T., Iwadate, Y., Takiguchi, M., and Hiwasa, T. (2009). Activation of NFAT signal by p53-K120R mutant. FEBS Letters 583, 1916–1922.

Stiewe, T., and Pützer, B.M. (2002). Role of p73 in malignancy: tumor suppressor or oncogene? Cell Death and Differentiation 9, 237–245.

Storici, F., Lewis, L.K., and Resnick, M.A. (2001). In vivo site-directed mutagenesis using oligonucleotides. Nature Biotechnology 19, 773–776.

Storici, F., and Resnick, M.A. (2003). Delitto perfetto targeted mutagenesis in yeast with oligonucleotides. Genetic Engineering 25, 189–207.

Suganuma, K., Miwa, H., Imai, N., Shikami, M., Gotou, M., Goto, M., Mizuno, S., Takahashi, M., Yamamoto, H., Hiramatsu, A., et al. (2010). Energy metabolism of leukemia cells: glycolysis versus oxidative phosphorylation. Leukemia & Lymphoma 51, 2112–2119.

Surazynski, A., Liu, Y., Miltyk, W., and Phang, J.M. (2005). Nitric oxide regulates prolidase activity by serine/threonine phosphorylation. Journal of Cellular Biochemistry 96, 1086–1094.

Suzuki, S., Tanaka, T., Poyurovsky, M. V, Nagano, H., Mayama, T., Ohkubo, S., Lokshin, M., Hosokawa, H., Nakayama, T., Suzuki, Y., et al. (2010). Phosphate-activated glutaminase (GLS2), a p53-inducible regulator of glutamine metabolism and reactive oxygen species. Proceedings of the National Academy of Sciences of the United States of America 107, 7461–7466.

Tennant, D.A., Frezza, C., MacKenzie, E.D., Nguyen, Q.D., Zheng, L., Selak, M.A., Roberts, D.L., Dive, C., Watson, D.G., Aboagye, E.O., et al. (2009). Reactivating HIF prolyl hydroxylases under hypoxia results in metabolic catastrophe and cell death. Oncogene 28, 4009–4021.

Teodoro, J.G., Parker, A.E., Zhu, X., and Green, M.R. (2006). p53-mediated inhibition of angiogenesis through up-regulation of a collagen prolyl hydroxylase. Science (New York, N.Y.) 313, 968–971.

Tomasini, R., Tsuchihara, K., Wilhelm, M., Fujitani, M., Rufini, A., Cheung, C.C., Khan, F., Itie-Youten, A., Wakeham, A., Tsao, M.-S., et al. (2008). TAp73 knockout shows genomic instability with infertility and tumor suppressor functions. Genes & Development 22, 2677–2691.

Torii, S., Kurihara, A., Li, X.Y., Yasumoto, K., and Sogawa, K. (2011). Inhibitory effect of extracellular histidine on cobalt-induced HIF-1alpha expression. Journal of Biochemistry 149, 171–176.

Tsunoda, T., and Takagi, T. (1999). Estimating transcription factor bindability on DNA. Bioinformatics (Oxford, England) 15, 622–630.

Tuderman, L., Myllylä, R., and Kivirikko, K.I. (1977). Mechanism of the prolyl hydroxylase reaction. 1. Role of co-substrates. European Journal of Biochemistry / FEBS 80, 341–348.

Ueda, Y., Hijikata, M., Takagi, S., Chiba, T., and Shimotohno, K. (2001). Transcriptional activities of p73 splicing variants are regulated by inter-variant association. The Biochemical Journal 356, 859–866.

Ulanet, D.B., and Hanahan, D. (2010). Loss of p19(Arf) facilitates the angiogenic switch and tumor initiation in a multi-stage cancer model via p53-dependent and independent mechanisms. PloS One 5, e12454.

Veprintsev, D.B., and Fersht, A.R. (2008). Algorithm for prediction of tumour suppressor p53 affinity for binding sites in DNA. Nucleic Acids Research 36, 1589–1598.

Vogelstein, B., and Kinzler, K.W. (2004). Cancer genes and the pathways they control. Nature Medicine 10, 789–799.

Vousden, K.H., and Prives, C. (2009). Blinded by the Light: The Growing Complexity of p53. Cell 137, 413–431.

Vousden, K.H., and Ryan, K.M. (2009). p53 and metabolism. Nature Reviews. Cancer 9, 691–700.

Wallace, D.C. (2012). Mitochondria and cancer. Nature Reviews. Cancer 12, 685–698.

Wang, B., Xiao, Z., and Ren, E.C. (2009). Redefining the p53 response element. Proceedings of the National Academy of Sciences of the United States of America 106, 14373–14378.

Wang, G.L., Jiang, B.H., Rue, E.A., and Semenza, G.L. (1995). Hypoxia-inducible factor 1 is a basic-helix-loop-helix-PAS heterodimer regulated by cellular O2 tension. Proceedings of the National Academy of Sciences of the United States of America 92, 5510–5514.

Warburg, O. (1956). On the origin of cancer cells. Science (New York, N.Y.) 123, 309–314.

Wei, J., Zaika, E., and Zaika, A. (2012). p53 Family: Role of Protein Isoforms in Human Cancer. Journal of Nucleic Acids 2012, 687359.

Weinberg, R.L., Veprintsev, D.B., Bycroft, M., and Fersht, A.R. (2005). Comparative binding of p53 to its promoter and DNA recognition elements. Journal of Molecular Biology 348, 589–596.

White, T.A., Krishnan, N., Becker, D.F., and Tanner, J.J. (2007). Structure and kinetics of monofunctional proline dehydrogenase from Thermus thermophilus. The Journal of Biological Chemistry 282, 14316–14327.

Yamakuchi, M., Lotterman, C.D., Bao, C., Hruban, R.H., Karim, B., Mendell, J.T., Huso, D., and Lowenstein, C.J. (2010). P53-induced microRNA-107 inhibits HIF-1 and tumor angiogenesis. Proceedings of the National Academy of Sciences of the United States of America 107, 6334–6339.

Yang, A., Schweitzer, R., Sun, D., Kaghad, M., Walker, N., Bronson, R.T., Tabin, C., Sharpe, A., Caput, D., Crum, C., et al. (1999). p63 is essential for regenerative proliferation in limb, craniofacial and epithelial development. Nature 398, 714–718.

Yang, A., Walker, N., Bronson, R., Kaghad, M., Oosterwegel, M., Bonnin, J., Vagner, C., Bonnet, H., Dikkes, P., Sharpe, A., et al. (2000). p73-deficient mice have neurological, pheromonal and inflammatory defects but lack spontaneous tumours. Nature 404, 99–103.

Yoon, K.-A., Nakamura, Y., and Arakawa, H. (2004). Identification of ALDH4 as a p53-inducible gene and its protective role in cellular stresses. Journal of Human Genetics 49, 134–140.

Yuan, Y., Hilliard, G., Ferguson, T., and Millhorn, D.E. (2003). Cobalt inhibits the interaction between hypoxia-inducible factor-alpha and von Hippel-Lindau protein by direct binding to hypoxia-inducible factor-alpha. The Journal of Biological Chemistry 278, 15911–15916.

Zabirnyk, O., Liu, W., Khalil, S., Sharma, A., and Phang, J.M. (2010). Oxidized low-density lipoproteins upregulate proline oxidase to initiate ROS-dependent autophagy. Carcinogenesis 31, 446–454.

Zhao, S., Lin, Y., Xu, W., Jiang, W., Zha, Z., Wang, P., Yu, W., Li, Z., Gong, L., Peng, Y., et al. (2009). Glioma-derived mutations in IDH1 dominantly inhibit IDH1 catalytic activity and induce HIF-1alpha. Science (New York, N.Y.) 324, 261–265.

**ACKNOWLEDGEMENTS.**

Foremost, I would like to express my sincere gratitude to my tutor Dott. Paola Campomenosi for the continuous support during my Ph.D study and research, for her patience, motivation, enthusiasm, and immense knowledge. Her guidance helped me in all the time of research and writing of this thesis.

Besides my advisor, I would like to thank all our collaborators: Prof. Loredano Pollegioni and all his group, for the enormous collaboration and financial contribution to our work; Prof. Douglas Noonan, Prof. Elena Monti and Dott. Marzia Gariboldi, for the constant support.

My sincere thanks also goes to Prof. Alberto Inga, for offering me stage opportunities in his group and leading me working on a different exciting work environment where I met fantastic people.

A special thanks to Dott. Raffaella Cinquetti and Elena Tallarita for being friends more than just simple colleagues during my Ph.D. adventure.

Thanks to my girlfriend Noemi, for her love and moral support.

Last but not the least, I would like to thank my mother, for giving birth to me at the first place and supporting me spiritually throughout my life.

## CONTRIBUTIONS

**From previous work.**

- Campomenosi P., Cinquetti R., Tallarita E., Lindqvist C., Raimondi I., Grassi P., Näsman J., Dell A., Haslam S.M., Taramelli R., et al. (2011) **Comparison of the baculovirus-insect cell and Pichia pastoris heterologous systems for the expression of the human tumor suppressor protein RNASET2.** Biotechnology and Applied Biochemistry 58, 39–49.

**From the work described in this Ph.D. thesis.**

- Raimondi I., Ciribilli Y., Monti P, Bisio A., Pollegioni L., Fronza G., Inga A., Campomenosi P. **P53 family members modulate the expression of PRODH, but not PRODH2, via intronic p53 response elements.** PLoS ONE submitted, currently under revision.

# Comparison of the baculovirus-insect cell and *Pichia pastoris* heterologous systems for the expression of the human tumor suppressor protein RNASET2

**Biotechnology and Applied Biochemistry**

*Paola Campomenosi,[1]* Raffaella Cinquetti,[1] Elena Tallarita,[1] Christer Lindqvist,[2] Ivan Raimondi,[1] Paola Grassi,[3] Johnny Näsman,[2] Anne Dell,[3] Stuart M. Haslam,[3] Roberto Taramelli,[1] and Francesco Acquati[1]*

[1]*Department of Biotechnology and Molecular Sciences, University of Insubria, Varese, Italy*

[2]*Department of Biosciences, Åbo Akademi University, Turku, Finland*

[3]*Division of Molecular Biosciences, Faculty of Natural Sciences, Imperial College London, London, UK*

## Abstract.

We report the expression of recombinant RNASET2, the only human member of the Rh/T2/S family of acid ribonucleases, in the yeast *Pichia pastoris* and the baculovirus-insect cell heterologous systems. In both models, the yield of recombinant protein was comparable and ranged between 5 mg/L (for a catalytically impaired mutant version of RNASET2) and 30 mg/L for the wild-type protein. Thus, the produced protein version rather than the expression system used appears to influence protein yield after optimization of culture conditions. The recombinant protein was found to undergo heterogeneous glycosylation in both systems, particularly in *P. pastoris*. Most importantly, the wild-type protein purified from both systems was found to be catalytically competent. The expression of recombinant RNASET2 in both systems will allow the implementation of functional assays *in vivo* and *in vitro* to better define the antioncogenic properties of this member of the Rh/T2/S ribonuclease family.


Volume 58, Number 1, January/February 2011, Pages 39–49 •
E-mail: paola.campomenosi@uninsubria.it; francesco.acquati@uninsubria.it

**Keywords:** RNASET2, tumor suppressor, ribonuclease, heterologous protein expression, protein glycosylation

## 1. Introduction

Ribonucleases have been the subject of extensive studies in recent years, due to their involvement in several biological processes besides RNA metabolism. Indeed, RNAses have been involved in a host of cellular processes such as viral infections, cell proliferation, tumor cell growth, and angiogenesis [1],[2]. The transferase-type ribonucleases have long been ranked into three main families (ribonuclease A, Rh/T2/S, and T1) according to their biochemical properties [1]. The main feature of the Rh/T2/S family of ribonucleases is represented by two conserved active-site segment (CAS) motives, in which two histidine residues play an essential role in catalysis [1],[2]. These proteins are acid ribonucleases displaying a pH optimum below 6.0 for catalytic activity and are either secreted extracellularly or targeted to the vacuolar or lysosomal compartments after their transit through the secretory pathway, where they usually undergo *N*-glycosylation and chaperone-assisted folding [2].

RNASET2 is to date the only member of the Rh/T2/S family described in humans [3]. Besides its activity as a ribonuclease [4], we previously demonstrated an oncosuppressive function for this protein [5–7]. Strikingly, this role appeared to be independent of catalytic activity because a mutant RNASET2 protein in which the two key CAS histidine residues were replaced by phenylalanine (H65/118F RNASET2) was found to be still highly effective in suppressing tumorigenesis *in vivo* when compared with the wild-type protein [6],[7]. However, in order to further characterize this protein (both structurally and functionally) and to better define its potential as an antitumorigenic agent, it would be crucial to have recombinant RNASET2 available.

Ribonucleases of the Rh/T2/S family have been purified from different sources, either directly from the host organisms in which they are expressed (such as in fungi or plants) or in different heterologous protein expression systems [1],[2]. As these proteins are usually modified post-translationally by *N*-glycosylation and targeted to the secretory pathway, the expression strategy of choice usually relies on a eukaryotic system, in particular the baculovirus expression vector system (BEVS) or the yeast *Pichia pastoris*.

However, finding the system that grants the best expression levels is mandatory for obtaining sufficient amounts of pure protein for *in vivo* experiments and for conformational and

Abbreviations: CAS, conserved active-site segment; H65/118F, mutant RNASET2 version with histidine at positions 65 and 118 substituted with phenylalanines; BEVS, baculovirus expression vector system; anti-HA, anti-hemagglutinin; $Mut^+$, methanol utilization plus; $Mut^S$, methanol utilization slow; MOI, multiplicity of infection.

*Address for correspondence: Paola Campomenosi, BSc, PhD, Department of Biotechnology and Molecular Sciences, University of Insubria, Via J.H. Dunant 3, 21100 Varese, Italy. Tel.: +39-0332-421518; Fax: +39-0332-421500; e-mail: paola.campomenosi@uninsubria.it.

*Address for correspondence: Francesco Acquati, BSc, PhD, Department of Biotechnology and Molecular Sciences, University of Insubria, Via J.H. Dunant 3, 21100 Varese, Italy. Tel.: +39-0332-421512; Fax: +39-0332-421500; e-mail: francesco.acquati@uninsubria.it.

Received 30 November 2010; accepted 20 December 2010
DOI: 10.1002/bab.7
Published online 30 March 2011 in Wiley Online Library (wileyonlinelibrary.com)

structural studies. In independent reports, yields of a few milligrams per liter of culture have been reported for members of this family of ribonucleases [1],[2]. However, to our knowledge, no comparisons have ever been made among the expression levels obtained in different systems for a specific ribonuclease of this family.

In this work, we set out to define the best conditions for RNASET2 production in heterologous systems and we report the expression of this protein in both *P. pastoris* and BEVS by showing that both systems produce a catalytically competent RNASET2 with comparable levels of expression and catalytic activity. *P. pastoris* thus represents the expression system of choice for this protein, being more cost-effective compared with the baculovirus system and allowing the secretion of the protein in a relatively protein-free supernatant from which RNASET2 can be easily purified [8–10].

## 2. Materials and methods

### 2.1. Reagents and media

All reagents were from Sigma–Aldrich (Milan, Italy), unless otherwise specified. The "easy select" *Pichia* expression kit was purchased from Invitrogen (Milan, Italy). Phusion high-fidelity DNA polymerase, restriction/modification enzymes, and peptide-*N*-glycosydase F were from New England Biolabs (Milan, Italy). Zeocin was purchased from InvivoGen (Milan, Italy), yeast nitrogen base from Difco BD, and Bradford reagent and Polyprep columns from Biorad. Ultrafree centrifugal concentrators (cutoff 5,000 Da) were purchased from Millipore and NiNTA resin from Qiagen (Milan, Italy). BA85 nitrocellulose membrane was from Schleicher & Schuell (Varese, Italy), supersignal *West Dura* extended duration chemiluminescent substrate and horseradish peroxidase-conjugated secondary antibodies were from Thermo Scientific (Milan, Italy).

A rabbit polyclonal antibody raised against a truncated version of human RNASET2 expressed in bacteria (anti-RNASET2) [6] and a rabbit polyclonal antibody against purified full-length human recombinant RNASET2 from the baculovirus-insect cell system (anti-RNASET2-2) were used as primary antibodies and were raised by Dabio (Germany). The mouse monoclonal anti-HA tag (clone 12CA5) was purchased from Roche (Monza, Italy).

The following media for insect cell culture were used: Sf900 II medium supplemented with 2 mM L-glutamine, 10 U/mL penicillin G (sodium salt), 10 μg/mL streptomycin sulfate (GIBCO, Invitrogen), and 0.1% pluronics (Sigma–Aldrich); TMN-FH (Fully Supplemented Grace's Medium) medium, supplemented with 2 mM L-glutamine, 10 U/mL penicillin G (sodium salt), and 10 μg/mL streptomycin sulfate plus 5% Fetal Bovine Serum (FBS) (GIBCO, Invitrogen, Milan, Italy). Media for *P. pastoris* cell growth and screening of the methanol utilization phenotype were prepared as described in the Invitrogen "EasySelect™ *Pichia* Expression kit."

#### *2.1.1. Cloning of the human RNASET2 coding sequence in plasmid vectors*

Cloning of RNASET2 coding sequence fused at the 3′ end to sequences coding for both HA (hemagglutinin) and 6× histidine tags into the pFASTBAC1 vector for expression in the BEVS has been described previously [4]. The RNASET2 coding sequence included the human endogenous N-terminal signal peptide. Two versions of RNASET2 were cloned, coding either for the wild-type protein or the catalytically impaired H65/118F mutant.

The same HA and 6× histidine-tagged RNASET2 coding sequence without endogenous signal peptide (aa 25–256) was PCR amplified for cloning in pPICZ A (Invitrogen) in order to express RNASET2 in frame with the vector-encoded *Saccharomyces cerevisiae* factor signal peptide for secretion of the recombinant protein.

Primers for PCR amplification were as follows:

RNASET2 Forward:
5′TGACGAATTCGACAAGCGCCTGCGTGACA3′
RNASET2 Reverse:
5′TGACGAATTCTCAGTGATGATGGTGGTGATGAGCGTAGTCTGGCACGTCGTATGGG3′

The PCR products were gel purified, digested with EcoRI, and cloned into pPICZ A before transformation in the JM109 *Escherichia coli* strain. Plasmid DNA was purified from several transformed colonies and, after sequencing (CRIBI, Padova, Italy), the empty vector and the two RNASET2-encoding constructs (pPICZ A-wtRNASE and pPICZ A-mutRNASE) were used to transform several *P. pastoris* strains.

#### *2.1.2. Transformation of P. pastoris and "methanol utilization" phenotype screening*

Five micrograms of each RNASET2 construct or empty vector were linearized within the 3′AOX region with PmeI and transformed into *P. pastoris* by the lithium chloride method [11]. Three strains were transformed: GS115 [His4] and X33 [wild type], which are both methanol utilization plus ($Mut^+$), and KM71H [arg4, AOX1::ARG4], which is methanol utilization slow ($Mut^S$). Transformants were selected on Yeast, Peptone, Dextrose (YPD) plates (1% yeast extract, 2% bactopeptone, 2% dextrose, 20 g/L bactoagar) containing 100 μg/mL zeocin and confirmed by streaking on the same plates. Zeocin-resistant clones were picked and lysed by boiling at 100°C for 10 Min in 20 mL of bidistilled water. Five microliters of each lysate was used for PCR amplification, using two pairs of primers. The first primer pair (5′AOX and 3′AOX) was designed according to manufacturer's instructions (Invitrogen) to discriminate integration of the empty vector (producing a 590 bp PCR product) from integration of RNASET2-containing constructs (producing a 1,340 bp PCR product). The second primer pair (RNASET2 *forward 2*: 5′ GACAAGCGCCTGCGTGACA 3′ and RNASET2 *reverse 2*: 5′ TGCTTGGTCTTTTTAGGTGG 3′) was RNASET2-specific and was expected to yield a 700 bp band only when RNASET2-containing constructs were integrated.

$Mut^+$ strain colonies positive for integration were also screened for the methanol utilization phenotype by streaking on MDH and MMH plates (Minimal Dextrose Histidine and Minimal Methanol Histidine: 1.34% yeast nitrogen base, $4 \times 10^{-5}$% biotin, 0.004% histidine, 15 g/L bactoagar, and either 2% dextrose for MDH or 0.5% methanol for MMH plates). Clones maintaining the $Mut^+$ phenotype grew approximately

at the same efficiency on both plates, whereas clones that have turned to $Mut^S$ phenotype grew very slowly on MMH plates.

## 2.2. Optimization of RNASET2 expression from *P. pastoris*

Buffered minimal glycerol or buffered minimal methanol medium (BMGH/BMMH) (100 mM potassium phosphates pH 6.0, 1.34% yeast nitrogen base, $4 \times 10^{-5}$% biotin, 0.004% histidine, and either 1% glycerol or 0.5% methanol) and buffered complex glycerol or buffered complex methanol medium (BMGY/BMMY) (1% yeast extract, 2% bactopeptone, 1.34% yeast nitrogen base, $4 \times 10^{-5}$% biotin, and either 1% glycerol or 0.5% methanol) media were used to grow cells and analyze the expression of RNASET2. Selected clones were freshly plated and grown for 2 days at 30°C. One colony was picked and inoculated into 50 mL of BMGH or BMGY medium. Cultures were grown at 30°C with 180 rpm shaking overnight until they reached an Optical Density at 600 nm ($OD_{600}$) between 2 and 6. They were then centrifuged and the pellet was resuspended in the appropriate methanol-containing medium at a starting $OD_{600}$ of 1 for induction of protein expression. Fresh methanol (0.5% final concentration) was added to the culture each day to replace for evaporation. From time 0 to 240 H, 300-mL aliquots were taken from the culture every 24 H. Cells at each time point were centrifuged at 2,000*g* and both pellets and supernatants were stored at −80°C for subsequent immunoblot analysis. To select the best RNASET2-expressing clones, eight clones transformed with either wild type or H65/118F mutant RNASET2 construct and two control clones transformed with empty vector were grown in 50 mL conical tubes in 5 mL of BMGY. When cultures reached an $OD_{600}$ of 3, the cells were transferred in BMMY medium at a density of 1 $OD_{600}$. Induction was performed for 168 H (optimal time as determined during the time course assay), then cultures were centrifuged and supernatants stored at −80°C for subsequent analysis.

### *2.2.1. Expression and purification of wild-type RNASET2 using the BEVS*

The Sf9 insect cell line [12] from the pupal ovarian tissue of the fall army worm *Spodoptera frugiperda* was cultured at 27°C as suspension and/or monolayer cultures and infected with the recombinant baculovirus batches FastBac1-wtRNASE (wild-type RNASET2) or FastBac1-MutRNASE (H65/118F mutant) at a multiplicity of infection (MOI) of 5–10 plaque-forming units per cell. Supernatants were collected 96–144 H after infection. Protein purification was performed as previously described [4].

### *2.2.2. Expression and purification of wild-type RNASET2 from P. pastoris strain X33*

One recombinant clone from the X33 strain was selected to express the protein for subsequent purification. The BMGY/BMMY medium was used for generating biomass and inducing expression and cultures were processed after 7 days from induction. After pelleting the cells at 2,500*g* in a swinging rotor, the supernatant was filtered with a 0.45 μm pore size filter unit and processed as described in ref. [4] for RNASET2 expressed in the baculovirus system. Briefly, supernatants were concentrated 10-fold on Ultrafree centrifugal concentrators and extensively dialyzed against 50 mM Tris–HCl, 100 mM KCl, and 5 mM 2-mercaptoethanol (base solution) at pH 8.0, to improve subsequent binding to the Ni-NTA resin (Qiagen). After addition of 10 mM imidazole, binding to the resin was allowed to proceed for 2 H at 4°C, before applying the solution onto an empty column. After washing with 10-column volumes of wash solution (base solution plus 20 mM imidazole), elution was performed with four column volumes (one volume at a time) of base solution plus 250 mM imidazole. The amount of protein in the eluted fractions was checked both spectrophotometrically and by Sodium Dodecyl Sulphate-Polyacrylamide Gel Electrophoresis (SDS-PAGE) followed by Coomassie R250 staining. Protein-containing fractions were pooled and dialyzed against 10 mM potassium phosphate, 0.2 mM 2-mercaptoethanol (pH 6.6), and stored at −20°C in small aliquots.

### *2.2.3. Analysis of RNASET2 expression by immunoblotting*

Ten/fifteen microliters of supernatant from RNASET2-expressing *Pichia* or baculovirus system cultures or 10–50 ng of purified recombinant proteins were prepared in LaemmLi sample buffer, denatured at 95°C for 5 Min, resolved on 13% SDS-PAGE and transferred to BA85 nitrocellulose membrane. Membranes were blocked with 4% nonfat dry milk in 0.1% Tween-20 in phosphate-buffered saline (PBST) overnight at 4°C, then incubated 1 H at room temperature with the appropriate primary antibody at the following dilution in 2% nonfat milk in PBST: rabbit polyclonal anti-RNASET2: 1:600; rabbit polyclonal anti-RNASET2-2: 1:1,000; mouse monoclonal anti-HA tag: 1:4,000. Subsequently, membranes were incubated with horseradish peroxidase-conjugated anti-mouse or anti-rabbit secondary antibodies at a 1:900 dilution in 2% nonfat milk in PBST. Detection was carried out with chemiluminescent substrate.

### *2.2.4. RNASET2 deglycosylation*

Five hundred nanograms of purified recombinant RNASET2 obtained from the baculovirus-insect cell system or supernatants from RNASET2-expressing *P. pastoris* clones were denatured and either treated with peptide-*N*-glycosydase F to remove all *N*-linked glycosylation or mock treated. After treatment, samples were processed for immunoblotting as described above.

## 2.3. Analysis of the glycosylation pattern of recombinant RNASET2 purified from the two expression systems

Approximately 10 μg of RNASET2 obtained from either baculovirus or *P. Pastoris* was subjected to reduction, carboxymethylation, and tryptic digestion; the samples were reduced at 37°C in water bath for 1 H in 1 mL of 50 mM Tris–HCl buffer (pH 8.5) containing 10 mg/mL dithiothreitol.

Carboxymethylation was carried out by the addition of iodoacetic acid (fivefold molar excess over dithiothreitol), and the reaction was allowed to proceed at room temperature in the dark for 1 and 5 H. After carboxymethylation, samples were dialyzed against $4 \times 4.5$ L of 50 mM ammonium bicarbonate (pH 8.5) at 4°C for 48 H, and subsequently lyophilized.

The reduced carboxymethylated proteins were then digested with *N-p*-tosyl-l-phenylalanine chloromethyl

ketone-pretreated bovine pancreas trypsin (EC 3.4.21.4; Sigma) for 16 H at 37°C in 50 mM ammonium bicarbonate buffer (pH 8.4). After trypsin digestion, samples were purified by C18 Sep-Pak® (Waters Corp., Milford, MA, USA) as described previously [13].

Releasing of *N*-glycans from tryptic glycopeptides was obtained by addition of *N*-glycosidase F in 50 mM ammonium bicarbonate (pH 8.5). The digestion was carried on for 20 H at 37°C with 5 units of enzyme (Roche Applied Science, UK). The released *N*-glycans were purified from O-glycopeptides and peptides by chromatography on a Sep-Pak C18 cartridge (Waters) and subsequently methylated using the sodium hydroxide permethylation procedure as described previously [14].

Briefly, five to seven NaOH pellets were ground to fine powder and mixed with 2–3 mL anhydrous dimethylsulfoxide (Romil, UK) before adding to each dried sample. This is followed by the addition of 0.6 mL of methyl iodide and vigorous shaking at room temperature for 15 Min. Permethylated glycans were extracted with chloroform and then purified by using Sep-Pak C18 cartridges.

The cartridges were successively conditioned with methanol (5 mL), water (5 mL), acetonitrile (5 mL), and water (15 mL). Each sample was dissolved in 200 μL of methanol/water (1:1) solution before loading onto the cartridges. The cartridges were washed with 5 mL of water and then eluted sequentially with 3 mL of each 15%, 35%, 50%, and 75% acetonitrile solution in water.

Acetonitrile/water fractions (35%, 50%, and 75%) were collected and then concentrated with a Savant SpeedVac (ThermoFisher Scientific, Horsham, West Sussex, UK) and subsequently lyophilized.

The permethylated glycans were subsequently analyzed by mass spectrometry (MS). Briefly, Matrix Assisted Laser Desorption/Ionization-Time of Flight (MALDI-TOF) data were acquired on a Voyager-DE STR mass spectrometer (Applied Biosystems, Foster City, CA, USA) in the reflectron mode with delayed extraction. Permethylated samples were dissolved in 10 μL of methanol, and 1 μL of dissolved sample was premixed with 1 μL of matrix [20 mg/mL 2,5-dihydroxybenzoic acid in 70% (v/v) aqueous methanol], spotted onto a target plate and dried under vacuum.

The MS data were processed using Data Explorer 4.9 software (Applied Biosystems, UK). The mass spectra were baseline corrected (default settings) and noise filtered (with correction factor of 0.7), and then converted to ASCII format. The processed spectra were then subjected to manual assignment and annotation with the aid of a glycobioinformatics tool known as GlycoWorkBench [15].

Peak picking was done manually and proposed assignments for the selected peaks were based on molecular mass composition of the $^{12}C$ isotope together with knowledge of the biosynthetic pathways.

### 2.4. Analysis of the catalytic activity of recombinant RNASET2

To assess the catalytic activity of RNASET2 purified from the baculovirus-insect cell system or *P. pastoris*, zymogram gel electrophoresis was performed as described [16],[17]. Briefly, SDS polyacrylamide gels were prepared according to standard procedures, except total RNA from torula yeast was added in resolving (2 mg/mL final concentration) and stacking (0.3 mg/mL final concentration) gel solutions. Proteins were prepared in nonreducing sample buffer (125 mM Tris–HCl pH 6.8, 2% SDS, 10% glycerol, 0.02% blue bromophenol) and directly loaded into gels without boiling. After electrophoresis, proteins were allowed to renature by removing SDS with 25% isopropanol prepared in 10 mM Tris–HCl (pH 7.4) and the gel was washed extensively with 10 mM Tris–HCl (pH 7.4) and incubated at 51°C in freshly prepared KCl 100 mM, Na acetate 100 mM at pH 5,0. After washing with 10 mM Tris–HCl (pH 7.4), enzymatic activity was detected by toluidine blue staining followed by destaining in 10 mM Tris–HCl (pH 7.4), leaving a negative image where RNase activity was present. After image acquisition with a Biorad GS800 densitometer, gels were destained as much as possible from toluidine blue with 10 mM Tris–HCl (pH 7.4), soaked for 30 Min in transfer buffer and processed for immunoblotting as described above. In this case, detection was performed with the sensitive anti-RNASET2-2 antibody.

#### *2.4.1. Spectrophotometric discontinuous method for catalytic activity measurement*

To better quantify the enzymatic activity of the two recombinant proteins, a spectrophotometric discontinuous method was also used. The protein concentration was estimated assuming an extinction coefficient at 280 nm of 61,920 $M^{-1}$ $cm^{-1}$ for the denatured amino acid sequence without the signal peptide (aa 25–256), calculated with the ProtParam bioinformatics tool at Expasy (www.expasy.ch) and measuring the absorbance of the protein solution in 8 M urea, sodium phosphate buffer (pH 6.5). Enzymatic activity toward torula yeast total RNA was measured by following the increase in absorbance at 260 nm due to acid soluble nucleotides release at pH 5.0 and 37°C. Briefly, 3 μg/mL of RNASET2 was added to a reaction mix, pre-equilibrated at 37°C, containing total RNA at a final concentration of 0.4 mg/mL in 0.1 M sodium acetate, 0.1 M KCl (pH 5.0). This concentration has been previously shown to ensure that we worked in excess of substrate. At each time point, a 300 μL aliquot of the reaction was taken and transferred to a tube containing 100 μL of 25% perchloric acid with 0.75% uranyl acetate. After centrifugation, supernatants, containing the free nucleotides, were diluted 1:5 and absorbance at 260 nm was measured. At least two measures were performed for each protein preparation and two independent protein preparations were analyzed for each type of recombinant RNASET2. The software Kaleidagraph was used to build and analyze kinetics.

## 3. Results

To express recombinant RNASET2 in *P. pastoris*, the coding sequences of both wild-type and H65/118F mutant RNASET2 were cloned into the pPICZ A vector. Both recombinant constructs and empty vector were transformed into three *Pichia* strains (GS115, KM71H, and X33) and several clones were checked by PCR for integration of the construct in the host genome. As expected, integrant clones containing the RNASET2-coding

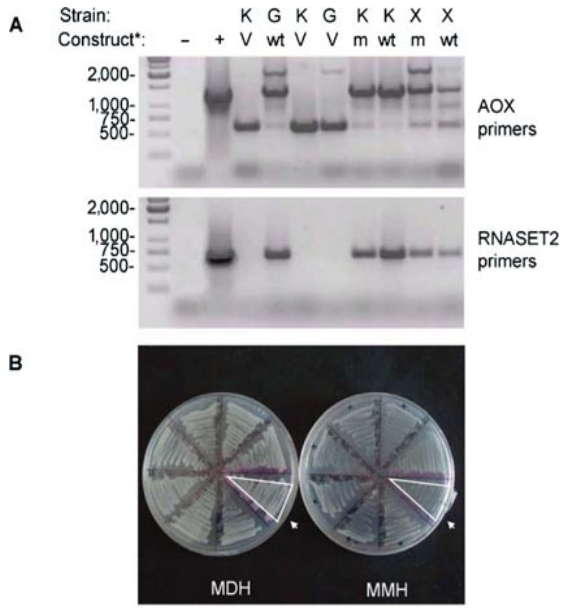


Fig. 1. Screening of *Pichia pastoris* zeocin-resistant clones for RNASET2–pPICZaA or pPICZaA vector integration and for methanol utilization phenotype. (A) AOX1-specific primers (upper panel) or RNASET2-specific primers (lower panel) were used for colony PCR to check for integration of the constructs into the AOX1 locus. Clone strains are indicated as X, K, and G for X33, KM71H, and GS115, respectively. The type of construct used for transformation (*) is also indicated as "V" (vector only), "wt" (wild-type RNASET2 construct), or "m" (H65/118F mutant RNASET2 construct). (B) MDH or MMH plates were used to screen for the methanol utilization phenotype. Arrows indicate a Mut$^S$ control that was streaked on both plates and shows a slower growth on MMH plates compared with MDH plates.

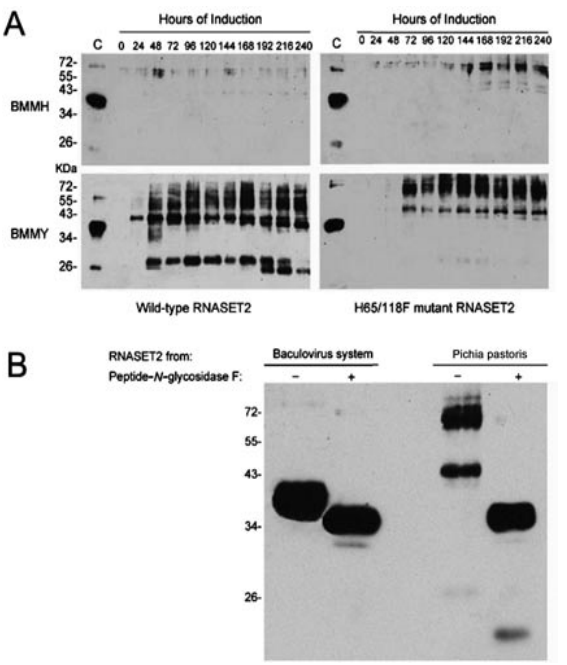


Fig. 2. Analysis of time-dependent RNASET2 expression in different media formulations. (A) Wild-type and H65/118F mutant RNASET2-expressing clones from the GS115 strain were induced up to 240 H in BMMH or BMMY media. Supernatants were immunoblotted and detected with anti-RNASET2-specific antibody. Lane C shows recombinant RNASET2 purified from the baculovirus-insect cell system. (B) Analysis of recombinant RNASET2 after peptide-*N*-glycosidase F treatment. Supernatants from RNASET2-expressing, baculovirus-infected cells or from a single *Pichia pastoris* clone were either treated with peptide-*N*-glycosidase F (+) or mock treated (–). Reactions were immunoblotted and detected with anti-HA specific antibody.

sequence showed a 700 and a 1,400 bp amplification product when RNASET2-specific primers or 5′ and 3′ AOX primer pairs were used, respectively (Fig. 1A). By contrast, integrants for the empty vector did not amplify with the RNASET2 primer pair and gave rise to a 600 bp band with the AOX primers (Fig. 1A). The orientation of the insert was also checked by PCR using a forward or a reverse RNASET2-specific primer together with the 3′ AOX primer (data not shown). Clones from Mut$^+$ strains were checked for maintenance of the methanol utilization phenotype. All clones in KM71H and X33 strains showed comparable growth rates on methanol or glycerol containing plates, indicating that they had maintained the Mut$^+$ phenotype (Fig. 1B).

One wild-type and one H65/118F mutant clone from the GS115 (Mut$^S$) strain were selected for pilot expression experiments aimed at defining the best conditions for RNASET2 expression. We chose this strain because it has already been used for expression of ribonucleases from the T2 family [18]. Cell pellets and supernatants were collected every 24 H for 10 days and stored until the end of the experiment. As shown in Fig. 2A, samples grown in BMMY medium showed a strong positivity to the anti-RNASET2-specific antibody in immunoblotting. These anti- RNASET2 positive bands showed a wide range of molecular masses, suggesting that following expression in *P. pastoris* RNASET2 undergoes a complex posttranslational modification. Indeed, besides proteins in the 38–45 kDa range, which is similar to that observed following expression of RNASET2 in the BEVS system, several bands in the 50–80 kDa range were also observed. Occasionally, a few bands were also observed at about 26 kDa in the wild-type RNASET2-expressing clone. This band(s) was recognized by two different anti-RNASET2 polyclonal antibodies and by the anti-HA antibody, confirming its identity as RNASET2 (Fig. 2, panel B and data not shown). A band of the same approximate molecular weight has been sometimes observed also in the baculovirus system and is likely to

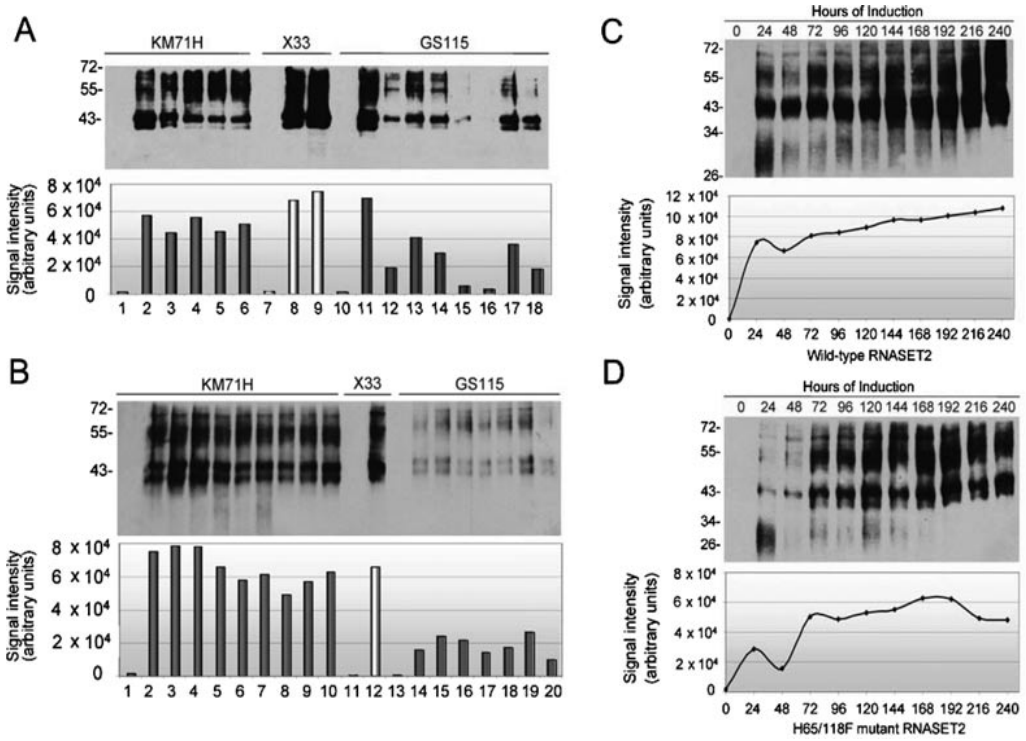


Fig. 3. Comparison of RNASET2 expression levels among different *Pichia pastoris* strains. Clones with integrated wild-type (A) or H65/118F mutant (B) RNASET2 constructs from strains GS115, X33, and KM71H were induced with methanol. Supernatants were collected after 168 H, immunoblotted and detected with anti-RNASET2-specific antibody. As a control, clones obtained by integration of empty pPICZaA vector were used (lanes and columns 1, 7, and 10 for wild- type and 1, 11, and 13 for mutant clones). (C, D) RNASET2 expression levels as a function of time in wild-type and mutant RNASET2-expressing clones from strain X33. The graphs below each immunoblot detected with anti-RNASET2 antibody show wild-type (C) or H65/118F mutant (D) expression levels as a function of induction time, and are reported as "signal intensity" arbitrary units which were calculated by band scanning and quantification with ImageJ software. The reported data represent the result of two independent experiments.

represent a degradative product. To investigate the nature of the different RNASET2 positive bands, supernatants from both RNASET2-expressing baculovirus-infected insect cells and a *Pichia* recombinant clone were treated with peptide-*N*-glycosidase F prior to Western blot analysis. A main band of 33 kDa was detected with an anti-HA antibody either in the sample from the baculovirus system or in that from *Pichia* after deglycosylation (Fig. 2B), suggesting that all anti-RNASET2 reactive forms shown in Fig. 2A represent mildly glycosylated or hyperglycosylated forms of RNASET2. The 26 kDa band, upon deglycosylation with PNGase F, shifted to a 19 kDa band and this confirmed that also this band was indeed glycosylated (Fig. 2B).

The time-course experiment in GS115 also allowed us to estimate the best time for optimal expression in this strain. At each time point, cell supernatants were immunoblotted and detected with anti-RNASET2-specific antibody. The expression levels were found to increase rapidly, reaching maximum levels between 144 and 168 H after induction (data not shown). We also tried to define the best RNASET2-expressing strain by the analysis of several clones from the three strains. Although we found evidence for intraclone variability in the expression levels, a trend was observed (for wild-type RNASET2-expressing clones), whereby the X33 strain was in general a better expressor when compared with both KM71H and GS115 strains (Fig. 3A), whereas for the H65/118F mutant RNASET2-expressing clones, the expression levels were quite similar in both X33 and KM71H strains and much higher when compared with strain GS115 (Fig. 3B). Being the best expressor strain for both RNASET2 forms, we thus chose the X33 strain for further expression experiments, and a new time course was performed on two selected wild-type and mutant clones, in order to define the best time for optimal expression in this strain. For both proteins, all clones showed a rapid increase in RNASET2 protein levels within 24 H from induction (Figs. 3C and 3D), followed by a flex between 24 and 72 H and a further wave of slow increased expression. As for clones in the GS115 strain, 168 H (7 days) was chosen as the best time for subsequent induction.

**Table 1**
**RNASET2 expression levels in the two heterologous expression systems**

| | *Pichia pastoris* | BEVS |
|---|---|---|
| Wild-type RNASET2 | 36 ± 4.26 | 33 ± 3.35 |
| H65/118F mutant RNASET2 | 6.9 ± 1.09 | 5.6 ± 1.39 |

Values are expressed in mg/L of cell culture supernatants and represent the mean of four independent experiments ± standard error.

Preliminary attempts to express recombinant RNASET2 in the baculovirus-insect cell system have been previously carried out in our laboratory [4], with estimated yields in the range of 1–2 mg/L of cell culture supernatant. We thus tried to optimize RNASET2 expression levels also in this heterologous system by using different media formulations and collecting supernatants at different times after infection (ranging from 96 to 144 H). Comparison among different media allowed us to conclude that maximum RNASET2 expression levels were obtained in TNM-FH medium supplemented with 5% FBS. In this medium, the wild-type protein was expressed at about 30 mg/L (Table 1), which represents a 15-fold improvement in expression levels compared with cultures in the previously used serum-free medium. The expression levels of the H65/118F mutant, however, did not improve as much as the wild type in the same conditions.

Next, we compared the expression levels of wild type and mutant RNASET2 in *P. pastoris* with those in the BEVS. To this aim, identical volumes of unprocessed supernatant samples were immunoblotted and detection was performed with anti-RNASET2 and anti-HA antibodies. A calibration curve was constructed on each immunoblot by loading increasing known amounts of pure recombinant RNASET2 previously purified from the BEVS. This allowed us to determine the concentration of RNASET2 in the supernatants, which was estimated to range between 30 and 40 mg/L for the wild-type form in both expression systems, whereas the H65/118F mutant was expressed at about 7 mg/L in *P. pastoris* and at about 5 and 6 mg/L in the BEVS (Table 1).

Purification of recombinant RNASET2 was performed from supernatants after 168 H (7 days) of induction in *P. pastoris* and from supernatants of recombinant baculovirus-infected insect cells 144 H (6 days) after infection. The same protocol previously described for purification of RNASET2 from the baculovirus-insect cell system [4] was applied to both types of supernatant. By SDS-PAGE analysis of the purified proteins, RNASET2 from the baculovirus system showed two main bands of 37 and 39 kDa (Fig. 4A, lanes 1–3), whereas RNASET2 purified from *P. pastoris* showed two bands of 41 and 43 kDa (Fig. 4A, lanes 4–6). The hyperglycosylated forms with a molecular weight above 55 kDa were barely visible only when high amounts (o, 5 μg) of

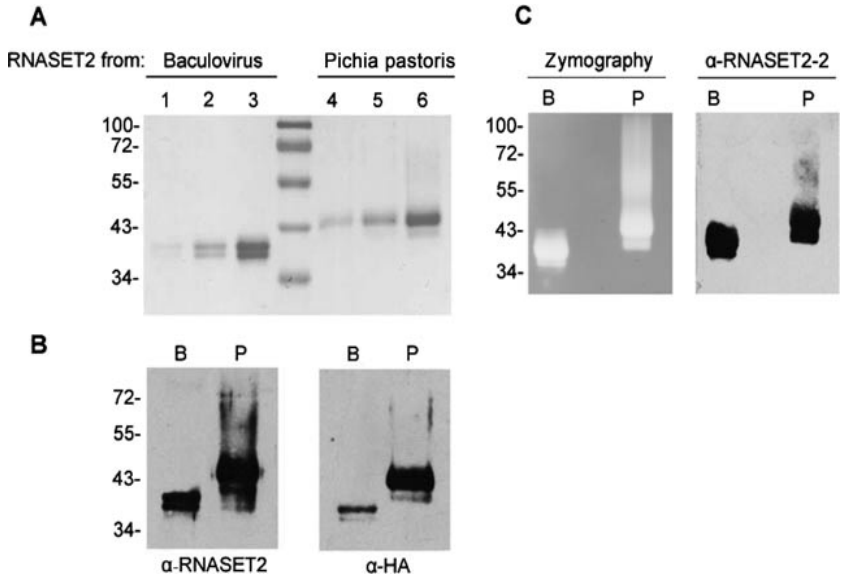


Fig. 4. Analysis of wild-type RNASET2 purified from baculovirus-infected insect cells or from a *Pichia pastoris* strain X33 clone. (A) Coomassie staining of an SDS-PAGE gel loaded with three different volumes of RNASET2 from either baculovirus-infected insect cells (lanes 1–3) or *P. pastoris* (lanes 4–6). A prestained protein marker was loaded in the middle lane. (B) Immunoblots were detected with anti-RNASET2 antibody (left) or anti-HA antibody (right) to confirm the identity of the purified proteins. (C) Zymography was performed using total RNA from torula yeast as substrate to analyze RNASET2 purified from the two heterologous systems. The identity of the bands showing ribonucleolytic activity was confirmed by immunodetection with anti- RNASET2-2 antibody. In all panels, P and B indicate supernatants from *P. pastoris* or the BEVS, respectively.

RNASET2 from *P. pastoris* were loaded (data not shown). Western blot analysis with anti-RNASET2 or anti-HA monoclonal antibodies confirmed the identity of the purified proteins (Fig. 4B). Both purified preparations were judged to be >95% pure by Coomassie staining of SDS-acrylamide gels.

Finally, as we previously showed that human RNASET2 is a functional ribonuclease [4], the purified proteins were checked for proper folding and functionality by zymographic analysis. Equal amounts of each purified protein, as determined both spectrophotometrically and by Coomassie blue staining, were loaded on a zymographic gel containing torula yeast's total RNA as a substrate. RNASET2 purified from both *P. pastoris* and baculovirus systems showed a strong signal after toluidine blue staining, indicative of ribonucleolytic activity (Fig. 4C, left panel). Molecular weights corresponding to RNA hydrolyzation activity were compatible with those observed from the forms obtained after purification. Moreover, the same forms showing ribonucleolytic activity were detected by the anti-RNASET2-2-specific antibody (Fig. 4C, right panel).

To evaluate whether the wild-type proteins from the two expression systems showed comparable levels of catalytic activity, a spectrophotometric method to measure the ribonucleolytic activity in solution was applied. At least two measures were performed for each protein preparation and two independent protein preparations were tested for each type of RNASET2. The two preparations of each recombinant protein gave very similar results, showing that the recombinant protein produced in the BEVS has an activity, expressed as Abs260/Min, of 0.67 $\pm$ 0.009 against an activity of 1.02 $\pm$ 0.013 Abs260/Min for the recombinant protein expressed in *P. pastoris*. Therefore, RNASET2 purified from *P. pastoris* shows a 30% higher activity than the protein purified from the baculovirus system in the conditions tested.

Defining one unit as the amount of enzyme which produces a change of 1 $OD_{260}$ absorbance in 15 Min at 37°C, wild-type human RNASET2 purified from baculovirus appeared to contain 3,390 units/mg of protein, whereas the protein purified from *P. pastoris* contained 5,100 units/mg of protein in the preparations and the conditions tested.

Taken together, these data show that recombinant RNASET2 expressed in both *P. pastoris* and BEVS expression systems have catalytic activity.

Finally, we investigated the nature of the carbohydrate modifications on the proteins purified from the two heterologous expression systems. Analysis of MALDI spectra of *N*-glycans released by PNGaseF digestion of the tryptic peptides and subsequently permethylated (spectra A and B in Fig. 5) showed a wide variation in molecular weight of the glycans attributable to the products from baculovirus and *P. Pastoris* systems. Thus, the protein purified from the baculovirus system is characterized by a major hexasaccharide whose composition is consistent with a core fucosylated trimannosyl *N*-glycan (*m*/*z* 1,345; see Fig. 5 A). Less abundant components are high mannose structures of composition Man5GlcNac2 (*m*/*z* 1,580), Man6GlcNac2 (*m*/*z* 1,784), and Man7GlcNac2 (*m*/*z* 1,988) (see Fig. 5 A). In contrast, the sample purified from *Pichia* is dominated by polymannose glycans of composition Man5GlcNac2 (*m*/*z* 1,580), Man6GlcNac2 (*m*/*z* 1,784), Man7GlcNac2 (*m*/*z* 1,988), Man9GlcNac2 (*m*/*z* 2,396), Man10GlcNac2 (*m*/*z* 2,600), Man11GlcNac2 (*m*/*z* 2,804), Man12GlcNac2 (*m*/*z* 3,008), Man13GlcNac2 (*m*/*z* 3,212), Man14GlcNac2 (*m*/*z* 3,416), and Man15GlcNac2 (*m*/*z* 3,623) (see Fig. 5 B), and has none of the hexasaccharide at *m*/*z* 1,345 detected in the protein from the baculovirus system.

## 4. Discussion

In this paper, we describe the expression of RNASET2, the only human member of the Rh/T2/S family of ribonucleases, in both *P. pastoris* and baculovirus-insect cell-based expression systems. The two systems were compared in terms of expression levels and functionality of the produced protein. To our knowledge, this is the first report comparing two different heterologous expression systems for expression of a ribonuclease of the Rh/T2/S family.

*Pichia pastoris* and baculovirus-insect cell systems were chosen because RNASET2 is a secreted protein which undergoes a series of posttranslational modifications in the endoplasmic reticulum and Golgi apparatus. Indeed, RNASET2 expression has been previously attempted in *E. coli* by our group, but the expression levels were quite low, likely due to either toxicity to the host cells or lack of stability in *E. coli*.

By contrast, in this work, RNASET2 was successfully expressed in both eukaryotic heterologous expression systems following optimization of culture conditions. The expression levels in these heterologous expression systems were comparable and ranged between 5 and 30 mg/L, depending on the protein version expressed (mutant or wild-type RNASET2), whereas the expression system did not appear to significantly influence the amount of protein produced. These expression levels represent the result of an accurate optimization strategy, as we previously described a yield of just 1–2 mg of protein/L of baculovirus-infected insect cell supernatants [4]. As long as expression in *P. pastoris* is concerned, three different strains were used as host cells and the X33 strain turned out to be a better expressor with respect to the GS115 and KM71H ($Mut^S$) strains. When compared with other proteins, the expression levels obtained for RNASET2 are rather low [8]; nevertheless, they rank in the high range of expression levels when published data reporting heterologous expression of members of the Rh/T2/S family of ribonucleases are taken into account [1],[2]. In one report, heterologous expression of RNase Rh from *Rhizopus niveus* in *S. cerevisiae* gave high expression levels, ranging from 40 to 70 mg/L, depending on the signal peptide used [19]. In another paper, two S-ribonucleases of *Petunia inflata* were expressed in the baculovirus expression system with yields of 1 mg of protein/L of cell supernatant [20]. Later, Huang et al. described expression of $E^{rns}$, a ribonuclease from classical swine fever virus, in *P. pastoris* at 27 mg/L [21]. The same protein had been previously produced in insect cells but expression levels were not reported [22]. Wild type and mutant versions of ribonuclease MC from *Momordica charantia* (bitter gourd) were expressed both in *E. coli* and *P. pastoris*. Although expression levels in bacteria were in the order of 0, 5 mg/L, the same protein was expressed

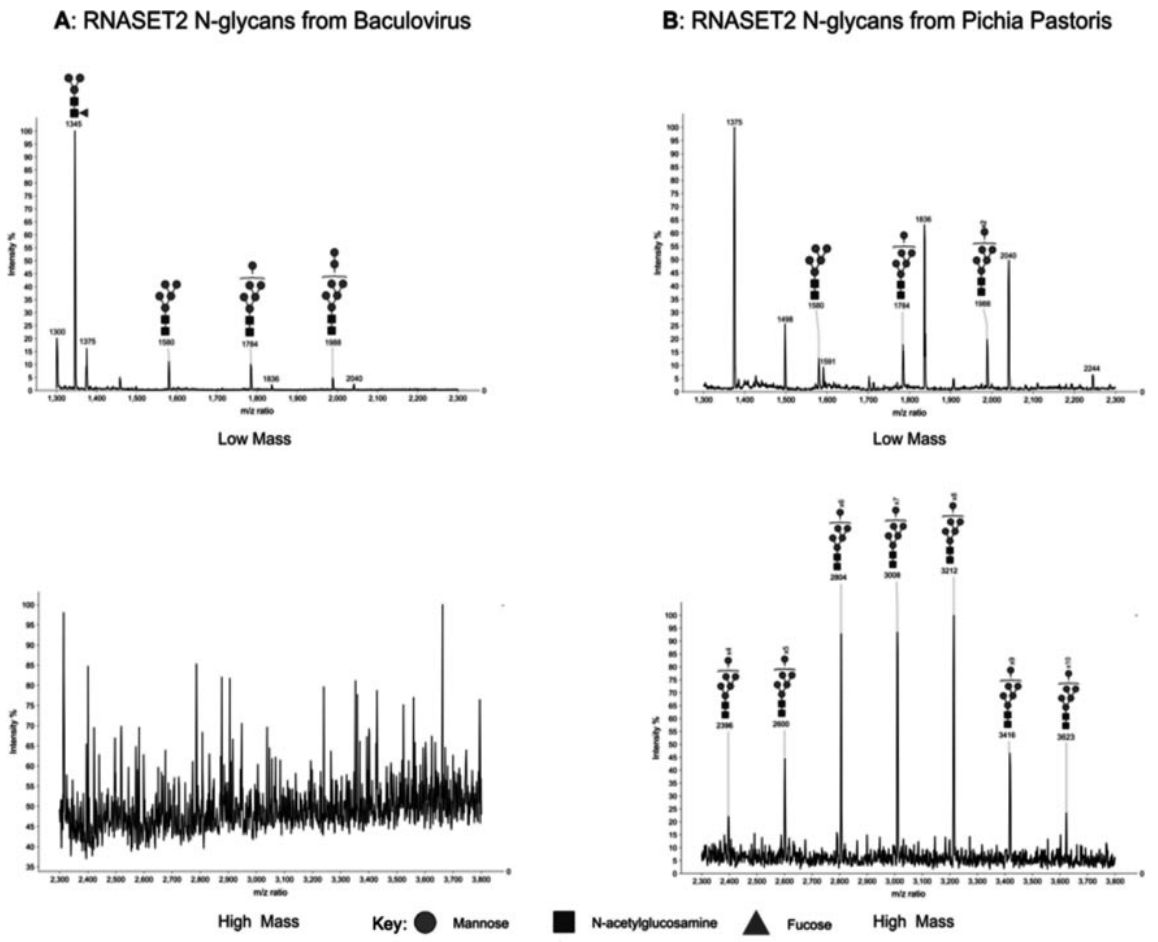


Fig. 5. *N*-glycan structures released from RNASET2 by PNGase F digestion and analyzed by MALDI-TOF MS. (A) Profile of total permethylated *N*-glycans in RNASET2 isolated from the baculovirus-insect cell heterologous systems. Upper panel: Low Masses (*m*/*z* interval: 1,300–2,300), fraction eluted in 50% acetonitrile/water during Sep-Pak purification. Annotated structures correspond to a core fucosylated glycan and high mannose glycans (Man2–Man4). Nonannotated peaks correspond to impurities and glycans originated from animal proteins included in the media used for baculovirus growth. Lower panel: High Masses (*m*/*z* interval: 2,300–3,800), fraction eluted in 75% acetonitrile/water during Sep-Pak purification. The signals spikes observed correspond to electrical and chemical noise. (B) Profile of total permethylated *N*-glycans in RNASET2 isolated from *Pichia pastoris.* Upper Panel: Low Masses (*m*/*z* interval: 1,300–2,300), fraction eluted in 50% acetonitrile/water during Sep-Pak purification. Annotated structures correspond to high mannose glycans (Man2–Man4). Nonannotated peaks correspond to impurities and glycans originated from animal proteins included in the media used for *P. Pastoris* growth. Lower panel: High Masses (*m*/*z* interval: 2,300–3,800), fraction eluted in 75% acetonitrile/water during Sep-Pak purification. Annotated *m*/*z* values correspond to high mannose glycans (Man6–Man12) detected in *P. Pastoris* sample.

with a yield of 7–20 mg/L in *P. pastoris* [23],[24]. Strikingly, in keeping with our data, a significant variation in expression levels between different protein versions was observed in the latter study, suggesting that intrinsic protein properties can influence expression levels.

RNASET2 is an *N*-glycosylated protein and three asparagines residues have been predicted *in silico* and experimentally validated as glycosylation sites *in vitro* [4]. Indeed, treatment of human cell extracts with peptide-*N*-glycosydase F confirmed that at least 7 kDa of the total apparent mass of RNASET2 in SDS-PAGE are contributed by carbohydrates [4]. In our hands, human recombinant RNASET2 expressed in the BEVS displayed a limited glycosylation heterogeneity, as demonstrated by the occurrence of bands ranging from 36 to 40 kDa detected with

an anti-RNASET2-specific antibody. By contrast, the same protein expressed in *P. pastoris* showed greater heterogeneity, as both mildly glycosylated (ranging from 38 to 45 kDa) and highly glycosylated forms (ranging from 50 to 80 kDa) of RNASET2 were detected in immunoblotting. As expected, all these forms turned into a single band of about 31 kDa in both *P. pastoris* and in the BEVS following enzymatic deglycosylation.

Preliminary data regarding the purification of RNASET2 from *P. pastoris* showed that the 39–45 kDa glycosylated forms were purified more efficiently than the hyperglycosylated forms. This could be explained by sterical hindrance of the abundant carbohydrates that could render the 6× histidine tag less accessible for binding to the resin. Therefore, although produced, these hyperglycosylated forms of RNASET2 (that do not usually occur in human cell extracts) represent a negligible fraction of the purified protein. In both heterologous expression systems used in this study, an anti-RNASET2 reactive form of 26 kDa was also occasionally observed, which probably represents a proteolytic degradation product, as deglycosylation treatment produced a further shift of MW down to 19 kDa. The 26-kDa form we observed is recognized by two different polyclonal antibodies against RNASET2 and also by an antibody against the C-terminal HA tag, suggesting that spontaneous proteolysis occurs at the N-terminus. Indeed, ribonucleases from the Rh/T2/S family have been described to possess protease-sensitive regions [25] and we previously showed that RNASET2 undergoes physiological proteolysis in mammalian cells, resulting in 31 and 27 kDa isoforms, which are targeted to the lysosome [4]. However, further analysis of the human forms showed that they were both generated by a cleavage event occurring in the C-terminal moiety of the RNASET2 protein. By contrast, the 26-kDa band occasionally observed in *Pichia* clones likely originated from a cleavage event at the N-terminus, as the C-terminal tag is still present. Taken together, these data suggest that the latter likely represents the result of a host-specific cleavage event of little physiological relevance.

Human RNASET2 was recently expressed in *P. pastoris* by another group [20], who described a single 27 kDa form whose expression levels were not reported. Although this molecular weight could be ascribed to the RNASET2 protein without signal peptide, it is not compatible with the glycosylation pattern that was described *in vivo* for RNASET2.

To better define the structural and functional features of recombinant RNASET2, we have also characterized the glycosylation pattern and the catalytic activity of the proteins purified from the two heterologous protein expression systems. Very distinct patterns of glycosylation were observed with the baculovirus system producing a largely glycosylated protein with a core fucosylated paucimannose glycan, whereas *P. Pastoris* expressed RNASET2 protein with polymannose structures, as expected for this expression system [8],[9].

Finally, recombinant wild-type RNASET2 purified from both systems was found to be catalytically competent. In the conditions tested, RNASET2 purified from *P. pastoris* showed a 30% higher activity than the protein purified from the baculovirus system, the activity of the first being 1.02 (0.013 Abs260/Min) against 0.67 (0.009 Abs260/Min) for the recombinant protein expressed in *P. pastoris*.

This result is of great practical relevance for future molecular and functional assays, whose goal is to achieve a detailed functional characterization of this protein. In recent years, RNASET2 has been shown by our group to behave as a potent oncosuppressor *in vivo* [5–7],[18]. This finding, coupled to the fact that RNASET2 is a secreted extracellular protein whose antiproliferative role was recently found to be carried out in a non-cell autonomous manner [26], makes the use of catalytically competent recombinant RNASET2 in both *in vitro* and *in vivo* cancer models a powerful tool to shed light on the functional roles of this unusual class of ribonucleolytic enzymes.

## Acknowledgements

We thank Luciano Piubelli for his help in evaluation of enzyme activity and Mauro Fasano and Tiziana Alberio for helpful discussion. Francesco Acquati was supported by a grant from the Fondazione Comunitaria del Varesotto ONLUS. Christer Lindqvist was supported by grants from The Academy of Finland and The Albin Johansson Foundation. The mass spectrometry work was supported by the Biotechnology and Biological Sciences Research Council (BBF0083091) and Marie Curie Initial Training Network, EuroglycoArrays Project, part of the FP7 People Programme.

## References

[1] Luhtala, N. and Parker, R. (2010) *Trends Biochem Sci.* **35**, 253–259.
[2] Deshpande, R. A. and Shankar, V. (2002) *Crit. Rev. Microbiol.* **28**, 79–122.
[3] Trubia, M., Sessa L., and Taramelli, R. (1997) *Genomics* **42**, 342–344.
[4] Campomenosi, P., Salis, S., Lindqvist, C., Mariani, D., Nordstrom T., Acquati F., and Taramelli, R. (2006) *Arch. Biochem. Biophys.* **449**, 17–26.
[5] Acquati, F., Morelli, C., Cinquetti R., Bianchi, M. G., Porrini, D., Varesco, L., Gismondi, V., Rocchetti, R., Talevi, S., Possati, L., Magnanini, C., Tibiletti, M. G., Bernasconi, B., Daidone, M. G., Shridhar, V., Smith, D. I., Negrini, M., Barbanti-Brodano, G., and Taramelli, R. (2001) *Oncogene* **22**, 980–988.
[6] Acquati, F., Possati, L., Ferrante, L., Campomenosi, P., Talevi, S., Bardelli, S., Margiotta, C., Russo, A., Bortolotto, E., Rocchetti, R., Calza, R., Cinquetti, R., Monti, L., Salis, S., Barbanti-Brodano, G., and Taramelli, R. (2005) *Int. J. Oncol.* **26**, 1159–1168.
[7] Monti, L., Rodolfo, M., Lo Russo, G., Noonan, D., Acquati, F., and Taramelli, R. (2008) *Oncol. Res.* **17**, 69–74.
[8] Cereghino, J. L. and Cregg, J. M. (2000) *FEMS Microbiol. Rev.* **24**, 45–66.
[9] Cregg, J. M., Cereghino, J. L., Shi, J., and Higgins, D. R. (2000) *Mol. Biotechnol.* **16**, 23–52.
[10] Daly, R. and Hearn, M. T. J. (2005) *Mol. Recognit.* **18**, 119–138.
[11] Gietz, R. D., Schiestl, R. H., Willems, A. R., and Woods, R. A. (1995) *Yeast* **11**, 355–360.
[12] Vaughn, J. L., Goodwin, R. H., Tompkins, G. J., and McCawley, P. (1977) *In Vitro* **13**, 213–217.
[13] Dell, A., Reason, A. J., Khoo, K. H., Panico, M., McDowell, R. A., and Morris H. R. (1994) *Methods Enzymol.* **230**, 108–132.
[14] Jang-Lee, J., North, S. J., Sutton-Smith, M., Goldberg, D., Panico, M., Morris, H., Haslam, S., and Dell, A. (2006) *Methods Enzymol.* **415**, 59–86.
[15] Ceroni, A., Maass, K., Geyer, H., Geyer, R., Dell, A., and Haslam, S. M. (2008) *J. Proteome Res.* **7**, 1650–1659.
[16] Blank, A. and Dekker, C. A. (1981) *Biochemistry* **20**, 2261–2267.
[17] Brown, P. H. and Ho, T. H. (1986) *Plant Physiol.* **82**, 801–806.
[18] Smirnoff, P., Roiz, L., Angelkovitch, B., Schwartz, B., and Shoseyov, O. (2006) *Cancer* **107**, 2760–2769.
[19] Ohgi, K., Horiuchi, H., Watanabe, H., Takagi, M., Yano, K., and Irie, M. (1991) *J. Biochem.* **109**, 776–785.
[20] Mu J. and Kao, T. H. (1992) *Biophys. Res. Commun.* **187**, 299–304.

[21] Huang, C., Chien, M. S., Hu, C. M., Chen, C. W., and Hsieh, P. C. J. (2006) *Virol. Meth.* **132**, 40–47.
[22] Hulst, M. M., Panoto, F. E., Hoekman, A., van Gennip, H. G., and Moormann, R. J. (2000) *J Virol.* **74**, 9553–9561.
[23] Numata, T., Suzuki, A., Kakuta, Y., Kimura, K., Yao, M., Tanaka, I., Yoshida, Y., Ueda, T., and Kimura, M. (2003) *Biochemistry* **42**, 5270–5278.
[24] Kimura, K., Numata, T., Kakuta, Y., and Kimura, M. (2004) *Biosci. Biotechnol. Biochem.* **68**, 1748–1757.
[25] Iwama, M., Kusano, A., Ogawa, Y., Ohgi, K., and Irie, M. (1998) *Biol. Pharm. Bull.* **21**, 634–637.
[26] Acquati, F., Bertilaccio, S., Grimaldi, A., Monti, L., Cinquetti, R., Bonetti, P., Lualdi, M., Vidalino, L., Fabbri, M., Sacco, M.G., van Rooijen, N., Campomenosi, P., Vigetti, D., Passi, A., Riva, C., Capella, C., Sanvito, F., Doglioni, C., Gribaldo, L., Macchi, P., Sica, A., Noonan, D.M., Ghia, P., and Taramelli, R. (2011) *Proc. Natl. Acad. Sci. USA.* **108**, 1104–1109.

PLoS ONE

# P53 family members modulate the expression of PRODH, but not PRODH2, via intronic p53 response elements

--Manuscript Draft--

| | |
|---|---|
| **Manuscript Number:** | |
| **Article Type:** | Research Article |
| **Full Title:** | P53 family members modulate the expression of PRODH, but not PRODH2, via intronic p53 response elements |
| **Short Title:** | PRODH and PRODH2 regulation by p53 family members |
| **Corresponding Author:** | Paola Campomenosi, Ph.D.<br>University of Insubria<br>Varese, ITALY |
| **Keywords:** | proline dehydrogenase/proline oxidase; response elements; p53 family; tumor suppressor; apoptosis; metabolism |
| **Abstract:** | The tumor suppressor p53 was previously shown to markedly up-regulate the expression of the PRODH gene, encoding the proline dehydrogenase (PRODH) enzyme, which catalyzes the first step in proline degradation. Also PRODH2, which degrades 4-hydroxy-L-proline, a product of protein (e.g. collagen) catabolism, was recently described as a p53 target. Here, we confirm p53-dependent induction of endogenous PRODH in response to genotoxic damage in cell lines of different histological origin and we establish that overexpression of p73β or p63β is sufficient to induce PRODH expression in p53-null cells. The p53 family-dependent transcriptional activation was linked to specific intronic response elements (REs), among those predicted by bioinformatics tools and experimentally validated by a yeast-based transactivation assay upon modulated expression of p53, p63 and p73 and by p53 occupancy measurements in HCT116 human cells. Instead, PRODH2 was not responsive to p63 nor p73 and was at best a weak p53 target, based on minimal levels of PRODH2 transcript induction by genotoxic stress observed only in one of four p53 wild-type cell lines tested. Consistently, all predicted p53 REs in PRODH2 were poor matches to the p53 RE consensus and showed limited responsiveness, only to p53, in the functional assay. Taken together, our results highlight that PRODH but not PRODH2 expression is likely under control of the entire p53 family members, supporting a deeper link between p53 proteins and metabolic pathways, as PRODH functions in modulating the balance of proline and glutamate levels and of their derivative alpha-keto-glutarate in the metabolism under normal and pathological (tumor) conditions. |
| **Order of Authors:** | Ivan Raimondi |
| | Yari Ciribilli |
| | Paola Monti |
| | Alessandra Bisio |
| | Loredano Pollegioni |
| | Gilberto Fronza |
| | Alberto Inga |
| | Paola Campomenosi, Ph.D. |
| **Suggested Reviewers:** | Giannino Del Sal<br>University of Trieste<br>delsal@lncib.it |
| | Thierry Soussi<br>Cancer Centre Karolinska (CCK)<br>thierry.soussi@ki.se |
| | Tim Crook |

| | |
|---|---|
| | University of Dundee<br>tr.crook@gmail.com |
| **Opposed Reviewers:** | |

**ABSTRACT**

The tumor suppressor p53 was previously shown to markedly up-regulate the expression of the *PRODH* gene, encoding the proline dehydrogenase (PRODH) enzyme, which catalyzes the first step in proline degradation. Also *PRODH2*, which degrades 4-hydroxy-L-proline, a product of protein (e.g. collagen) catabolism, was recently described as a p53 target. Here, we confirm p53-dependent induction of endogenous *PRODH* in response to genotoxic damage in cell lines of different histological origin and we establish that overexpression of p73β or p63β is sufficient to induce *PRODH* expression in p53-null cells. The p53 family-dependent transcriptional activation was linked to specific intronic response elements (REs), among those predicted by bioinformatics tools and experimentally validated by a yeast-based transactivation assay upon modulated expression of p53, p63 and p73 and by p53 occupancy measurements in HCT116 human cells. Instead, PRODH2 was not responsive to p63 nor p73 and was at best a weak p53 target, based on minimal levels of PRODH2 transcript induction by genotoxic stress observed only in one of four p53 wild-type cell lines tested. Consistently, all predicted p53 REs in PRODH2 were poor matches to the p53 RE consensus and showed limited responsiveness, only to p53, in the functional assay. Taken together, our results highlight that PRODH but not PRODH2 expression is likely under control of the entire p53 family members, supporting a deeper link between p53 proteins and metabolic pathways, as PRODH functions in modulating the balance of proline and glutamate levels and of their derivative alpha-keto-glutarate in the metabolism under normal and pathological (tumor) conditions.

## INTRODUCTION

The p53 protein exerts its tumour suppressive function acting primarily as a transcription factor, that controls the expression of a large and ever increasing number of target genes in response to a variety of stresses [1-3]. Well known outcomes are cell cycle arrest, DNA repair, apoptosis, but more recently also p53 involvement in the induction of autophagy and regulation of metabolism have been described [4,5].

Historically, p53 represents the founder member of the p53 family, to which also p63 and p73 belong. These proteins share the highest level of homology in the DNA binding domain and often recognize the same REs in the promoter of target genes. However, the pattern of transcribed genes upon induction of the different family members does not overlap completely [6] and neither do the biological functions, as exemplified by their different roles during embryonic development [7].

To complicate matters, the various p53 family members can also influence each other's function and transactivation activity through a complex network created by the different transactivation efficiency of the various isoforms and the presence of "p53" REs in their own regulatory regions [8,9]. Clearly, there is a complex transactivation network within the p53 family and between the p53 family and other transcription factors in the regulation of target genes [10,11].

This underlines the importance of understanding how transactivation specificity arises through the mapping and the characterization of the REs present in target genes. Regulatory regions within genes are a complex field of investigation. Nevertheless, their thorough characterization in terms of sequence and location may help assessing coordinated regulation by transcription factors, as well as cell type and cell context (type of stress, kinetics) dependencies on gene expression, ultimately contributing to define gene functions [11,12].

Several years ago Polyak and colleagues identified *PIG6*, also known as *PRODH/POX*, among the apoptotic genes induced by p53 after adriamycin treatment [13]. Nevertheless, a systematic search and validation of the p53 REs in these genes have never been carried out. As a consequence, PRODH is not considered as a proven p53 target in most of the published reviews. Since its discovery, evidence has been accumulating on the role that proline dehydrogenase, the protein encoded by the *PRODH* gene, could play in suppressing tumorigenesis, suggesting its contribution as an apoptosis effector through ROS induction [14]. Very recently, a PRODH-dependent induction of autophagy has also been described [15]. The biochemical function of PRODH (EC 1.5.99.8) is the oxidation of proline to ∆'-pyrroline-5-carboxylic acid (P5C), which is converted to glutamate by P5C dehydrogenase (EC 1.5.1.12). Notably, also the gene encoding P5C dehydrogenase, *ALDH4*,

has been reported to be a target of p53 [16], suggesting the importance of the proline to glutamate conversion in mediating p53 functions.

More recently, also 4-hydroxy-L-proline (OH-proline) dehydrogenase (EC 1.1.1.104), encoded by the *PRODH2* gene, was shown to be induced by p53 [17], although there are conflicting results in the literature [18]. Like proline, OH-proline, the substrate of hydroxy-proline dehydrogenase, is present in some cellular, extracellular and dietary proteins, such as collagen, that therefore represent an abundant source of substrate. Nevertheless, while downstream metabolism of proline can impact several aspects of cellular metabolism, metabolism of OH-proline yields compounds that can be used to generate ATP or ROS but do not have anaplerotic or regulatory functions [17].

The aim of this study was to identify and validate the p53-REs present in the *PRODH* and *PRODH2* genes and to investigate their responsiveness to the other p53 family members. Here we show that four intronic p53 REs, located in introns 2 and 3 of the *PRODH* gene, are the most active among the REs examined. Interestingly, one of them is efficiently transactivated by all p53 family members. Conversely, the putative REs identified in the *PRODH2* gene respond poorly even in the presence of high p53 levels and are inactive with p63 and p73, as revealed with a yeast functional assay. Moreover, PRODH2 expression was weakly detectable following genotoxic stress in only one of the p53 wild-type cell lines we tested, consistent with contradictory results in the literature [17,18].

## MATERIALS AND METHODS

### Reagents

Doxorubicin and 5-fluorouracil (5FU) were from Sigma–Aldrich (Milan, Italy), Nutlin-3A was purchased from Alexis Biochemicals (Enzo Life Sciences, Exeter, UK). All oligonucleotides were from *Eurofins MWG Operon* (Ebersberg, Germany). Bacteriological reagents (Bactoagar, Yeast extract, Peptone) were from DIFCO (BD Biosciences, Milan, Italy) and all other reagents were from Sigma Aldrich (Milan, Italy) unless otherwise specified.

### Cell lines and treatments

The human breast adenocarcinoma-derived MCF7 cell line was obtained from the InterLab Cell Line Collection bank, ICLC (Genoa, Italy); the colon adenocarcinoma HCT116 ($p53^{+/+}$) cell line and its p53−/− derivative were a gift from B. Vogelstein (The Johns Hopkins Kimmel Cancer Center, Baltimore, Maryland, USA) [19]. LoVo colon adenocarcinoma cells were a gift from M. Broggini (Istituto Farmacologico Mario Negri, Milan Italy) [20], while the hepatocellular carcinoma derived HepG2 cells were a generous gift from A. Provenzani (Laboratory of Genomic Screening, CIBIO, University of Trento) [21]. Cells were maintained in DMEM or RPMI supplemented with 10% FCS, 1% glutamine and antibiotics (100 units/ml penicillin plus 100 µg/ml streptomycin).

To study PRODH expression in response to p53 induction or stabilization, cells were seeded at 80% confluence and treated with genotoxic agents or Nutlin-3A at the indicated concentrations for 16 hours.

For transient transfection experiments with HCT116 $p53^{-/-}$, 7 x $10^5$ cells were seeded in 6-well plates 24 hours before transfection to reach ~70% confluency on transfection day. Cells were transfected using 2 µg plasmid DNA/well and the TransIT-LT1 transfection reagent (Mirus, Milan, Italy) according to the manufacturer's instructions. Human p53 was expressed from the pC53-SN3 plasmid [22], while p63beta and p73beta cDNAs were expressed either from pCDNA3.1 [11] or pCI-Neo vectors (Monti et al., unpublished). All mammalian constructs were extracted from XL1blue *E. coli* cells using the endotoxin free PureYield plasmid midi-prep kit, according to the manufacturer's protocol (Promega, Milan, Italy). In all experiments, cells were harvested 24 hours after transfection, trypsinized and collected for RNA extraction.

### Analysis of PRODH and PRODH2 transcript levels

To quantify PRODH and PRODH2 mRNAs following treatments or transfections, cells were harvested and washed once with PBS. Total RNA was extracted using the RNeasy Kit (Qiagen, Milan, Italy) according to the manufacturer's instructions. For real-time quantitative PCR (qPCR), cDNA was generated from 2 µg of RNA by using the RevertAid First Strand cDNA Synthesis Kit (Fermentas, Milan, Italy) or the iScript Reverse Transcription Supermix for RT-qPCR (Biorad). qPCR was performed on a RotorGene 3000 thermal cycler (Corbett Life Science, Ancona, Italy) or on a StepOne thermal cycler (AB, Milan, Italy) using the KAPA Probe Fast Universal 2X qPCR Master Mix (Resnova, Rome, Italy) with Taqman assays (AB, Milan, Italy) or the Sso Advanced Sybr Green Supermix (Biorad). Primers are reported in Table S2. Relative mRNA quantification was obtained using the ΔΔCt method, where the glyceraldehyde 3-phosphate dehydrogenase (*GAPDH*) or the β2-microglobulin (B2-M) genes served as internal control. *P21* was used as positive control for the efficacy of the induction of p53 family members by the specific treatment.

**Construction of yeast reporter strains and media**

Nine different *Saccharomyces cerevisiae* reporter strains were constructed, containing the firefly luciferase gene under the control of the p53 RE found by bioinformatics tools (see below) in the *PRODH* and *PRODH2* genes. To insert the putative p53 RE upstream of the luciferase reporter genes the "*delitto perfetto approach"* for *in vivo* mutagenesis was used [23], starting from the available master reporter strain yLFM-ICORE. The master strain contains the luciferase cDNA integrated in the yeast genome downstream a minimal promoter derived from the CYC1 gene. The counter selectable ICORE cassette is located 5' to the minimal promoter and confers high targeting efficiency of the locus by oligonucleotides that contain the desired RE sequences (Table S1) [23]. The recombinant yeast strains were checked by colony PCR and direct sequencing for proper positioning of the inserted REs (BMR Genomics, Padua, Italy).

Yeast cells were grown in YPDA medium (1% yeast extract, 2% peptone, 2% dextrose with the addition of 200 mg/L adenine). For plating, YPDA medium was supplemented with 2% bactoagar, while selective minimal plates lacking tryptophan or leucine but containing adenine (200 mg/L) and dextrose as carbon source were used to isolate transformant clones with expression vectors for p53 family proteins. 5-Fluoroorotic acid (FOA) and geneticin (G418) were added to the plates when necessary [23].

**Constructs for the expression of p53 family members in *S. cerevisiae***

To express members of the p53 family in yeast, the pTSG- (TRP1) or pLSG-based (LEU2) constructs, harbouring respectively p73β and p63β cDNAs (TA isoforms) under the control of the

*GAL1,10* inducible promoter, were used [24,25]. This promoter allows to modulate the expression of the proteins under study by varying the galactose concentration in the culture medium The wild type p53 cDNA was similarly expressed using the pLS89 expression vector (TRP1) [24]. Empty vectors pRS-314 or pRS-315 were used as a controls; these vectors contain respectively the TRP1 (as pTSG-) or LEU2 (as pLSG-) yeast selectable markers.

**Luciferase assays in yeast**

To measure the transactivating capacity of p53 family members on the putative p53 REs identified in *PRODH* and *PRODH2* genes, the expression vectors described above were transformed into the yLFM-RE strains using the lithium acetate method. After transformation the yeast strains were grown on minimal medium lacking tryptophan or leucine but containing adenine (200 mg/L) and dextrose as carbon source, to keep the expression of p53 family members inhibited. After 2-3 days at 30°C, transformants were streaked onto the same type of plates and grown for an additional day. For each reporter strain, the basal luciferase activity was measured from the empty vectors pRS314- or pRS315-transformed colonies.

Transformant colonies were grown in 100 µL of selective medium containing raffinose as the sole carbon source in a transparent 96-well plate for 16-24 hours at 30°C. Different concentrations of galactose (0.008% and 1%) were added to induce low or high levels of expression of the p53 family members. $OD_{600}$ was directly measured in the multi-well plate to normalize for cell density using a multilabel plate reader (Infinite M200-Pro, Tecan, Milan, Italy). Ten µL of cells suspension were transferred to a white 384 plate (BrandTech Scientific Inc., Essex, CT, USA) and mixed with an equal volume of PLB buffer 2X (Passive Lysis Buffer, Promega). After 15 minutes of shaking at room temperature, 10 µL of *Firefly* luciferase substrate (Bright Glo Luciferase Reporter Assay, Promega) were added. Luciferase activity was measured and results were expressed as fold of induction compared to empty vectors.

**Chromatin immunoprecipitation experiments in MCF7 or HCT116 cell lines.**

Chromatin immunoprecipitation (ChIP) assays were performed as previously described (Menendez et al 2007) using the EZ Magna ChIP kit (Upstate Biotechnology, Millipore, Lake Placid, NY, USA). Briefly, HCT116 $p53^{+/+}$ and $p53^{-/-}$ cells were plated onto 150-mm dishes, let to grow for one day and treated with 1.5 µM doxorubicin for 16 h or left untreated. Cells were then cross-linked with 1% formaldehyde for 10 min at 37 °C and treated subsequently with 125 mM glycine for 5 min. Samples were processed following the manufacturer's instructions. Cell lysates were then sonicated using conditions that enabled us to evaluate the distinct contribution of the different REs.

Sonication was done using a Misonix 4000 instrument equipped with a multiplate horn (Misonix, Qsonica LLC., Newtown, CT, USA). Samples were sonicated using twelve cycles of 20 seconds pulses at 80% of amplitude with a 40 seconds pause in-between and the accuracy of shared chromatin fragments was checked on a 2% agarose gel. The p53-specific monoclonal antibody DO-1 (Santa Cruz Biotechnology, Milan, Italy) and magnetic Protein G beads were used in the ChIP assay. As a negative control we used mouse IgG (Santa Cruz Biotechnology). Once reverted the crosslinks, PCR amplifications were performed on immunoprecipitated and purified chromatin using primers to amplify specific regions in the PRODH promoter and introns and in the *CCNB1* gene, that does not contain any p53 REs (No Binding Site, NBS) (Table S2). Furthermore, qPCR was used to quantify the fold change in site occupancy. The qPCR reaction was performed with 2 µL of each sample and using the Power SYBR® Green PCR Master Mix (Applied Biosystems, Foster City, CA, USA) following manufacturer's procedures. To determine the fold change in site occupancy the SuperArray ChIP-qPCR Data Analysis tool was used (SA Biosciences, Frederick, MD, USA). The enrichment values were obtained after normalization against the input, then computing the ratio between the doxorubicin vs mock treatment.

**Bioinformatics analysis**

Sequences of the human PRODH and PRODH2 reference mRNAs (NM_016335.4 and NM_021232.1, respectively) were retrieved from NCBI (http://www.ncbi.nlm.nih.gov/nucleotide), and the genomic organization was obtained with the UCSC Blat algorithm at http://genome.ucsc.edu/ followed by extension of the promoter region retrieved, using the function "gene sorter" at UCSC.

To search for the p53 REs in the *PRODH* and *PRODH2* genes, the following sites were consulted:

-TESS (http://www.cbil.upenn.edu/tess.);

-p53MH algorithm (http://linkage.rockefeller.edu/ott/p53MH.htm.) [26];

-p53 FamTaG ( http://p53famtag.ba.itb.cnr.it/index.php.) [27];

-TFBIND (http://tfbind.hgc.jp/) [28].

## RESULTS

### 1. PRODH levels increase upon genotoxic stress or p53 stabilization

To confirm that *PRODH* is inducible by genotoxic stress via p53, we treated cell lines known to harbour wild type p53 with doxorubicin or 5-fluorouracil. PRODH transcript was readily induced by doxorubicin in all cell lines tested except in HCT116 $p53^{-/-}$ cells, confirming that induction was indeed p53 dependent (Figure 1). PRODH expression also increased in a dose dependent manner when cells were treated with the p53 stabilizer Nutlin-3A (Figure 1).

As PRODH induction occurred upon increase of p53 levels due to either genotoxic stress or treatment with a p53 stabilizer, we suggest that it is indeed p53 dependent.

### 2. The *PRODH* gene contains numerous putative p53 REs

A combination of four bioinformatic tools for identifying p53 specific or transcription factors binding sites in general (p53MH, p53FamTag, Tess, TFBIND) along with manual search was used to scan the *PRODH* gene. Nine putative p53 REs were identified and named according to their distance from the Transcription Start Site (TSS) based on reference sequence NM_016335.4 (Table 1).

Six REs were selected for validation, based on the evaluation of the following parameters: number and position of mismatches with respect to the consensus, presence of a spacer sequence between the two decameric sites, and position in the gene (Table 1). Two putative REs were located in the promoter of the *PRODH* gene, at positions -3.1 and -0.9 kb from TSS; the latter has already been described [29] and was selected, although it did not completely fulfilled the chosen parameters. The other REs were located in intron 2 (+1.7, +2.8 and +4.7 kb) and 3 (+6.8 kb), respectively. The latter RE, +6.8, falls within a genomic region previously identified in a ChIP-sequencing experiment but not further characterized [30].

The two REs in the promoter contained only one half-site with either one (-3.1) or no (-0.9) mismatches. An additional half-site with two mismatches, one of which involving a base in the CWWG core sequence, was present in the -3.1 RE, separated from the first half-site by a 5 bp spacer; in the -0.9 RE, a quarter site with one mismatch and a half-site with three mismatches (which can alternatively be considered a quarter site with one mismatch) were present, separated by the first half-site by 7 or 5 nucleotide spacers, respectively. Among the intronic REs, two of them (+1.7 and +6.8) had no spacers, while the +4.7 had a 3 bp spacer; the +4.7 and +6.8 REs had a consensus half-site and a second half-site with two mismatches outside the CWWG core motif, while the +1.7 had mismatches (one or two) in each half-site (Table 1). The +2.8 RE was identified

as a full site composed of the two half-sites GctCATGCCT AGGCATGgTg by the TFbind software. Upon careful analysis of the nearby sequence, this RE turned out to be surrounded by other half-sites, thus constituting a cluster with a total of 5 half-sites, of which the 3 central contained a CATG core and were devoid of any spacers, while the two external half-sites were separated from the central 3 REs by 3 bp spacers (Table 1). All of the 5 half-sites in the +2.8 RE contained at least 2 mismatches each, none involving the CWWG core motif of the consensus. Interestingly, the +6.8 was the only RE identified by the p53SCAN algorithm in the genomic region encompassing the *PRODH* gene [31].

**3. The p53 family members differentially transactivate from the PRODH REs in yeast**

Six yeast reporter strains, corresponding to the six selected REs in the *PRODH* gene (-3.1; -0.9; +1.7; +2.8; +4.7; +6.8, Figure 2A), were constructed using the *delitto perfetto* approach [23,32]. A well-established yeast transactivation assay was then applied to analyze the induction of the luciferase reporter gene upon expression of p53, p63β or p73β proteins. The expression of the p53 family members was regulated by using the galactose inducible promoter *GAL1,10*. Two different galactose concentrations were exploited to induce different levels of the transcription factors. The four intronic REs (+1.7, +2.8, +4.7 and +6.8) were induced by p53 in a dose dependent manner and showed strong response at the higher level of induction (1% galactose) (Figure 2B). At moderate induction (0.008% galactose), the +2.8, +4.7 and +6.8 already showed at least a 35-fold increase above background in luciferase activity. The REs in the promoter (-3.1 and -0.9) instead, showed no induction over the basal level even at 1% galactose, suggesting complete lack of responsiveness to p53. Also the other p53 family members can transactivate luciferase reporter expression from some REs, but only at 1% galactose. More specifically, the +1.7, +2.8 and + 6.8 REs were transactivated upon p63β expression (Figure 2B), while only +6.8 RE driven luciferase activity was increased more than 5-fold following p73β expression (Figure 2B). At low galactose induction of p63β and p73β, no detectable increase in luciferase activity was observed in any of the PRODH REs (Figure 2B).

**4. p63 and p73 can potentially transactivate PRODH also in mammalian cells**

To determine if p63 and p73 were capable of driving expression of the endogenous *PRODH* gene in mammalian cells, expression constructs for p53, p63β, p73β were transiently transfected into HCT116 $p53^{-/-}$ cells. p63β and p73β expressing cells showed a 3-fold induction of PRODH compared to vector transfected cells (Figure 3). Therefore, all members of the p53 family exhibit the potential to transactivate the *PRODH* gene.

**5. The +6.8 RE shows the highest p53 binding *in vivo***

To study the p53 binding to the PRODH gene *in vivo*, HCT116 $p53^{+/+}$ cell line and its p53 knock-out derivative HCT116 $p53^{-/-}$, were treated with doxorubicin or left untreated (mock) and cell extracts were subjected to chromatin immunoprecipitation analysis (ChIP).

The data confirmed that the +6.8 RE is the most efficiently bound by p53 in HCT116 $p53^{+/+}$ under the conditions tested, followed by +2.8, +1.7 and finally -3.1 REs. The -0.9 and +4.7 REs showed very low enrichment (Figure 4).

In conclusion, the +6.8 RE showed the highest p53 binding *in vivo* (Figure 4). Interestingly, this RE is the one most efficiently transactivated by all p53 family members in yeast assays (Figure 2B) and was the only RE in the genomic region encompassing the *PRODH* gene to be enriched in a ChIP-sequencing experiment conducted in the U2OS cell line after genotoxic treatment or p53 stabilization with Nutlin-3A (D. Menendez and M. Resnick, personal communication).

.

**6. p53, but not p63 and p73, weakly transactivates from the PRODH2 REs in yeast**

Five putative p53 consensus sequences were identified in the PRODH2 gene, three of which were in the promoter, while two were located in intron 9 at more than 10 kb from the TSS (first nucleotide present in the NM_021232.1 reference PRODH2 mRNA). The latter two REs consisted of just one half-site (Table 2); for this reason and for the distance from the TSS, they were excluded from further analysis. Of the three REs identified in the promoter (Table 2), two had a 3 bp spacer and at least four mismatches in the two half-sites, not involving the core sequence (-1.3 and -0.5), and the third (-0.27) had a 6 bp spacer and one or two mismatches in the two half-sites (Table 2).

Yeast strains carrying the -1.3, -0.5 and -0.27 REs upstream of the chromosomally located luciferase reporter, and otherwise isogenic with the previously describer PRODH RE strains, were constructed. Activity of the reporter was only slightly increased by high-level p53 expression in the three strains, with -0.27 being the most efficiently transactivated (9-fold induction) (Figure 5B). A 4-fold increase in luciferase activity was obtained with the -1.3 RE but only a 2-fold with the -0.5 RE. Expression of p63β and p73β did not result in a detectable induction of luciferase activity (Figure 5B).

Taken together the results suggested a weak responsiveness of PRODH2 gene to p53.

**7. p53 weakly transactivates the *PRODH2* gene in mammalian cells**

To confirm that PRODH2 is weakly inducible by genotoxic stress via p53, we treated different cell lines known to harbour wild type p53 with doxorubicin or 5-fluorouracil as previously described. Consistent with the literature, these genotoxic treatments resulted in a slight increase of PRODH2 transcript in LoVo cells, but we were unable to calculate the fold induction as basal levels fell below the detection limits of our qPCR. In HCT116 $p53^{+/+}$ and MCF7 cell lines, basal levels were undetectable and no induction was observed (data not shown). Finally, when the HepG2 hepatocarcinoma cell line, which turned out to have detectable basal levels, was treated with doxorubicin, no induction of the PRODH2 gene was observed (Figure 6).

Taken together, and compared with the induction levels obtained with PRODH, PRODH2 should be considered as a weak p53 target with low expression levels and limited responsiveness in human cells.

**Discussion**

In the present study, the identification and characterization of the p53 REs in the *PRODH* and *PRODH2* genes is described. These genes have been previously described as p53 targets [13,17,29], although the REs were not characterized, and their encoded proteins are involved in similar but not identical metabolic processes in the cell, i.e. a) their catalytic activity is directed on very similar substrates with limited cross-reactivity with each other [33], b) their substrates have common origin (dietary protein or collagen degradation) and c) they are both capable of inducing apoptosis via ROS production [14,17].

In spite of the fact that the role of PRODH as p53 apoptosis effector has been known for a long time [13], there is very limited information on the regulatory elements that mediate p53 responsiveness of this gene. This could explain why PRODH was not included in the list of 129 genes responding to at least three out of four of the criteria -namely the presence of a p53 RE, demonstration of its up-regulation by wild-type p53, functional confirmation of responsiveness of the identified RE in functional assays and physical binding of RE by p53- to be classified as a p53 regulated gene [2,34].

We extended the characterization of PRODH responsiveness to p53 beyond genotoxic induction, by showing that it was also strongly induced by p53 stabilization following Nutlin-3A treatment (Figure 1). We also showed, by use of a yeast transactivation assay, that p53 exhibits transactivation potential towards all intronic REs in the *PRODH* gene (Figure 2B). The identified intronic REs presented at least two complete half-sites and no mismatches in the core sequences, in contrast to the REs present in the promoter (Table 1). Ultimately, the extent of p53-dependent transactivation of the *PRODH* gene may be due to the sum of the contribution of each RE that can be bound and transactivated. Moreover, depending on p53 levels of induction one might expect titration of p53 to the REs based on its affinity and therefore different levels of PRODH induction, which may influence its activity [15,35,36].

Concerning PRODH2, our results could not conclusively demonstrate its responsiveness to p53, in fact the experimental results suggest that it is at best a very weak p53 target gene. This conclusion is based on the functional analysis of identified p53 REs in yeast and on the quantification of the endogenous gene expression in different cell lines upon genotoxic stress-dependent induction of p53 (Figures 5 and 6). The latter analysis was limited by the extremely low level of PRODH2 expression in several cell lines examined (i.e. HCT116, MCF7, LoVo), with the exception of HepG2. However, we did not observe any induction of PRODH2 by activation of p53 in this cell line, confirming the results obtained by Shinmen et al [18]. The detection of PRODH2 in basal conditions only in the hepatocellular carcinoma cell line confirms that this gene is indeed liver- and

kidney-specific, although recently the group led by Phang demonstrated its expression in RKO and its induction by p53 in RKO and LoVo cell lines [17]. In our experimental conditions LoVo cells did not show any detectable basal levels of PRODH2 but showed a potential activation upon genotoxic stress, that was however at the limit of detection by qPCR.

Therefore, although a coordinated expression of PRODH and PRODH2 would be justified by the existence of proteins, like collagen, rich both in proline and OH-proline, respectively the substrates of the two enzymes, this does not seem the case [37]. Indeed, PRODH has a broad expression and could contribute to cell metabolism, by the production of glutamate and α-KG from P5C, compounds in turn involved in many metabolic reactions and pathways in the cell.

On the lack of a coordinated p53-dependent expression of PRODH and PRODH2 some considerations can be taken into account. First, and notably, the step downstream of the PRODH reaction in the pathway leading from proline to glutamate, is catalyzed by P5C dehydrogenase, whose gene (*ALDH4*) was reported as a p53 target [16]. Second, other p53 transcriptional targets, such as TIGAR [38,39], can modulate α-KG levels. This suggests an important, and only partially elucidated, contribution of the latter compound in p53 mediated responses and stresses the contribution of PRODH in the metabolic pathways controlled by p53 [4].

Finally, in this work we also addressed the responsiveness of the *PRODH* gene to other members of the p53 family. Indeed, we found that p63β and p73β could also induce PRODH even though at lower levels compared to p53 (Figure 2A). To our knowledge, no data are available on p73 ability to transcriptionally regulate PRODH expression, while PRODH was found as one of the genes expressed more than 4-fold upon expression of a tetracyclin-inducible TAp63γ isoform [40]. The lower levels of induction with respect to p53 were not unexpected, as several other p53 targets show a decreased responsiveness to p63 and p73. Furthermore, this result could be explained, among others, by the fact that p63 and p73 show somewhat different DNA binding affinity and transactivation potential towards canonical p53 REs, possibly in part dependent on tetramer assembly and conformation stability, as recently revealed by the comparison of crystal structures of p63 and p73 bound to DNA [41-44]. It is interesting to note that the three REs that were transactivated by p63 (namely +1.7, +2.8 and +6.8) and the one transactivated by p73 (+6.8) have no spacer, consistent with previous studies indicating both for p63 and p73 a marked preference for adjacent half-site REs [12,43,45]. The +6.8kb RE turned out to be the most efficiently recognized not only by p53 but also by p63 and p73. The reason for this may be that this RE has no spacer and that the mismatches present in one half-site affects the first and last base of the consensus, which is not involved in establishing direct protein:DNA interactions and does not preclude high affinity binding of p53 [34,46-48]. However, as in mammalian cells p63 and p73 transactivated equally the

*PRODH* gene, induction appears not to be strictly correlated to the relative transactivation potentials measured in the yeast-based assay. Notably, also p73, besides p53, has been recently implicated in regulation of metabolism and autophagy and was shown to be regulated by mTOR [49-51]. As proline dehydrogenase is induced by rapamycin [52] it is tempting to speculate that this may be achieved at least in part through p73.

In conclusion, this work demonstrates that PRODH is a target of the p53 family and provides new clues for a deeper involvement of p53 proteins in metabolic pathways. In fact, in light of the recently described link between glutamine and proline, p53 acquires a more profound role in metabolism of these non essential aminoacids as well as their derivative alpha-ketoglutarate and in antagonizing c-Myc, that was recently found to downregulate PRODH as an important contribution to Myc metabolic reprogramming and induction of cell proliferation [53-56].

**Acknowledgements**

We thank Daniel Menendez and Michael A. Resnick for sharing their results on ChIP seq experiments and members of the Biochemistry laboratory at University of Insubria for their support. Dr. Raimondi is a Ph.D. student in the Molecular and Cellular Biology Ph.D. course at University of Insubria, Varese.

**References**


1. Beckerman R, Prives C (2010) Transcriptional Regulation by p53. Cold Spring Harbor Perspectives in Biology 2.
2. Riley T, Sontag E, Chen P, Levine A (2008) Transcriptional control of human p53-regulated genes. Nature Reviews Molecular Cell Biology 9: 402-412.
3. Brady CA, Attardi LD (2010) p53 at a glance. Journal of Cell Science 123: 2527-2532.
4. Vousden KH, Ryan KM (2009) p53 and metabolism. Nature Reviews Cancer 9: 691-700.
5. Gottlieb E, Vousden KH (2010) p53 Regulation of Metabolic Pathways. Cold Spring Harbor Perspectives in Biology 2.
6. Harms K, Nozell S, Chen X (2004) The common and distinct target genes of the p53 family transcription factors. Cell Mol Life Sci 61: 822-842.
7. Dotsch V, Bernassola F, Coutandin D, Candi E, Melino G (2010) p63 and p73, the Ancestors of p53. Cold Spring Harbor Perspectives in Biology 2.
8. DeYoung MP, Ellisen LW (2007) p63 and p73 in human cancer: defining the network. Oncogene 26: 5169-5183.
9. Murray-Zmijewski F, Lane DP, Bourdon JC (2006) p53/p63/p73 isoforms: an orchestra of isoforms to harmonise cell differentiation and response to stress. Cell Death and Differentiation 13: 962-972.
10. Menendez D, Inga A, Resnick MA (2010) Estrogen receptor acting in cis enhances WT and mutant p53 transactivation at canonical and noncanonical p53 target sequences. Proceedings of the National Academy of Sciences of the United States of America 107: 1500-1505.
11. Ciribilli Y, Andreotti V, Menendez D, Langen JS, Schoenfelder G, et al. (2010) The Coordinated P53 and Estrogen Receptor Cis-Regulation at an FLT1 Promoter SNP Is Specific to Genotoxic Stress and Estrogenic Compound. Plos One 5.
12. Menendez D, Inga A, Resnick MA (2010) Potentiating the p53 network. Discov Med 10: 94-100.
13. Polyak K, Xia Y, Zweier JL, Kinzler KW, Vogelstein B (1997) A model for p53-induced apoptosis. Nature 389: 300-305.
14. Donald SP, Sun XY, Hu CAA, Yu J, Mei JM, et al. (2001) Proline oxidase, encoded by p53-induced gene-6, catalyzes the generation of proline-dependent reactive oxygen species. Cancer Research 61: 1810-1815.
15. Zabirnyk O, Liu W, Khalil S, Sharma A, Phang JM (2010) Oxidized low-density lipoproteins upregulate proline oxidase to initiate ROS-dependent autophagy. Carcinogenesis 31: 446-454.
16. Yoon KA, Nakamura Y, Arakawa H (2004) Identification of ALDH4 as a p53-inducible gene and its protective role in cellular stresses. Journal of Human Genetics 49: 134-140.
17. Cooper SK, Pandhare J, Donald SP, Phang JM (2008) Novel function for hydroxyproline oxidase in apoptosis through generation of reactive oxygen species. Journal of Biological Chemistry 283: 10485-10492.
18. Shinmen N, Koshida T, Kumazawa T, Sato K, Shimada H, et al. (2009) Activation of NFAT signal by p53-K120R mutant. Febs Letters 583: 1916-1922.
19. Bunz F, Dutriaux A, Lengauer C, Waldman T, Zhou S, et al. (1998) Requirement for p53 and p21 to sustain G2 arrest after DNA damage. Science 282: 1497-1501.
20. Drewinko B, Romsdahl MM, Yang LY, Ahearn MJ, Trujillo JM (1976) Establishment of a human carcinoembryonic antigen-producing colon adenocarcinoma cell line. Cancer Res 36: 467-475.
21. Aden DP, Fogel A, Plotkin S, Damjanov I, Knowles BB (1979) Controlled synthesis of HBsAg in a differentiated human liver carcinoma-derived cell line. Nature 282: 615-616.
22. Kern SE, Pietenpol JA, Thiagalingam S, Seymour A, Kinzler KW, et al. (1992) Oncogenic forms of p53 inhibit p53-regulated gene expression. Science 256: 827-830.
23. Storici F, Lewis LK, Resnick MA (2001) In vivo site-directed mutagenesis using oligonucleotides. Nature Biotechnology 19: 773-776.

24. Inga A, Iannone R, Monti P, Molina F, Bolognesi M, et al. (1997) Determining mutational fingerprints at the human p53 locus with a yeast functional assay: a new tool for molecular epidemiology. Oncogene 14: 1307-1313.
25. Jordan JJ, Menendez D, Inga A, Nourredine M, Bell D, et al. (2008) Noncanonical DNA Motifs as Transactivation Targets by Wild Type and Mutant p53. Plos Genetics 4.
26. Hoh J, Jin S, Parrado T, Edington J, Levine AJ, et al. (2002) The p53MH algorithm and its application in detecting p53-responsive genes. Proc Natl Acad Sci U S A 99: 8467-8472.
27. Sbisa E, Catalano D, Grillo G, Licciulli F, Turi A, et al. (2007) p53FamTaG: a database resource of human p53, p63 and p73 direct target genes combining in silico prediction and microarray data. BMC Bioinformatics 8 Suppl 1: S20.
28. Tsunoda T, Takagi T (1999) Estimating transcription factor bindability on DNA. Bioinformatics 15: 622-630.
29. Maxwell SA, Kochevar GJ (2008) Identification of a p53-response element in the promoter of the proline oxidase gene. Biochem Biophys Res Commun 369: 308-313.
30. Wei CL, Wu Q, Vega VB, Chiu KP, Ng P, et al. (2006) A global map of p53 transcription-factor binding sites in the human genome. Cell 124: 207-219.
31. Smeenk L, van Heeringen SJ, Koeppel M, van Driel MA, Bartels SJ, et al. (2008) Characterization of genome-wide p53-binding sites upon stress response. Nucleic Acids Res 36: 3639-3654.
32. Storici F, Resnick MA (2003) Delitto perfetto targeted mutagenesis in yeast with oligonucleotides. Genet Eng (N Y) 25: 189-207.
33. Downing SJ, Phang JM, Kowaloff EM, Valle D, Smith RJ (1977) Proline oxidase in cultured mammalian cells. J Cell Physiol 91: 369-376.
34. Menendez D, Inga A, Resnick MA (2009) The expanding universe of p53 targets. Nature Reviews Cancer 9: 724-737.
35. Phang JM, Donald SP, Pandhare J, Liu YM (2008) The metabolism of proline, a stress substrate, modulates carcinogenic pathways. Amino Acids 35: 681-690.
36. Phang JM, Liu W, Zabirnyk O (2010) Proline Metabolism and Microenvironmental Stress. Annual Review of Nutrition, Vol 30 30: 441-463.
37. Phang JM, Pandhare J, Liu YM (2008) The metabolism of proline as microenvironmental stress substrate. Journal of Nutrition 138: 2008S-2015S.
38. Bensaad K, Tsuruta A, Selak MA, Vidal MNC, Nakano K, et al. (2006) TIGAR, a p53-inducible regulator of glycolysis and apoptosis. Cell 126: 107-120.
39. Green DR, Chipuk JE (2006) p53 and metabolism: Inside the TIGAR. Cell 126: 30-32.
40. Osada M, Park HL, Nagakawa Y, Yamashita K, Fomenkov A, et al. (2005) Differential recognition of response elements determines target gene specificity for p53 and p63. Mol Cell Biol 25: 6077-6089.
41. Chen C, Gorlatova N, Kelman Z, Herzberg O (2011) Structures of p63 DNA binding domain in complexes with half-site and with spacer-containing full response elements. Proc Natl Acad Sci U S A 108: 6456-6461.
42. Chen C, Gorlatova N, Herzberg O (2012) Pliable DNA conformation of response elements bound to transcription factor p63. J Biol Chem 287: 7477-7486.
43. Ethayathulla AS, Tse PW, Monti P, Nguyen S, Inga A, et al. (2012) Structure of p73 DNA-binding domain tetramer modulates p73 transactivation. Proc Natl Acad Sci U S A 109: 6066-6071.
44. Kitayner M, Rozenberg H, Kessler N, Rabinovich D, Shaulov L, et al. (2006) Structural basis of DNA recognition by p53 tetramers. Mol Cell 22: 741-753.
45. Jegga AG, Inga A, Menendez D, Aronow BJ, Resnick MA (2008) Functional evolution of the p53 regulatory network through its target response elements. Proceedings of the National Academy of Sciences of the United States of America 105: 944-949.

46. Weinberg RL, Veprintsev DB, Bycroft M, Fersht AR (2005) Comparative binding of p53 to its promoter and DNA recognition elements. J Mol Biol 348: 589-596.
47. Espinosa JM, Emerson BM (2001) Transcriptional regulation by p53 through intrinsic DNA/chromatin binding and site-directed cofactor recruitment. Mol Cell 8: 57-69.
48. Veprintsev DB, Fersht AR (2008) Algorithm for prediction of tumour suppressor p53 affinity for binding sites in DNA. Nucleic Acids Res 36: 1589-1598.
49. Rosenbluth JM, Mays DJ, Pino MF, Tang LJ, Pietenpol JA (2008) A gene signature-based approach identifies mTOR as a regulator of p73. Mol Cell Biol 28: 5951-5964.
50. Rosenbluth JM, Pietenpol JA (2009) mTOR regulates autophagy-associated genes downstream of p73. Autophagy 5: 114-116.
51. Rosenbluth JM, Mays DJ, Jiang A, Shyr Y, Pietenpol JA (2011) Differential regulation of the p73 cistrome by mammalian target of rapamycin reveals transcriptional programs of mesenchymal differentiation and tumorigenesis. Proc Natl Acad Sci U S A 108: 2076-2081.
52. Pandhare J, Donald SP, Cooper SK, Phang JM (2009) Regulation and Function of Proline Oxidase Under Nutrient Stress. Journal of Cellular Biochemistry 107: 759-768.
53. Liu W, Le A, Hancock C, Lane AN, Dang CV, et al. (2012) Reprogramming of proline and glutamine metabolism contributes to the proliferative and metabolic responses regulated by oncogenic transcription factor c-MYC. Proc Natl Acad Sci U S A.
54. Dang CV (2011) Therapeutic Targeting of Myc-Reprogrammed Cancer Cell Metabolism. Cold Spring Harb Symp Quant Biol.
55. Suzuki S, Tanaka T, Poyurovsky MV, Nagano H, Mayama T, et al. (2010) Phosphate-activated glutaminase (GLS2), a p53-inducible regulator of glutamine metabolism and reactive oxygen species. Proc Natl Acad Sci U S A 107: 7461-7466.
56. Hu W, Zhang C, Wu R, Sun Y, Levine A, et al. (2010) Glutaminase 2, a novel p53 target gene regulating energy metabolism and antioxidant function. Proc Natl Acad Sci U S A 107: 7455-7460.

**Legend to figures**

**Figure 1. Genotoxic stress and p53 stabilization result in a p53-dependent increase of PRODH transcript levels.** HCT116 $p53^{+/+}$, HCT116 $p53^{-/-}$ and MCF7 cell lines were treated with the genotoxic compounds Doxorubicin (DOXO, 1.5 μM) and 5-Fluorouracil (5FU, 375 μM) or with the p53 stabilizer Nutlin-3A (Nutlin, 5 or 10 μM) for 16 hours before proceeding to total RNA extraction, cDNA preparation and real time q-PCR.

PRODH (darker bars) was induced by DOXO and, albeit less efficiently, 5-FU in all cell lines tested, except in the p53 null HCT116 cell line, confirming that induction is indeed p53 dependent. Treatment of HCT116$p53^{+/+}$ with Nutlin-3A also resulted in induction of PRODH. The established p53 target gene p21 is shown for a comparison (lighter bars). In all cases, the values obtained in untreated cell lines were normalized to 1 and the average fold of induction is plotted together with the standard deviation of three biological replicates.

**Figure 2. The *PRODH* gene contains several putative p53 REs, some of which are differentially transactivated by p53 family members in yeast. A.** Scheme depicting chromosomal location and sequence of the p53 REs in the PRODH gene that were selected for further analyses. The sequence of the REs at the various indicated locations is shown (lowercase = mismatches from consensus; italics = spacer between half sites) **B.** The REs in the *PRODH* gene respond differently to different p53 family members (p53, p63β and p73β) and to different levels of galactose induction (0.008% and 1%) in the yeast transactivation assay. p53 is a very effective inducer of the four intronic REs and shows transactivation of the +2.8, +4.7 and +6.8 REs also at low levels of p53 induction, obtained at 0.008% galactose. Three of the four intronic REs are also transactivated by p63β, while only the +6.8 RE responds to p73β.

**Figure 3. Ectopic expression of p53 family members p53, p63β, p73β induces PRODH expression in mammalian cells.** Transfection of expression constructs for p53, p63β, p73β leads to a 7-fold (p53) or 3-fold increase (p63β and p73β) in PRODH transcript in HCT116$p53^{-/-}$ cells.

**Figure 4. Relative p53 occupancy levels at PRODH sites containing p53 REs.** Chromatin Immunoprecipitation experiments were performed in the HCT116 $p53^{+/+}$ colon cancer cell line and its isogenic derivative HCT116 $p53^{-/-}$, used as control, treated with DOXO or left untreated. Binding of p53 to the different REs was analysed by qPCR. The +6.8 RE showed the strongest binding to p53, followed by the +2.8, +1.7 and -3.1 REs. The -0.9 and +4.7 REs did not show any enrichment

in site occupancy compared to the "no binding site" (NBS) used as control. The dotted line indicates the level of p53 bound to the NBS after doxorubicin treatment of HCT116 $p53^{+/+}$ cells, taken as reference.

**Figure 5. The *PRODH2* gene contains three putative p53 REs, that are poorly transactivated only by p53 in yeast. A.** Scheme depicting chromosomal location and sequence of the p53 REs in the *PRODH2* gene, selected for analysis in the yeast transactivation assay. **B.** The REs identified in the *PRODH2* gene were very weakly transactivated by p53 even when the p53 levels were induced with high concentrations of galactose (1%), as measured by firefly luciferase specific activity. The -0.27 RE is the most responsive, being induced 9 fold by p53 (for comparison see the behaviour of the REs in the PRODH gene, Figure 2B).

**Figure 6. p53 does not induce PRODH2 expression in the HepG2 cell line.** The ability of genotoxic compound doxorubicin to induce expression from the *PRODH2* gene was analysed in the HepG2 hepatocellular carcinoma cell line that harbours wild type p53. This cell line contained detectable basal levels of PRODH2 (darker bars) but showed a slight repression of the transcript upon treatment with doxorubicin. The established p53 target gene p21 is shown for a comparison (lighter bars). The value obtained in the untreated cell line was normalized to 1 and the reported values derive from three biological replicates.

Table 1. p53 Response elements in the *PRODH* gene

| | Name | Location (bp from TSS) | Mismatches HS 1 | Mismatches HS 2 | Spacer (bp) | Sequence |
|---|---|---|---|---|---|---|
| 1 | **-3.1** | Promoter, -3,158 | 1 | 2 | 5 | **cGACTTGTCC***TCAAT***GAcCAcGCTC** |
| 2 | **-0.9** | Promoter, -917 | - | 1 in ¼ site, 3 in a HS | 7, 5 | CACC**AGgCT***CCACTAT***GGGCTTGTCT***TCGTG***tGACTTcTgT** * |
| 3 | **+1.7** | Int 2, +1,694 | 2 | 1 | - | **GGGCAAGgaCGGGCATGCTa** |
| 4 | **+2.8** | Int 2, +2,816 | 2, 2, 2, 2, 3 in each of the 5 half-sites | | 3,0,0,3 bp respectively | **ttACAAGCCC***TAG***GctCATGCCTAGGCATGgTgGctCATGCCT***GTA***AttCTAGCaC** ° |
| 5 | **+4.7** | Int 2, +4,727 | 3 | - | 3 | **GtcCTTGTTg***CCA***GGGCATGCCT** |
| 6 | +6.4 | Int 3, +6,453 | 1 | 2 | 8 | **GGtCTTGCTC***TGTTGCCC***AGGCTAGagT** |
| 7 | **+6.8** | Int 3, +6,817 | - | 2 | - | **AGGCTTGCCTcAGCATGTCg** |
| 8 | +14.3 | Int 8, +14,269 | 2 | 1 | 2 | **AGcCATGgTT***CC***AGcCAAGCCC** |
| 9 | +15.8 | Int 9, +15,832 | - in ¼ site | 1 | 5 | **TGTTT***GTTAG***AAGCATGTCa** |

* same RE described in [29].
° Cluster formed by 5 half-sites: the 3 central half-sites contain a CATG core and are separated by 0 bp spacer, while the two external half-sites are separated by the central 3 by 3 bp spacers. All of the 5 half-sites contain at least 2 mismatches each, although they never involve the core of the consensus.
Bold name: REs selected for experimental validation.
Bold/underlined: bases belonging to the indicated RE; italic: spacers; minuscule: mismatches within RE

Table 2. p53 Response elements in the *PRODH2* gene

| | Name | Location (bp from TSS) | Mismatches HS 1 | Mismatches HS 2 | Spacer (bp) | Sequence |
|---|---|---|---|---|---|---|
| 1 | **-1.3** | Promoter, -1,281 | 2 | 2 | 3 | **cAGCATGTTg***GGA***GGACAAGTag** |
| 2 | **-0.5** | Promoter, -0,534 | 2 | 3 | 3 | **ActCTAGCCT***GGG***cAACAAGagT** |
| 3 | **-0.27** | Promoter, -0,267 | 1 | 2 | 6 | **GtACATGTTT***CCTGCT***GtcCATGTTT** |
| 4 | +10.5 | Intron 9, +10,519 | 2 | NA | NA | **cAGCAAGaCC** |
| 5 | +10.7 | Intron 9, +10,685 | - | NA | NA | **AAGCAAGTCC** |

Bold: REs selected for experimental validation.
Bold/underlined: bases that are part of the indicated RE; italic: spacers; minuscule: mismatches within RE

Figure 1

Click here to download high resolution image

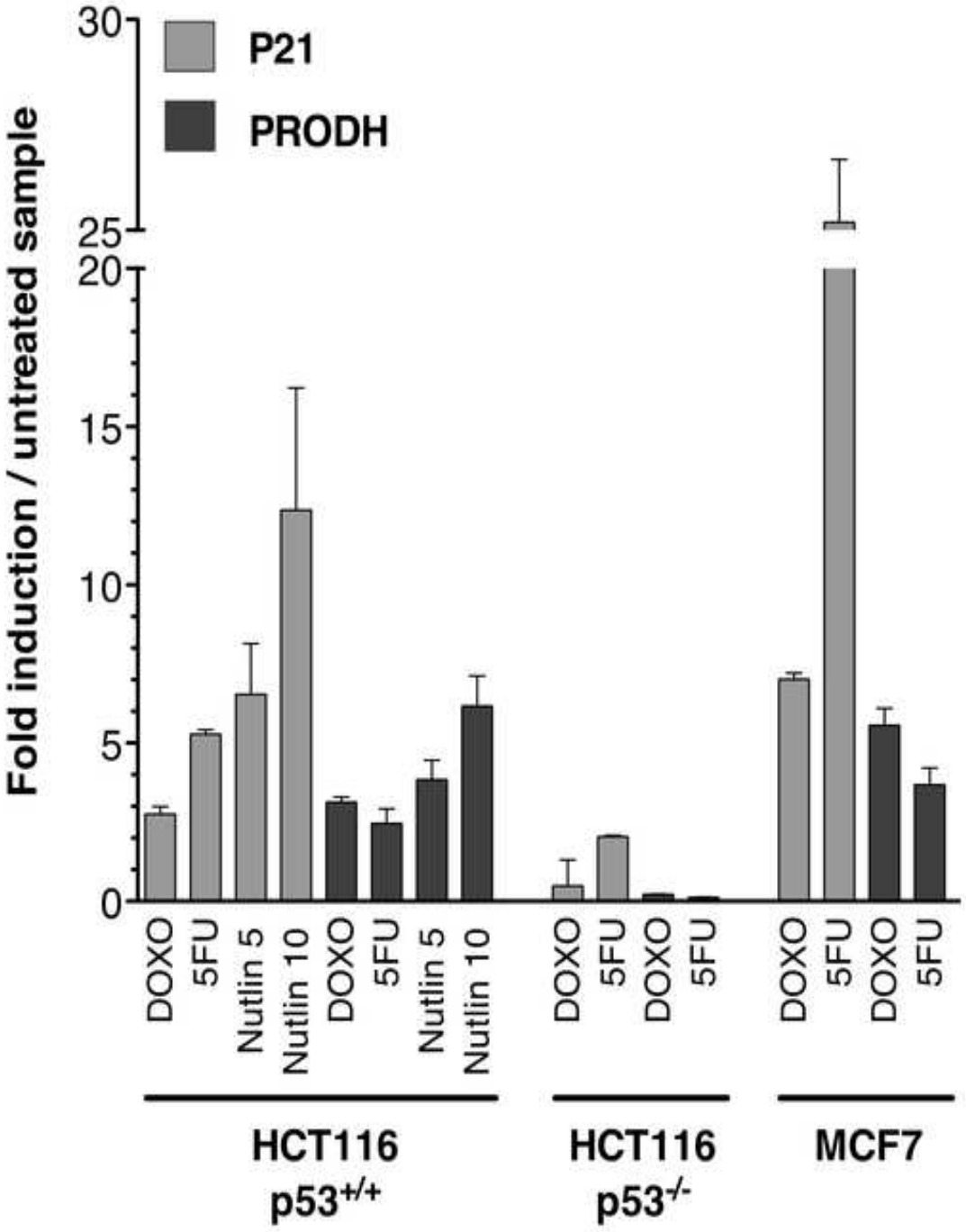

Figure 2
Click here to download high resolution image

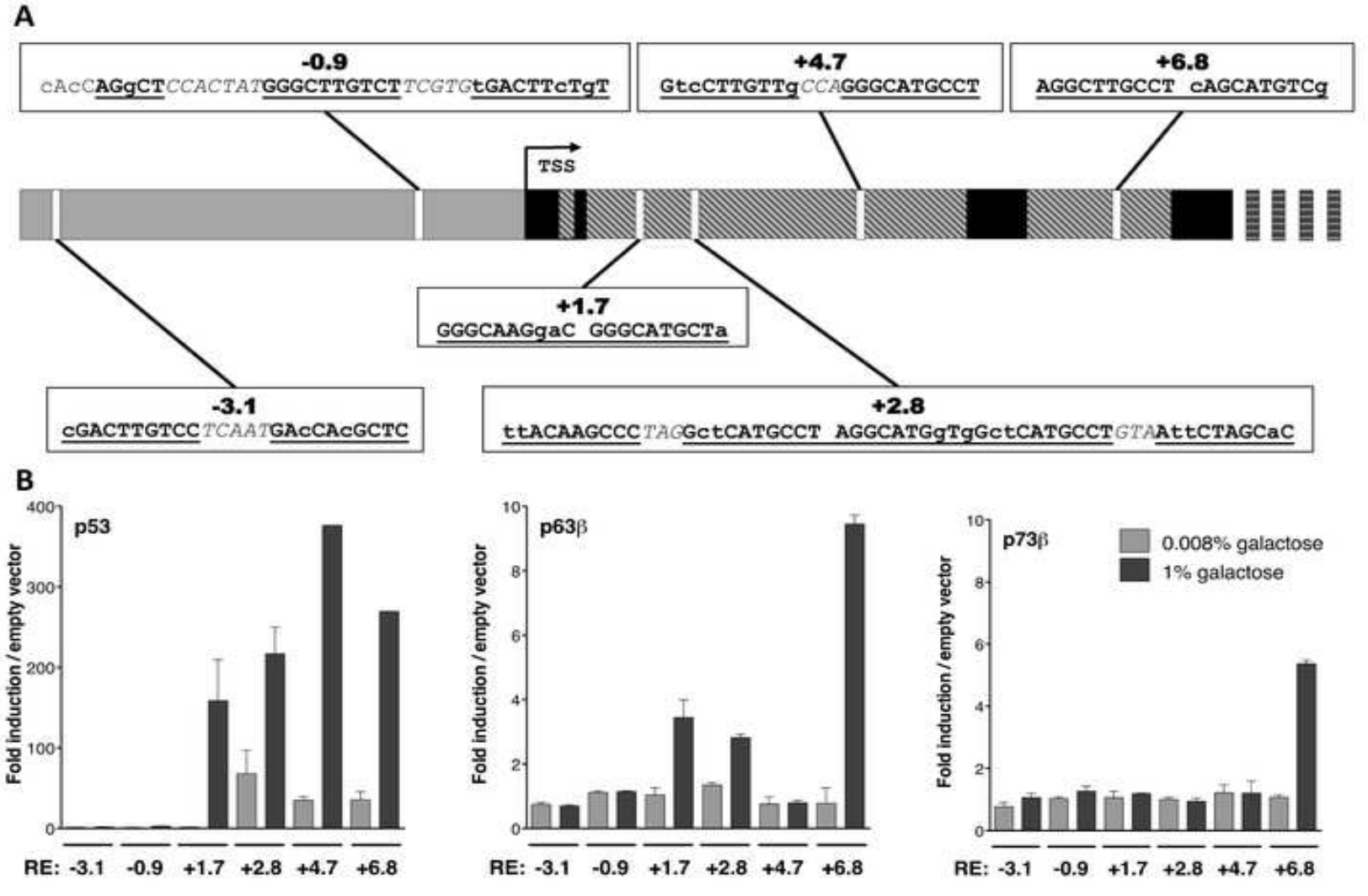

Figure 3
Click here to download high resolution image

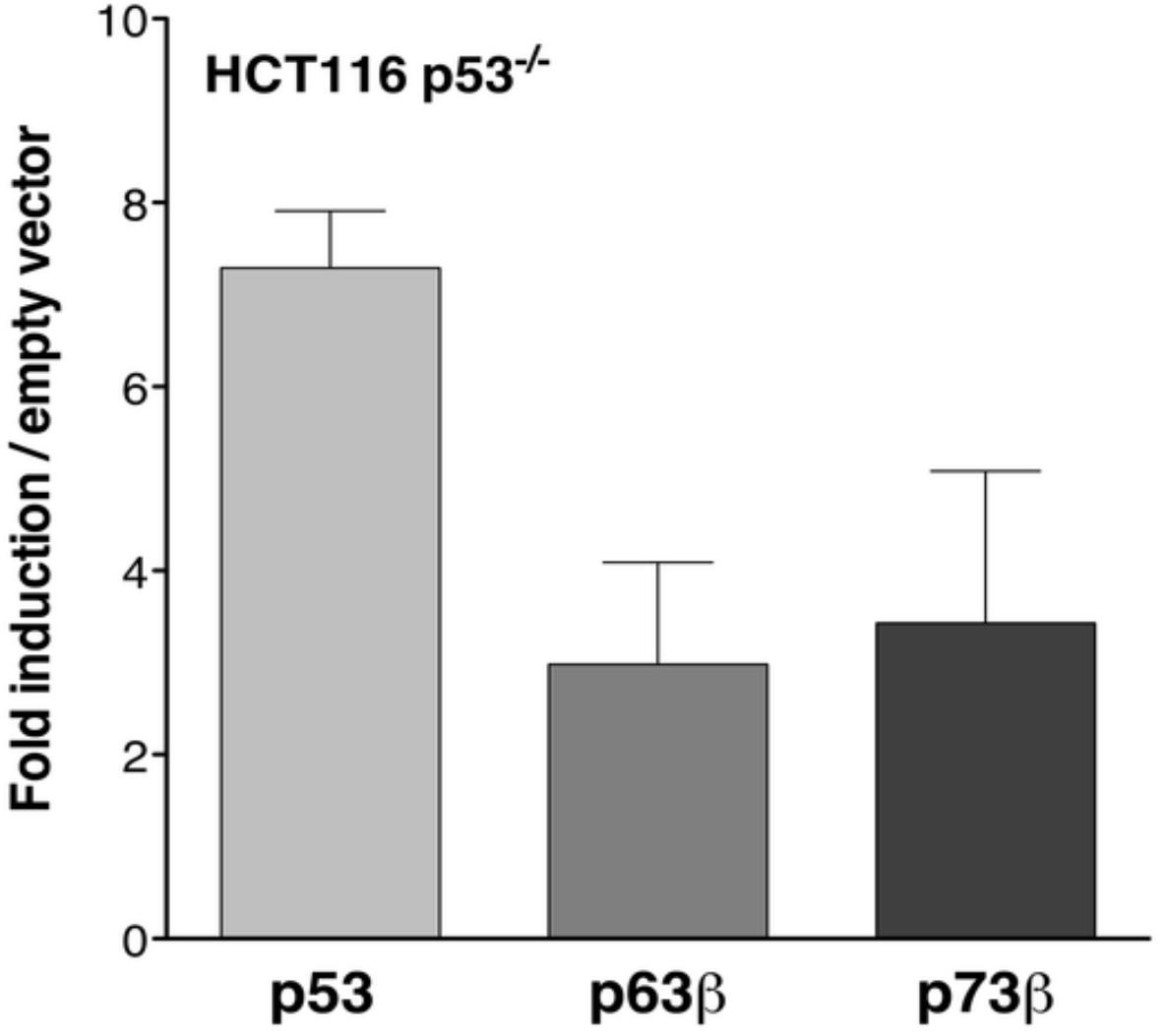

Figure 4
Click here to download high resolution image

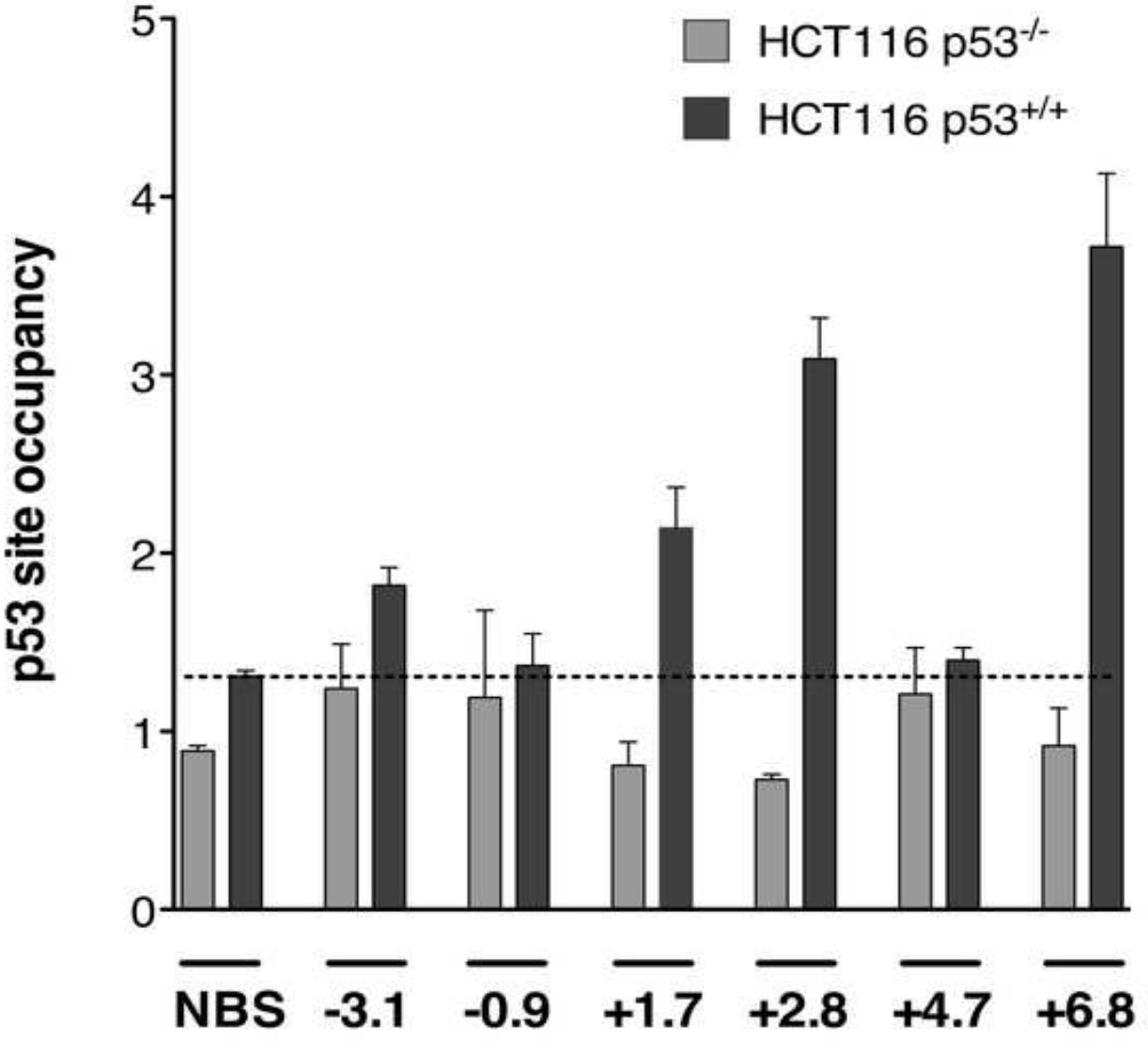

Figure 5
Click here to download high resolution image

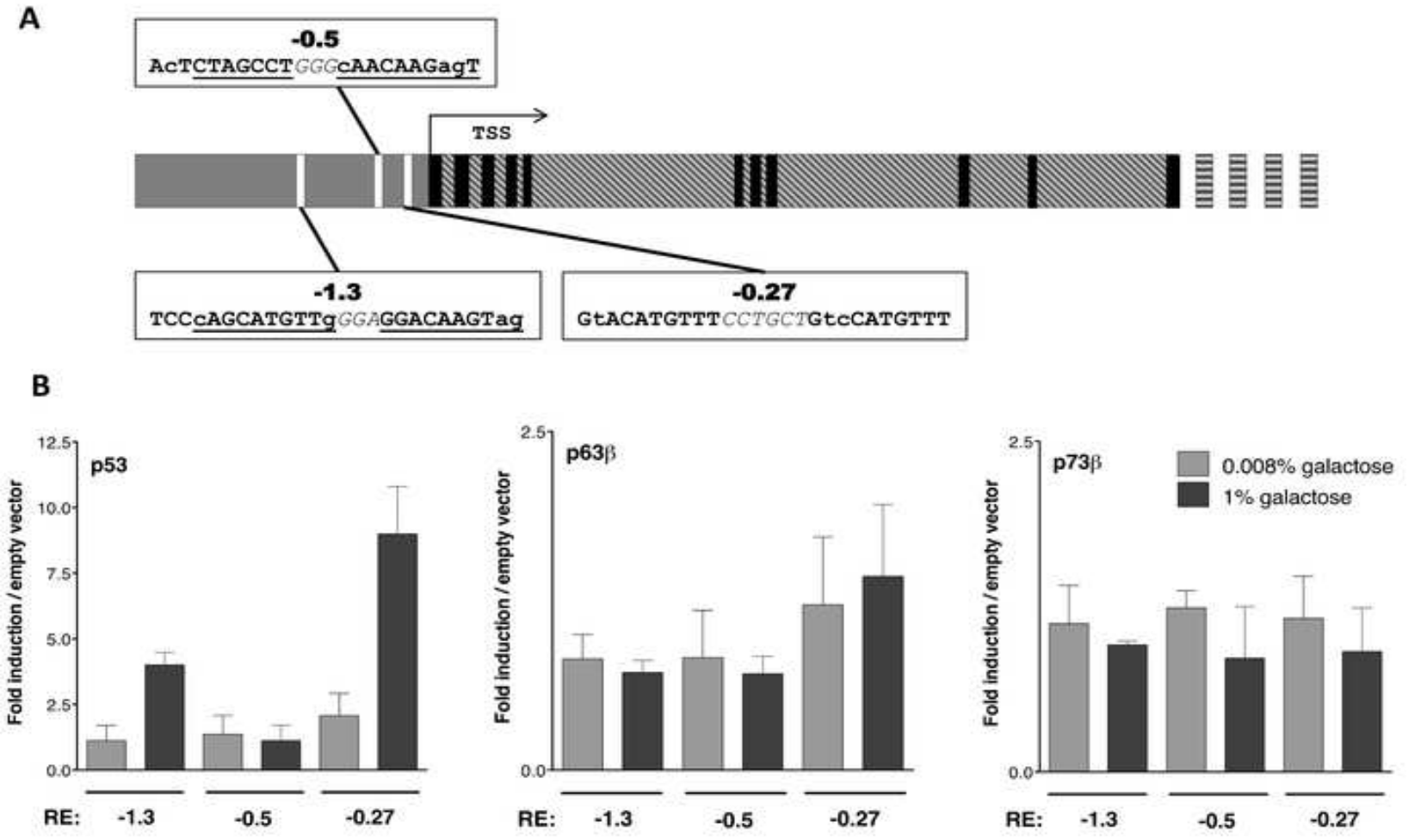

Figure 6
Click here to download high resolution image